

Dark Matter γ -ray searches in Galaxy Clusters: status and prospects



SMASH
machine learning for science and humanities postdoctoral program



Co-funded by
The European Union

Judit Pérez Romero
[*judit.perez@ung.si*](mailto:judit.perez@ung.si)

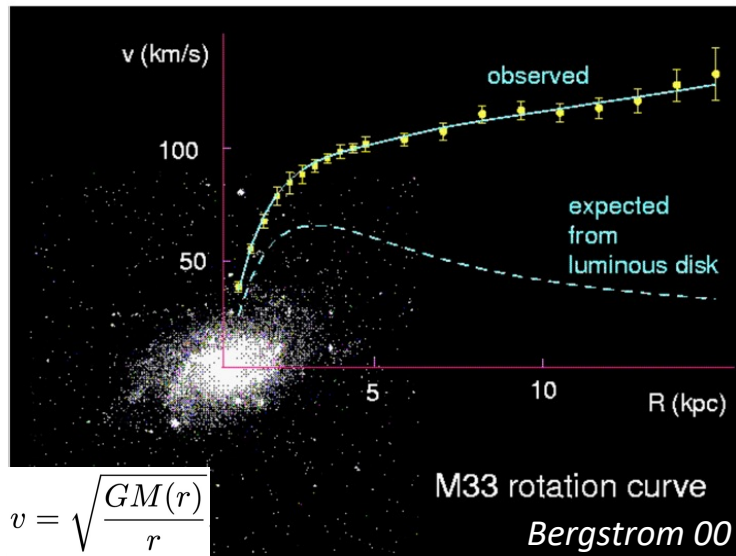


IRMP-CP3 Seminar, UC Louvain
28/05/2024

AI generated image combining different algorithms
interpreting:
"Gamma-rays from dark matter"

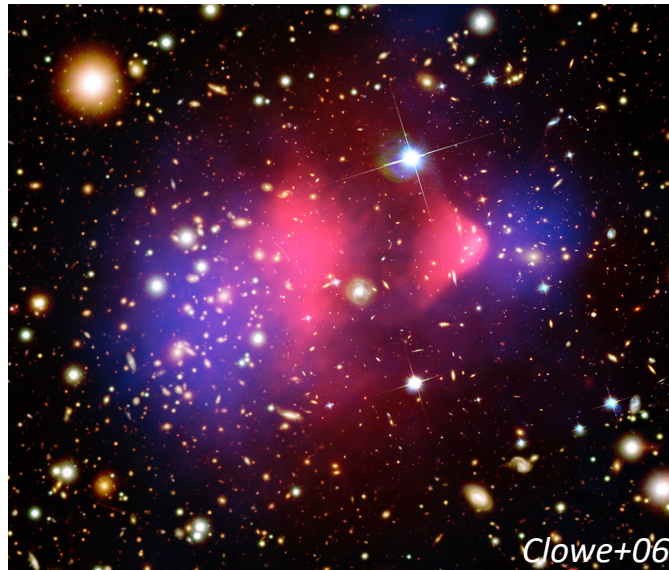
DARK MATTER (DM) EVIDENCE

Galactic scales



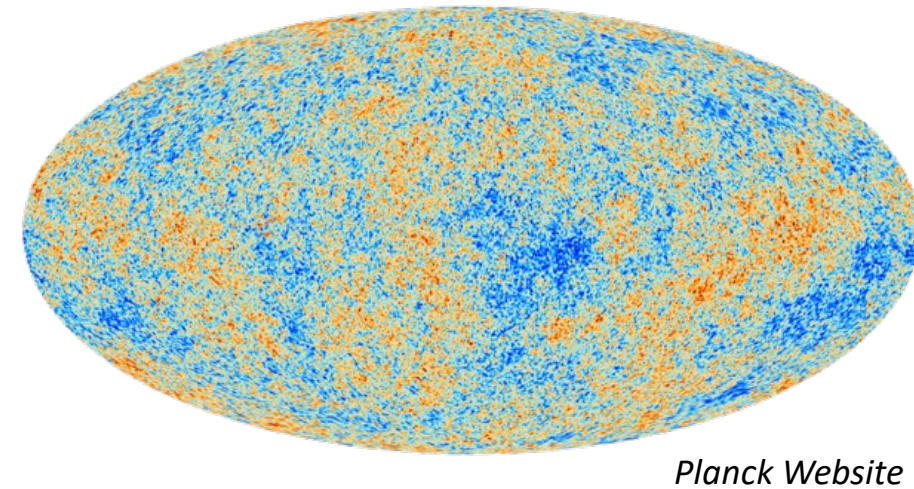
- Rotational curves
- Velocity dispersion

Galaxy cluster scales



- Peculiar velocity flows
- Mass tracers (X-rays, Sunyaev–Zeldovich, strong&weak lensing)
- Dynamical systems

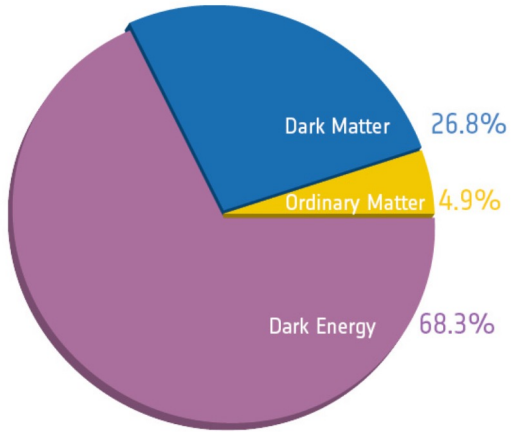
Cosmological scales



- Cosmic Microwave Background (CMB) anisotropies
- Large Scale Structure (LSS)

DM IN Λ CDM COSMOLOGY

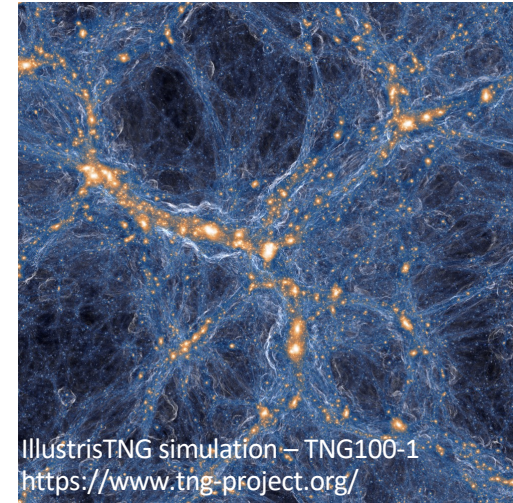
- Observational DM evidences



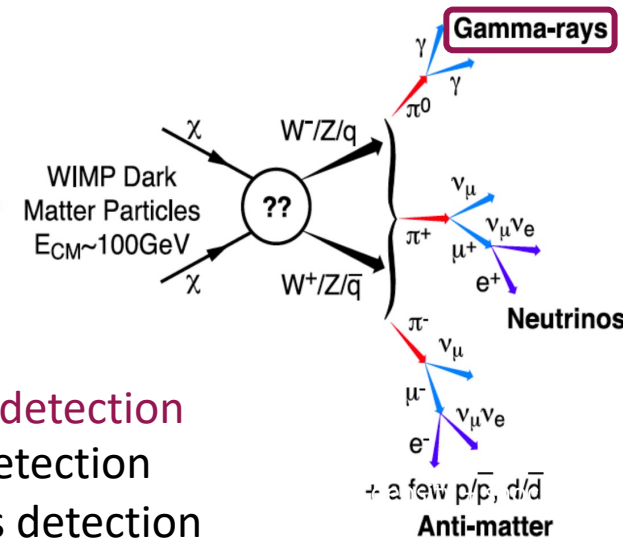
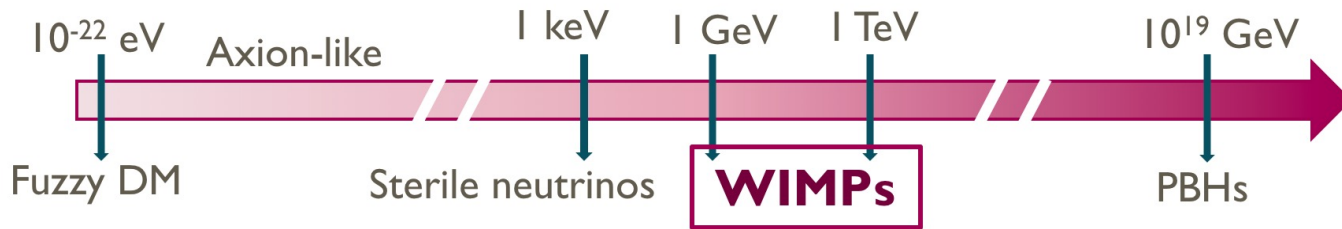
Component of Λ CDM Cosmology

- Structure formation driven by DM
- Bottom-up scenario: smaller structures form first

DM distribution in Halos and Subhalos



- Different DM candidates:

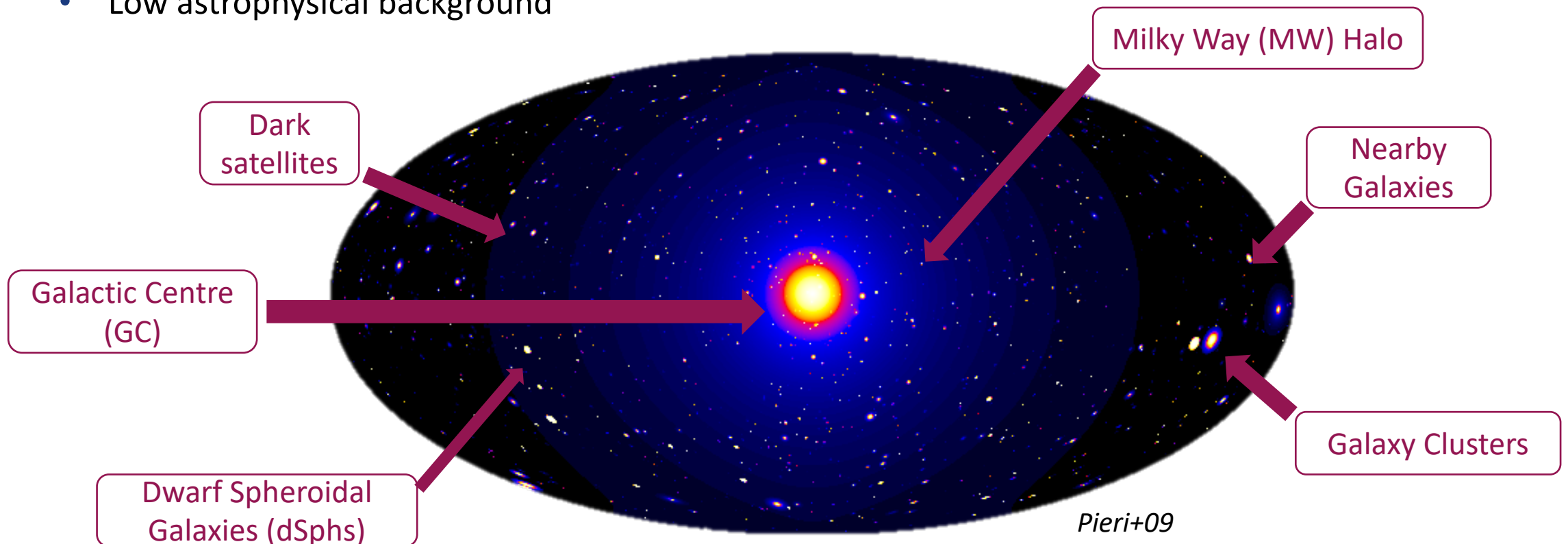


This γ -ray emission allows to perform Indirect DM Searches with current telescopes

- The search for the WIMP
 - Annihilation/Decay \rightarrow Indirect detection
 - Collision \rightarrow Direct detection
 - Production \rightarrow Colliders detection

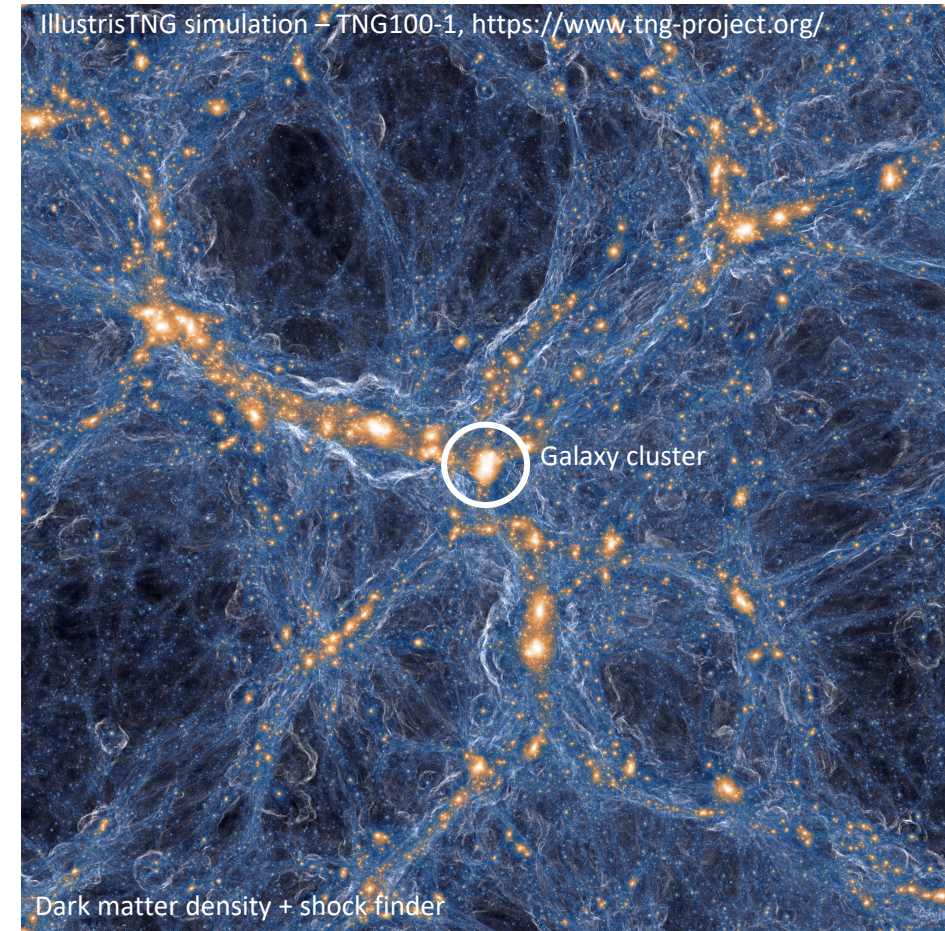
γ -RAY DM SEARCHES

- Optimal conditions for indirect DM searches:
 - High DM density ($\phi_{\text{DM}} \propto \rho_{\text{DM}}^2$ for annihilation, $\phi_{\text{DM}} \propto \rho_{\text{DM}}$ for decay)
 - Massive nearby objects ($\phi_{\text{DM}} \propto M/d_{\text{Earth}}^2$)
 - Low astrophysical background



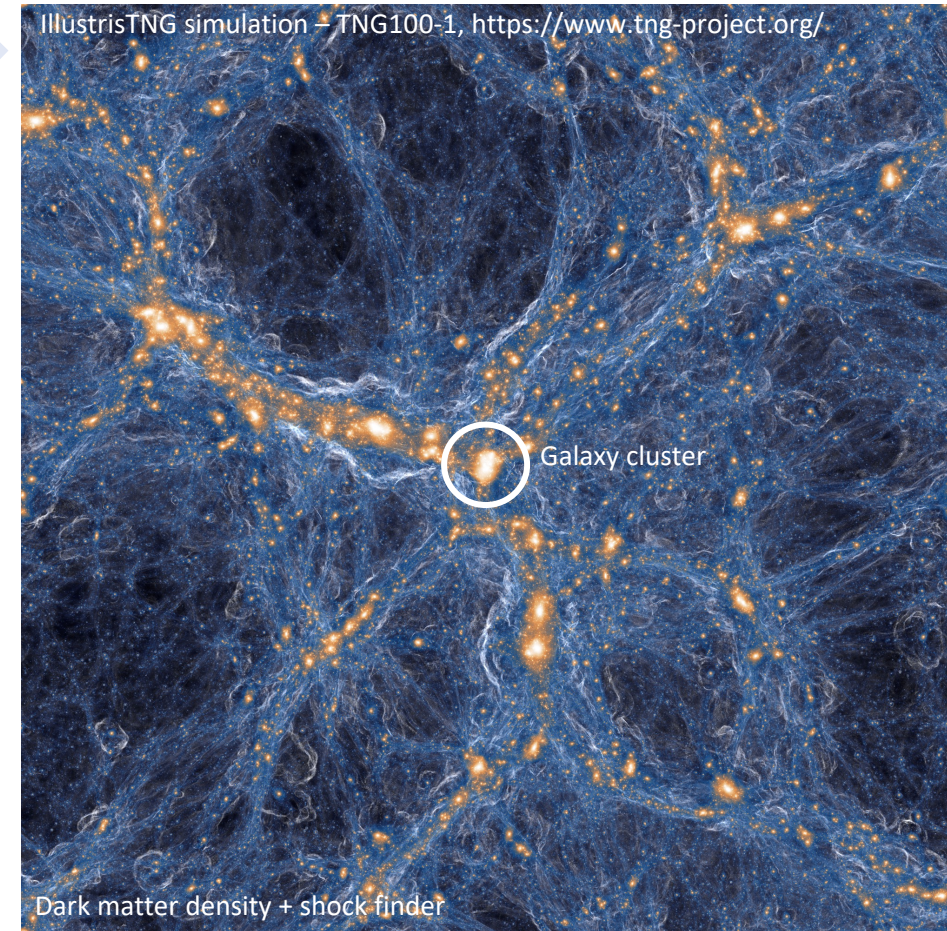
γ -RAY DM SEARCHES IN CLUSTERS

- Largest **gravitationally bound** structures formed by gravitational collapse
- Masses of order $\sim 10^{14}$ - $10^{15} M_{\odot}$
- Components:
 - Baryonic Matter
 - **Dark Matter (~80%)**
- Several in local Universe



γ -RAY DM SEARCHES IN CLUSTERS

- Largest **gravitationally bound** structures formed by gravitational collapse
- Masses of order $\sim 10^{14}$ - $10^{15} M_{\odot}$ ← Very massive objects ✓
- Components:
 - Baryonic Matter
 - **Dark Matter (~80%)** ← High DM density ✓
- Several in local Universe ← Closeby ✓



γ -RAY DM SEARCHES IN CLUSTERS

- Largest **gravitationally bound** structures formed by gravitational collapse
- Masses of order $\sim 10^{14}$ - $10^{15} M_{\odot}$
- Components:
 - Baryonic Matter
 - **Dark Matter (~80%)**
- Several in local Universe

Very massive objects ✓

High DM density ✓

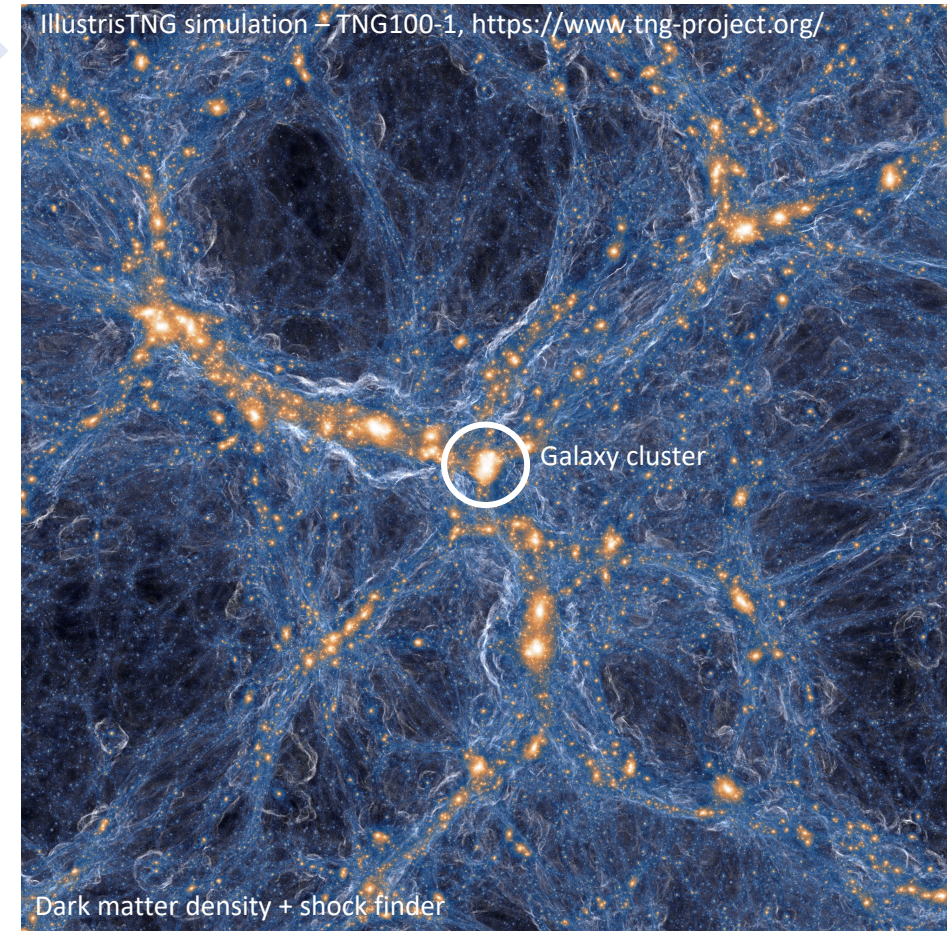
Closeby ✓

Decay

- Best possible targets to consider $\longrightarrow \phi_{\text{DM}} \propto \rho_{\text{DM}}$

Annihilation

- Competitive to other prime targets



γ -RAY DM SEARCHES IN CLUSTERS

- Largest **gravitationally bound** structures formed by gravitational collapse
- Masses of order $\sim 10^{14}$ - $10^{15} M_{\odot}$
- Components:
 - Baryonic Matter
 - **Dark Matter (~80%)**
- Several in local Universe

Very massive objects ✓

High DM density ✓

Closeby ✓

Decay

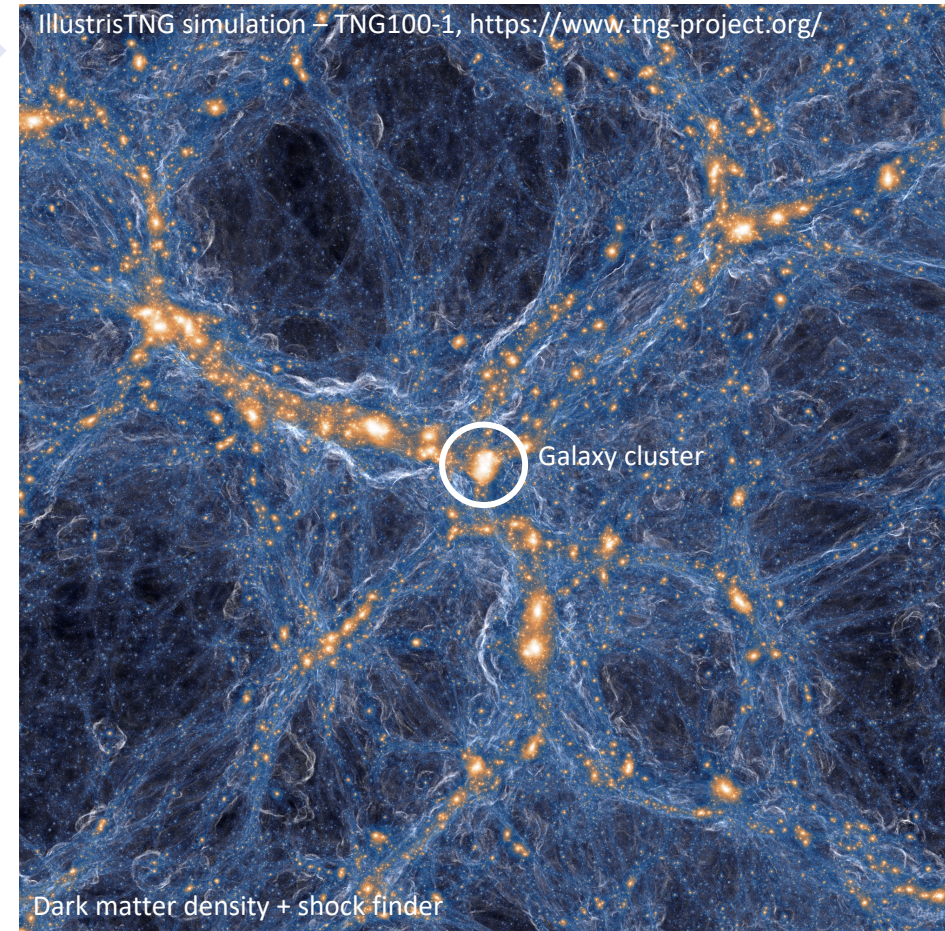
- Best possible targets to consider $\rightarrow \phi_{\text{DM}} \propto \rho_{\text{DM}}$

Annihilation

- Competitive to other prime targets

Caveat

Expected γ -ray emission from astrophysical processes



ASTROPHYSICAL γ -RAY EMISSION IN GALAXY CLUSTERS

- Components:

- Dark Matter
- **Baryonic Matter**
 - Galaxies ($\sim 3\% - 5\%$)
 - Intra Cluster Medium ($\sim 15\% - 17\%$)

- Even supposedly virialized objects, a lot of activity

- Merger events
- Feedback from galaxies and AGNs
- Magnetic fields
- Turbulence

Acceleration mechanisms

Cosmic-rays (CRs)

Diffuse synchrotron emission ← Leptons

γ -rays

← Hadrons

Chandra: NASA/CXC/SAO/Bulbul+14; XMM: ESA

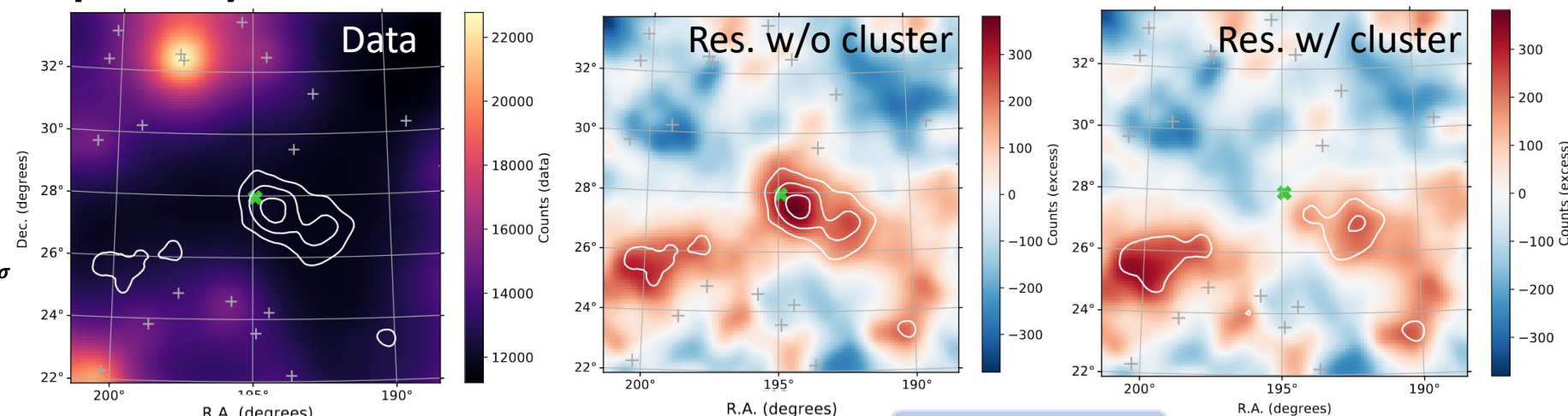
NGC 1275 in Perseus Galaxy Cluster

PREVIOUS γ -RAY DM SEARCHES IN GALAXY CLUSTERS

- Galaxy clusters should shine brightly in the γ -ray sky
- The search of diffuse γ -rays from clusters has been going on for over two decades (either originated from DM or/and CRs), but such signal has remained elusive

Reimer+03
 Aharonian+08 [HESS Collab.]
 Ackermann+10 [Fermi-LAT Collab.]
 Aleksic+10 [MAGIC Collab.]
 Dugger+10
 Colafrancesco+10
 Han+12 – Various clusters, *hint*
 Ando & Nagai 12
 Huang+12
 Aleksic+12 [MAGIC Collab.]
 Arlen+12 [VERITAS Collab.]
 Nezri+12
 Abramowski+12 [HESS Collab.]
 Cirelli+12
 Hektor+12 – Various clusters, 3.6σ
 Huber+13
 Prokhorov & Churazov 14 – Various clusters, $4-5\sigma$
Ackermann+14 [Fermi-LAT Collab.] – Various clusters, 2.4σ
 Griffin+14
 Zandanel & Ando 14
 Ackermann+15 [Fermi-LAT Collab.] – Virgo cluster, *hint*
 Ahnen+16 [MAGIC Collab.]
 Ackermann+16 [Fermi-LAT Collab.] – Coma cluster, *hint*
 Xi+18 – Coma cluster, *hint*
 Aleksic+18 [MAGIC Collab.]
 Lisanti+18
 Colavizzeno+19 – Various clusters, $3.5-3.8\sigma$
 Tan & Colavizzeno 19
 Adam+21 – Coma cluster, $4.9-5.8\sigma$
 Thorpe-Morgan+21

[Adam+21] – Fermi-LAT data of the Coma cluster



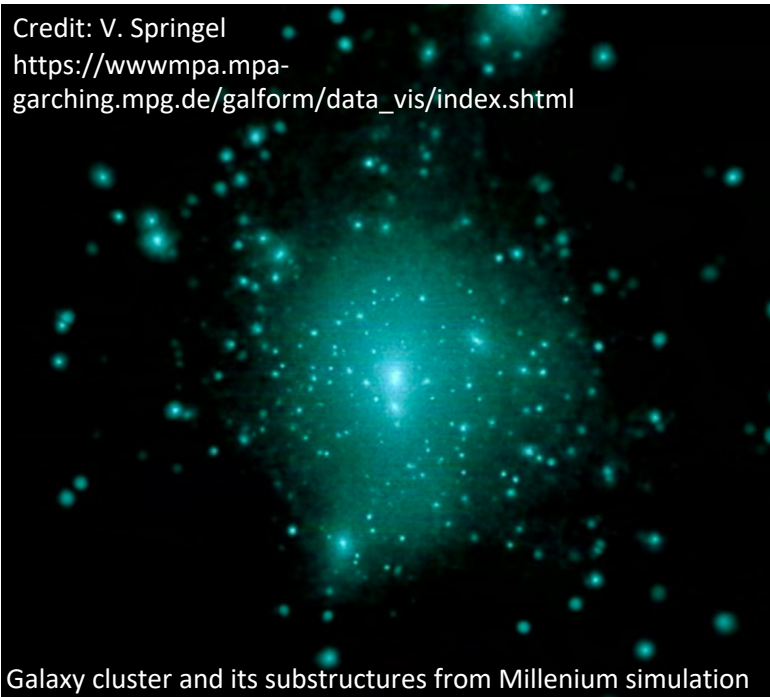
Hints of signal

PREVIOUS γ -RAY DM SEARCHES IN GALAXY CLUSTERS

- For annihilation of WIMPs:

- $\phi_{\text{DM}} \propto \rho_{\text{DM}}^2$
 - $\phi_{\text{DM}} \propto 1/d^2$
- DM distribution becomes extremely relevant

Credit: V. Springel
https://www.mpa-garching.mpg.de/galform/data_vis/index.shtml



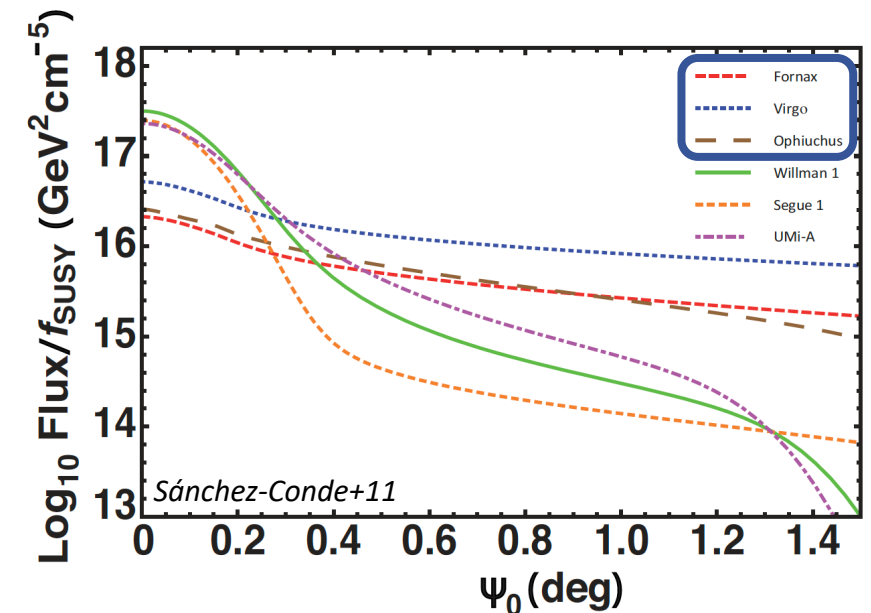
Galaxy cluster and its substructures from Millenium simulation

Large impact on the DM flux if we include:

- Smooth component (historical approach)
- + Substructure

Sánchez-Conde+11

| Object | Type | J_{tot} ($\text{GeV}^2\text{cm}^{-5}$) |
|-----------|---------|---|
| Fornax | Cluster | 1.48×10^{18} |
| Willman 1 | DSPH | 8.51×10^{17} |
| Coma | Cluster | 6.92×10^{17} |
| Perseus | Cluster | 5.37×10^{17} |
| Segue 1 | DSPH | 5.13×10^{17} |
| Draco | DSPH | 3.72×10^{17} |



Sánchez-Conde+11

PREVIOUS γ -RAY DM SEARCHES IN GALAXY CLUSTERS

What can we do to elucidate the mystery of γ -ray emission from galaxy clusters?

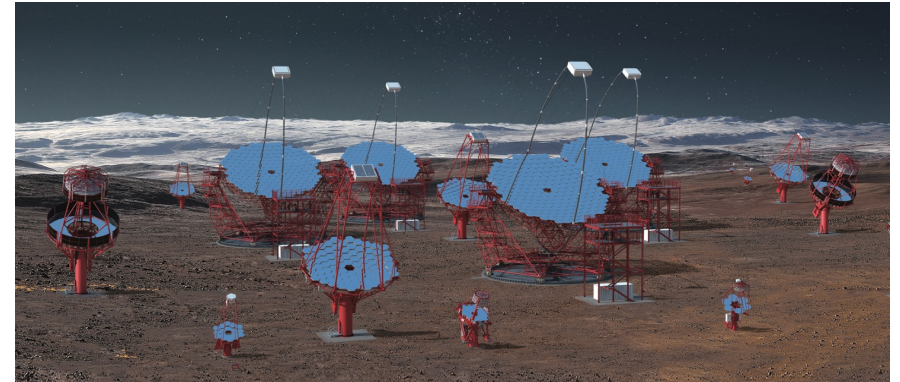
Present: *Fermi*-LAT



- Energy range: 400 MeV – 1 TeV
- Best sensitivity at ~ 200 GeV
- Angular resolution up to 0.1 deg
- 16 years of all-sky data



Future: Cherenkov Telescope Array Observatory (CTAO)



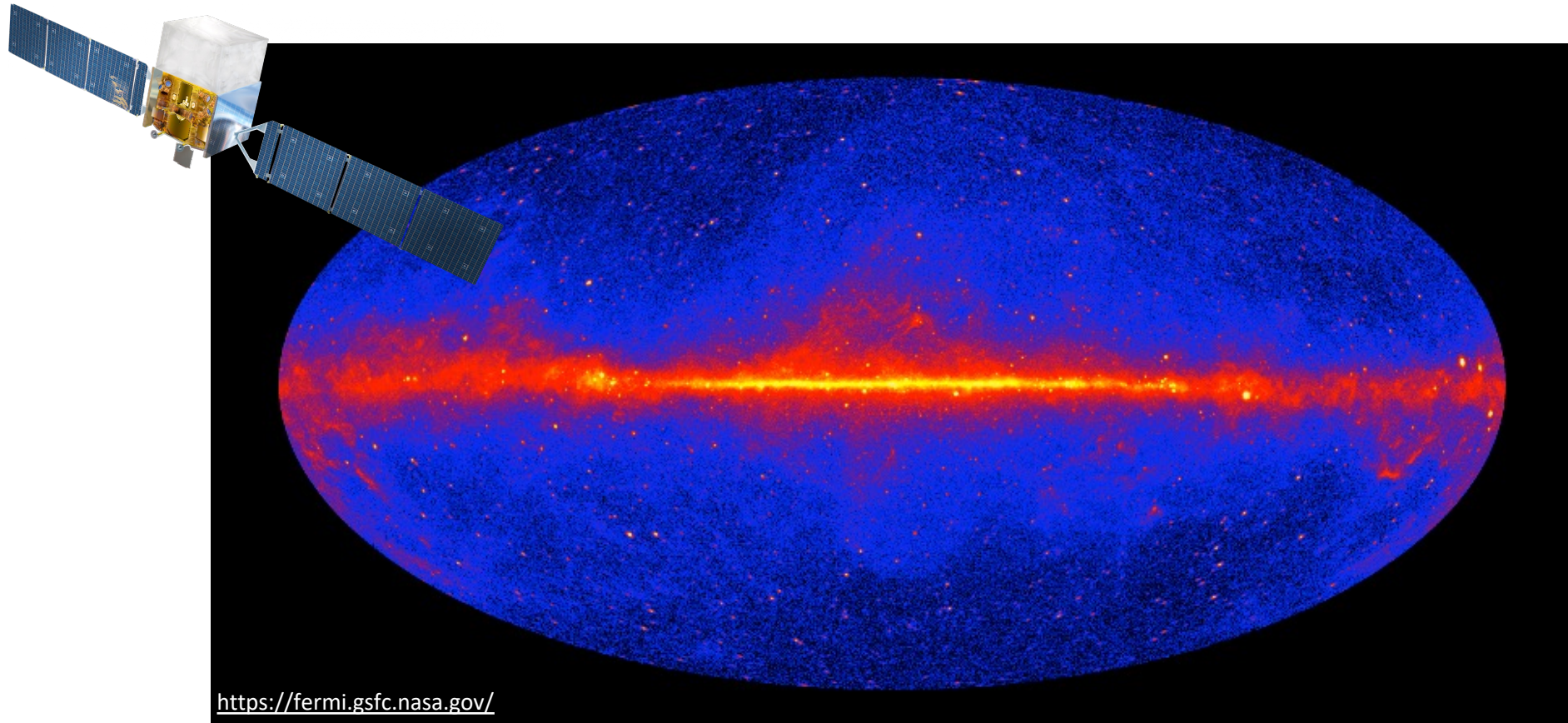
- First telescope in operation since 2022
- Energy range: 20 GeV – 100 TeV
- Best sensitivity at ~ 1 TeV
- Angular resolution up to 0.05 deg
- Deep dedicated surveys

γ -RAY DM SEARCHES IN GALAXY CLUSTERS WITH *FERMI*-LAT

Constraining the dark matter contribution of gamma-rays in cluster of galaxies using Fermi-LAT data

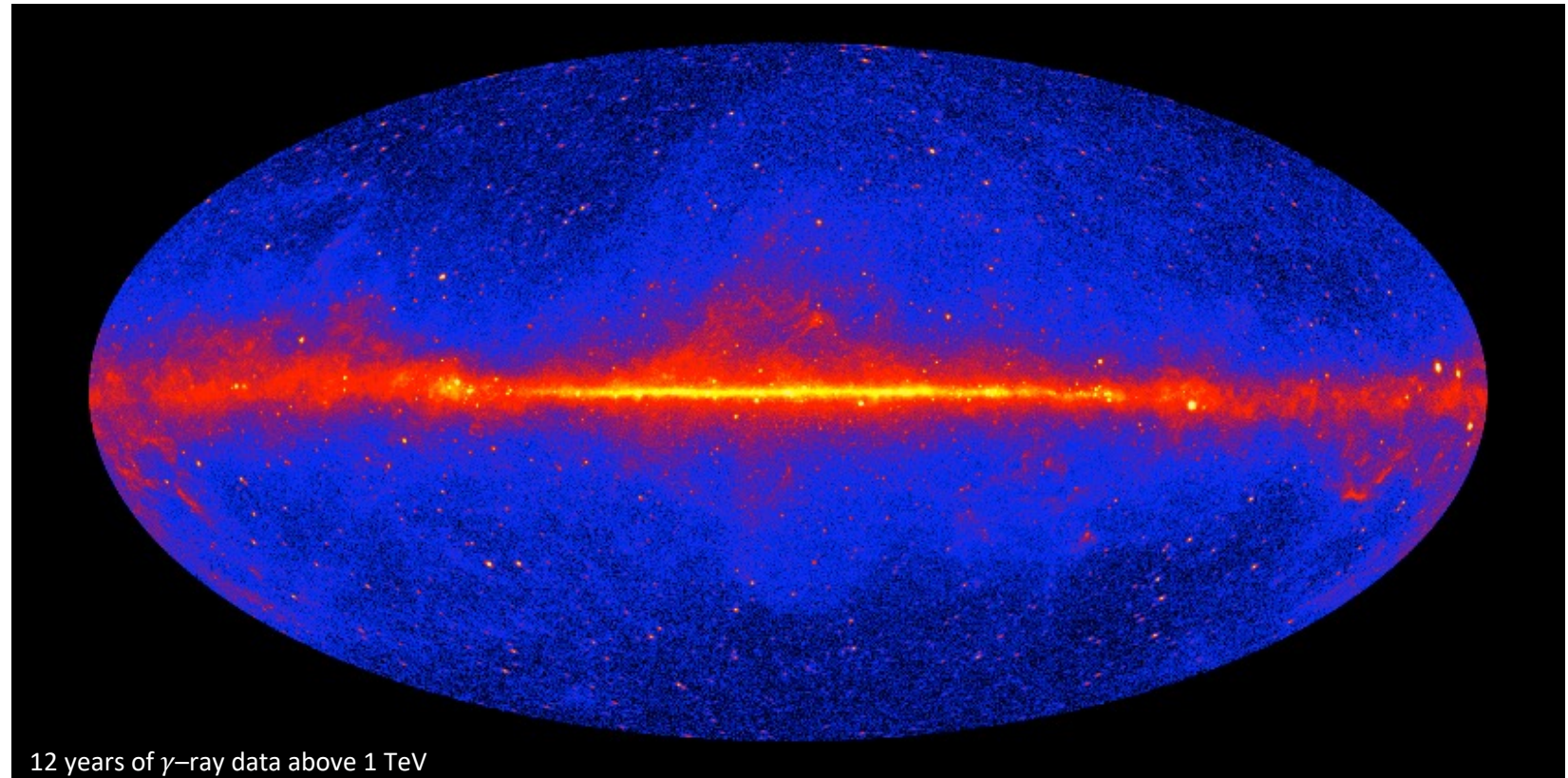
M. di Mauro, JPR, M. A. Sánchez-Conde, N. Fornengo

Phys. Rev. D 107, 083030, [[arXiv:2303.16930](https://arxiv.org/abs/2303.16930)]



FERMI LARGE AREA TELESCOPE (LAT)

- Satellite-based telescope launched in June 2008 – 16 years of γ -ray data
- All sky survey mode, image of whole sky every 3 hours
- The γ -ray produces a pair of electron-positron, tracked and used to determine the energy of the primary γ -ray

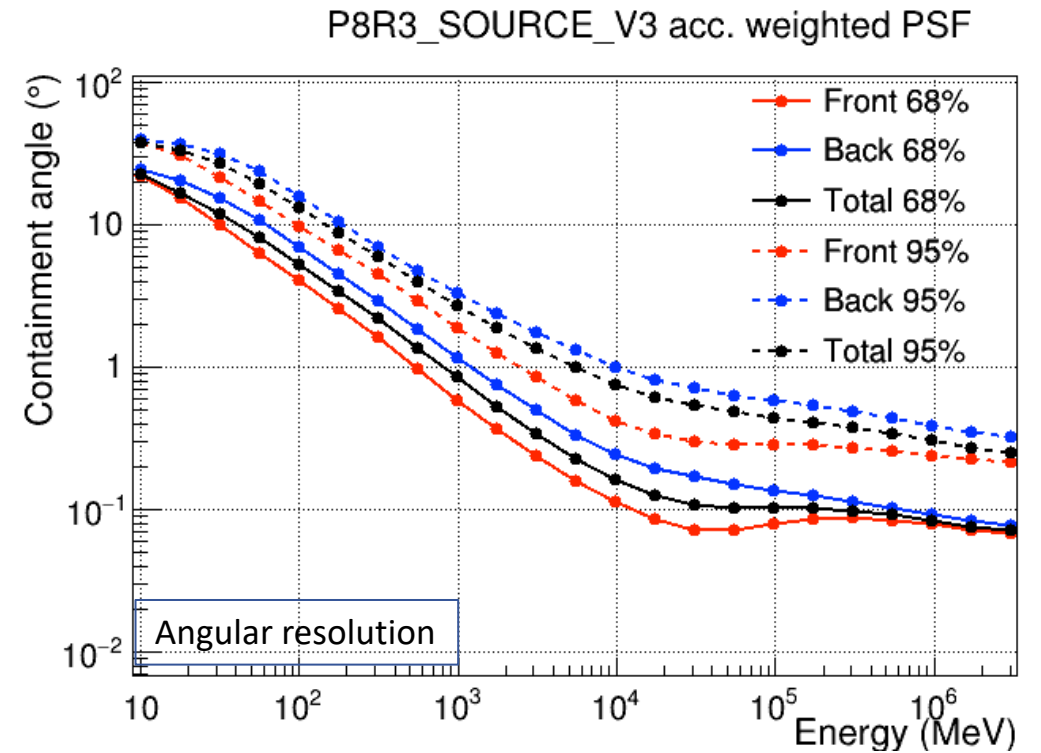
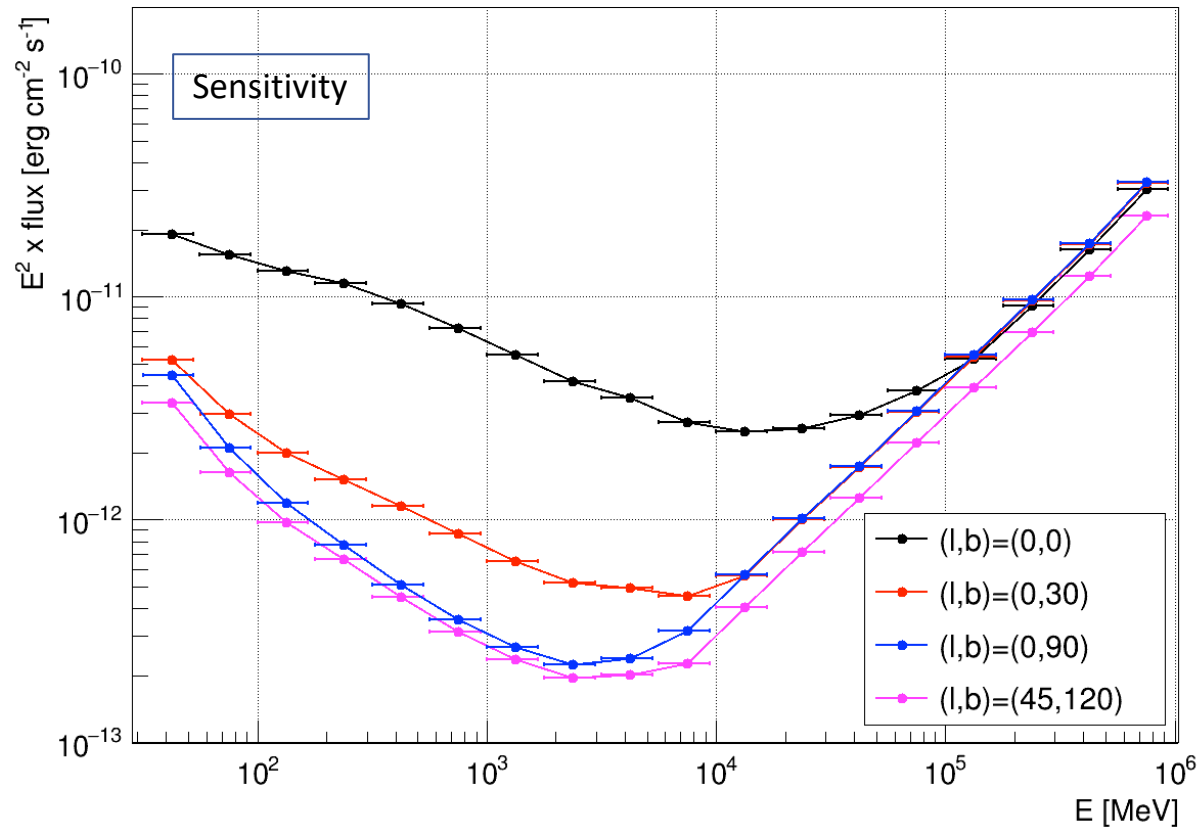


FERMI-LAT PERFORMANCE

10y Performance Capabilities

Instrument Response Functions (IRFs)

Diff. flux sensitivity (P8R3_SOURCE_V3, 10 years, TS=25, > 10 photons per bin)



https://www.slac.stanford.edu/exp/glast/groups/canda/lat_Performance.htm

CLUSTERS TARGET SELECTION

- *Fermi*-LAT does not have constraints on observation time



Sample of best clusters for DM searches

- Selection criteria:
 - Well-known M_{200} from X-rays measurements
 - Local clusters
 - Mask of $|b| < 20$ deg to avoid galactic diffuse emission
 - Separation of at least 2 deg to account for cluster extension

TARGET SELECTION

- *Fermi*-LAT does not have constraints on observation time

Sample of best clusters for DM searches

- Selection criteria:

- Well-known M_{200} from X-rays measurements
- Local clusters
- Mask of $|b| < 20$ deg to avoid galactic diffuse emission
- Separation of at least 2 deg to account for cluster extension

HIFLUGCS catalogue (*Reiprich&Böhringer02*)

- 50 local clusters
- $f_x \geq 1.7 \cdot 10^{-11}$ erg s⁻¹ cm⁻²
- biased towards cool-cored clusters (*Käfer+19*)

↓ BUT

- Observational inconveniences
- Outdated X-rays data

TARGET SELECTION

- *Fermi*-LAT does not have constraints on observation time

Sample of best clusters for DM searches

- Selection criteria:

- Well-known M_{200} from X-rays measurements
- Local clusters
- Mask of $|b| < 20$ deg to avoid galactic diffuse emission
- Separation of at least 2 deg to account for cluster extension

HIFLUGCS catalogue (*Reiprich&Böhringer02*)

- 50 local clusters
- $f_x \geq 1.7 \cdot 10^{-11}$ erg s⁻¹ cm⁻²
- biased towards cool-cored clusters (*Käfer+19*)



- Clusters used in previous searches:

Ackermann+10 [Fermi-LAT Coll.]

Sánchez-Conde+11

Ackermann+14 [Fermi-LAT Coll.]

TARGET SELECTION

- *Fermi*-LAT does not have constraints on observation time

Sample of best clusters for DM searches

- Selection criteria:

- Well-known M_{200} from X-rays measurements

Masses from *Schellenberger&Reiprich17*
(X-rays data from Chandra)

- Local clusters

$z < 0.1$

- Mask of $|b| < 20$ deg to avoid galactic diffuse emission
- Separation of at least 2 deg to account for cluster extension

HIFLUGCS catalogue (*Reiprich&Böhringer02*)

- 50 local clusters
- $f_x \geq 1.7 \cdot 10^{-11}$ erg s⁻¹ cm⁻²
- biased towards cool-cored clusters (*Käfer+19*)



- Clusters used in previous searches:

Ackermann+10 [Fermi-LAT Coll.]

Sánchez-Conde+11

Ackermann+14 [Fermi-LAT Coll.]

TARGET SELECTION

- *Fermi*-LAT does not have constraints on observation time

Sample of best clusters for DM searches

- Selection criteria:

- Well-known M_{200} from X-rays measurements

Masses from *Schellenberger&Reiprich17*
(X-rays data from Chandra)

- Local clusters

$z < 0.1$

- Mask of $|b| < 20$ deg to avoid galactic diffuse emission
- Separation of at least 2 deg to account for cluster extension

HIFLUGCS catalogue (*Reiprich&Böhringer02*)

- 50 local clusters
- $f_x \geq 1.7 \cdot 10^{-11}$ erg s⁻¹ cm⁻²
- biased towards cool-cored clusters (*Käfer+19*)



- Clusters used in previous searches:

Ackermann+10 [*Fermi*-LAT Coll.]

Sánchez-Conde+11

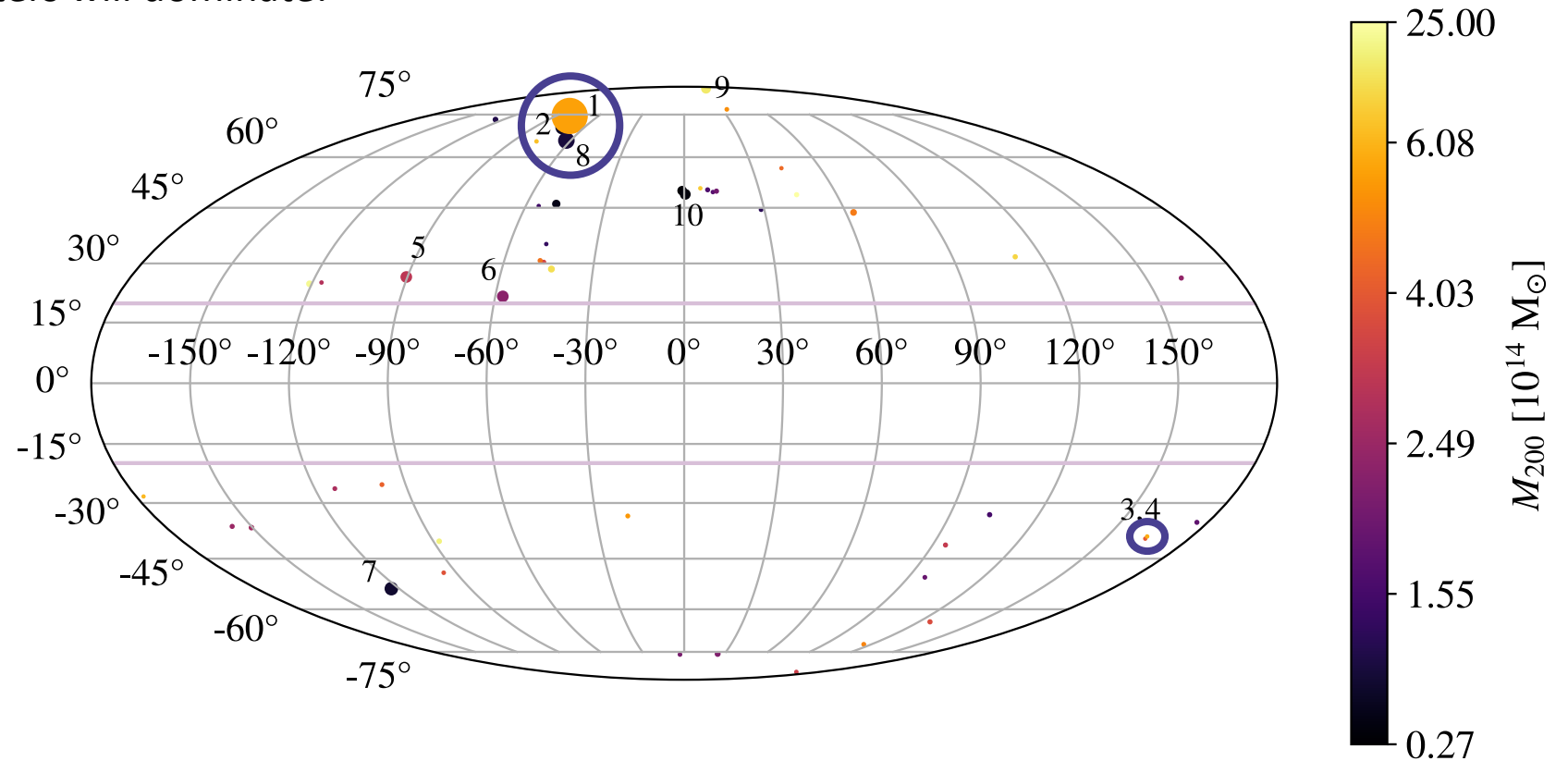
Ackermann+14 [*Fermi*-LAT Coll.]

Sample of 49 local
galaxy clusters

TARGET SELECTION

- Most massive and closest clusters will dominate:

- 1 - Virgo
- 2 - M49
- 3 - A0399
- 4 - A0401
- 5 - A1060 - Hydra
- 6 - A3526 - Centaurus
- 7 - NGC 1399 - Fornax
- 8 - NGC 4636
- 9 - A1656 - Coma
- 10 - NGC 5813



DARK MATTER MODELLING

$$\frac{d\Phi_{DM}}{dE}(E, l.o.s, \Delta\Omega, z) = \frac{d\phi}{dE}(E, z) \times \text{Astrophysical factor}$$


Charbonnier+12,
Bonnivard+15, Hütten+18
<https://clumpy.gitlab.io/CLUMPY/>

DM-induced γ -ray flux from an astrophysical object

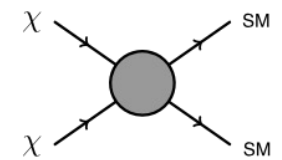
Particle Physics Model
Cirelli+12 (EW corrections)

Annihilation

$$J(l.o.s, \Delta\Omega, z) = \int_{\Delta\Omega} \int_{l.o.s} \rho_{DM}^2(r) dr$$

DM density profile

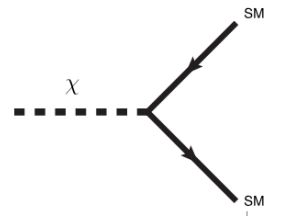
$$J \propto \frac{M_{200} c_{200}^3}{D_{Earth}^2}$$



Decay

$$D(l.o.s, \Delta\Omega, z) = \int_{\Delta\Omega} \int_{l.o.s} \rho_{DM}(r) dr$$

$$D \propto \frac{M_{200}}{D_{Earth}^2}$$



CLUSTERS DM MODELLING (I): MAIN HALO

Annihilation

$$J(l.o.s, \Delta\Omega, z) = \int_{\Delta\Omega} \int_{l.o.s} \rho_{DM}^2(r) dr$$

DM density profile

$$D(l.o.s, \Delta\Omega, z) = \int_{\Delta\Omega} \int_{l.o.s} \rho_{DM}(r) dr$$

Decay

- State-of-the-art parametrization of the DM in galaxy clusters:

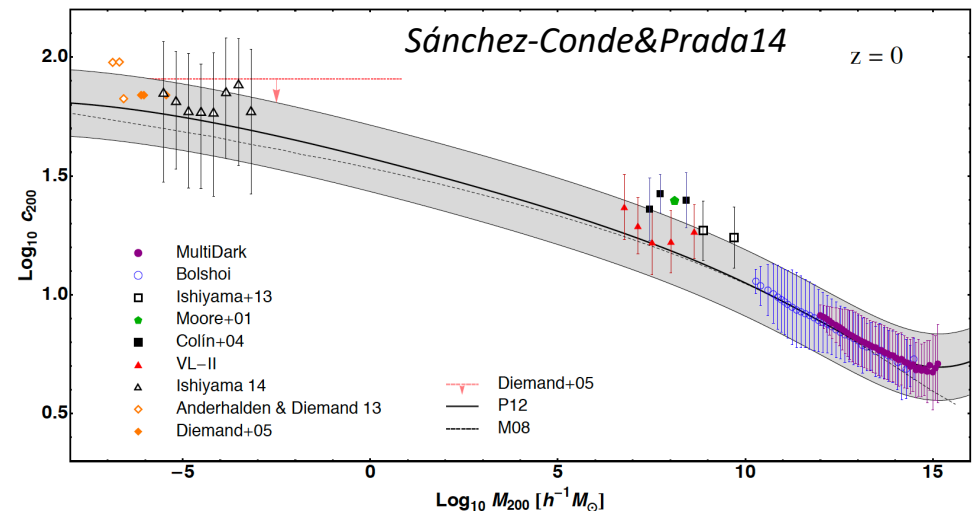
Assume density profile

$$\langle \rho_{\text{tot}} \rangle(r) = \rho_{\text{sm}}(r) + \langle \rho_{\text{subs}} \rangle(r) \longrightarrow \rho(r) = \frac{\rho_0}{\left(\frac{r}{r_s}\right) \left(1 + \frac{r}{r_s}\right)^2}$$

Navarro – Frenk – White (NFW)
Navarro+96, Navarro+97

- “Cuspy”-like profile

- To build the DM profile, we assume a concentration-mass relation ($c_{200} - M_{200}$):



CLUSTERS DM MODELLING (II): SUBSTRUCTURES

- Galaxy clusters are the most massive objects today, large amount of substructure expected
- Inclusion through ρ_{DM} using state-of-the-art subhalo models

$$\langle \rho_{\text{tot}} \rangle(r) = \rho_{\text{sm}}(r) + \langle \rho_{\text{subs}} \rangle(r)$$

DM subhalo profile: NFW

$$\rho(r) = \frac{\rho_0}{\left(\frac{r}{r_s}\right) \left[1 + \frac{r}{r_s}\right]^2}$$



$$\frac{d^3 N}{dV dM dc} = N_{\text{tot}} \frac{d\mathcal{P}_V}{dV}(r) \cdot \frac{d\mathcal{P}_M}{dM}(M) \cdot \frac{d\mathcal{P}_c}{dc}(M, c)$$



CLUSTERS DM MODELLING (II): SUBSTRUCTURES

- Galaxy clusters are the most massive objects today, large amount of substructure expected
- Inclusion through ρ_{DM} using state-of-the-art subhalo models

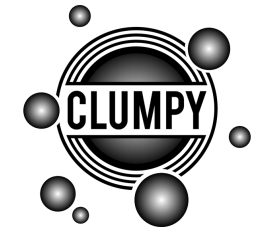
$$\langle \rho_{tot} \rangle(r) = \rho_{sm}(r) + \langle \rho_{subs} \rangle(r)$$

DM subhalo profile: NFW

$$\rho(r) = \frac{\rho_0}{\left(\frac{r}{r_s}\right) \left[1 + \frac{r}{r_s}\right]^2}$$

Subhalo Radial Distribution (SRD)

$$\frac{d^3 N}{dV dM dc} = N_{tot} \frac{d\mathcal{P}_V}{dV}(r) \cdot \frac{d\mathcal{P}_M}{dM}(M) \cdot \frac{d\mathcal{P}_c}{dc}(M, c)$$



$$\rho_{sub}^{VLI}(R) = \frac{\rho_{tot}^{VLI}(R) (R/R_a)}{\left(1 + \frac{R}{R_a}\right)} \quad \rho_{sub}^{Aq}(r) = \rho_s \exp\left(-\frac{2}{\alpha} \left[\left(\frac{r}{r_s}\right)^\alpha - 1\right]\right)$$

Via Lactea - II
Anti-biased relation
Diemand+08

Aquarius
Biased relation
Springel+08

CLUSTERS DM MODELLING (II): SUBSTRUCTURES

- Galaxy clusters are the most massive objects today, large amount of substructure expected
- Inclusion through ρ_{DM} using state-of-the-art subhalo models

$$\langle \rho_{\text{tot}} \rangle(r) = \rho_{\text{sm}}(r) + \langle \rho_{\text{subs}} \rangle(r)$$

DM subhalo profile: NFW

$$\rho(r) = \frac{\rho_0}{\left(\frac{r}{r_s}\right) \left[1 + \frac{r}{r_s}\right]^2}$$

Subhalo Radial Distribution
(SRD)

$$\rho_{\text{sub}}^{\text{VLII}}(R) = \frac{\rho_{\text{tot}}^{\text{VLII}}(R) (R/R_a)}{\left(1 + \frac{R}{R_a}\right)} \quad \rho_{\text{sub}}^{\text{Aq}}(r) = \rho_s \exp\left(-\frac{2}{\alpha} \left[\left(\frac{r}{r_s}\right)^\alpha - 1\right]\right)$$

Via Lactea - II
Anti-biased relation
Diemand+08

Aquarius
Biased relation
Springel+08

$$\frac{d^3 N}{dV dM dc} = N_{\text{tot}} \frac{d\mathcal{P}_V}{dV}(r) \cdot \frac{d\mathcal{P}_M}{dM}(M) \cdot \frac{d\mathcal{P}_c}{dc}(M, c)$$

Subhalo Mass Function
(SHMF)

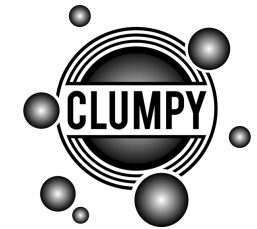
$$dN/dm = A/M (m/M)^{-\alpha}$$

$$\alpha = 1.9$$

Springel+08

$$\alpha = 2.0$$

Diemand+08



CLUSTERS DM MODELLING (II): SUBSTRUCTURES

- Galaxy clusters are the most massive objects today, large amount of substructure expected
- Inclusion through ρ_{DM} using state-of-the-art subhalo models

$$\langle \rho_{tot} \rangle(r) = \rho_{sm}(r) + \langle \rho_{subs} \rangle(r)$$

DM subhalo profile: NFW

$$\rho(r) = \frac{\rho_0}{\left(\frac{r}{r_s}\right) \left[1 + \frac{r}{r_s}\right]^2}$$

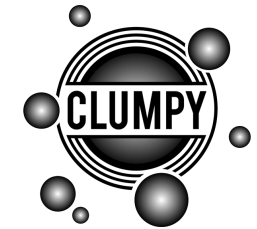
Subhalo Radial Distribution (SRD)

$$\rho_{sub}^{VLII}(R) = \frac{\rho_{tot}^{VLII}(R) (R/R_a)}{\left(1 + \frac{R}{R_a}\right)} \quad \rho_{sub}^{Aq}(r) = \rho_s \exp\left(-\frac{2}{\alpha} \left[\left(\frac{r}{r_s}\right)^\alpha - 1\right]\right)$$

Via Lactea - II
Anti-biased relation
Diemand+08

Aquarius
Biased relation
Springel+08

$$\frac{d^3 N}{dV dM dc} = N_{tot} \frac{d\mathcal{P}_V}{dV}(r) \cdot \frac{d\mathcal{P}_M}{dM}(M) \cdot \frac{d\mathcal{P}_c}{dc}(M, c)$$



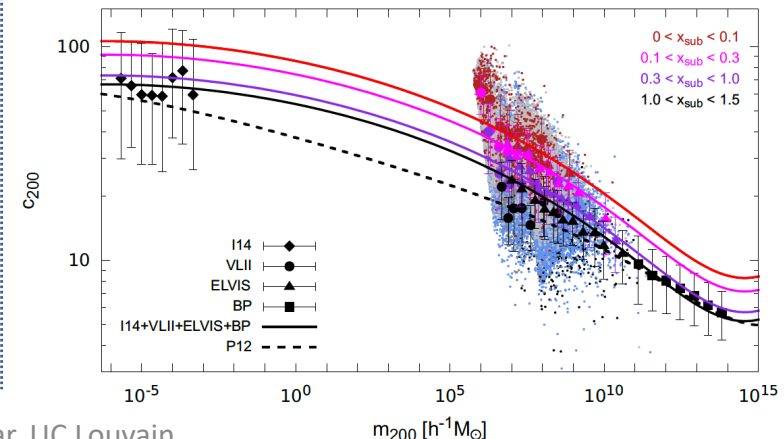
Subhalo Mass Function (SHMF)

$$dN/dm = A/M(m/M)^{-\alpha}$$

$\alpha = 1.9$
Springel+08

$\alpha = 2.0$
Diemand+08

Subhalo Concentration-Mass relation ($c_{200}-M_{200}$)

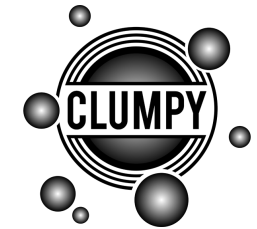


Dependence on the subhalo position
 $c_{200}(m_{200}, x_{sub})$
 $x_{sub} \equiv R_{sub}/R_\Delta$
Moliné+17

CLUSTERS DM MODELLING (II): SUBSTRUCTURES

- Galaxy clusters are the most massive objects today, large amount of substructure expected
- Inclusion through ρ_{DM} using state-of-the-art subhalo models

$$\langle \rho_{\text{tot}} \rangle(r) = \rho_{\text{sm}}(r) + \langle \rho_{\text{subs}} \rangle(r) \longrightarrow \frac{d^3 N}{dV dM dc} = N_{\text{tot}} \left(\frac{d\mathcal{P}_V}{dV}(r) \right) \cdot \left(\frac{d\mathcal{P}_M}{dM}(M) \right) \cdot \left(\frac{d\mathcal{P}_c}{dc}(M, c) \right)$$



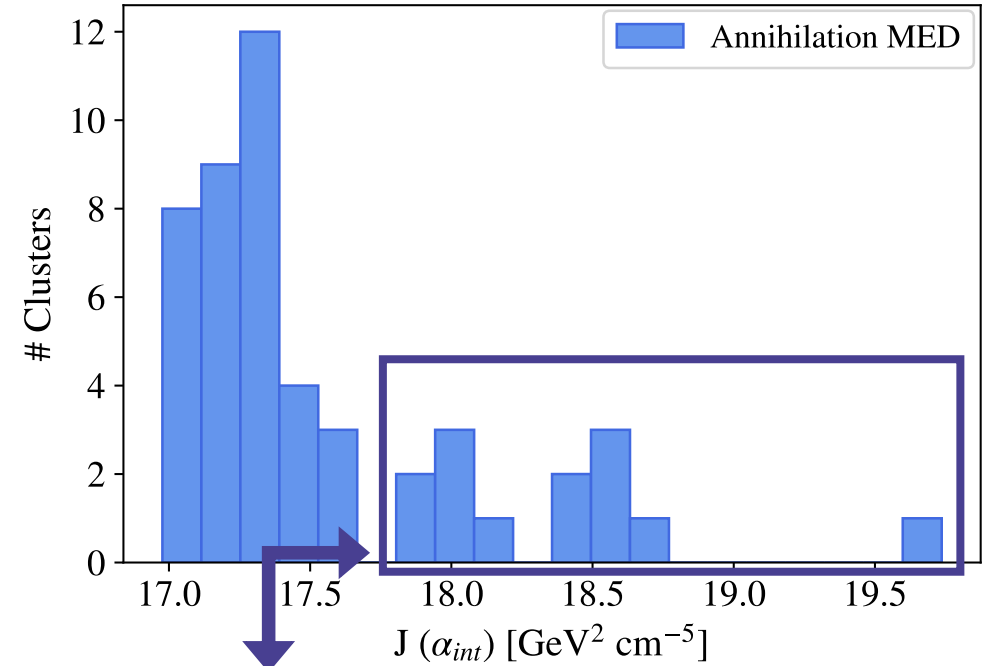
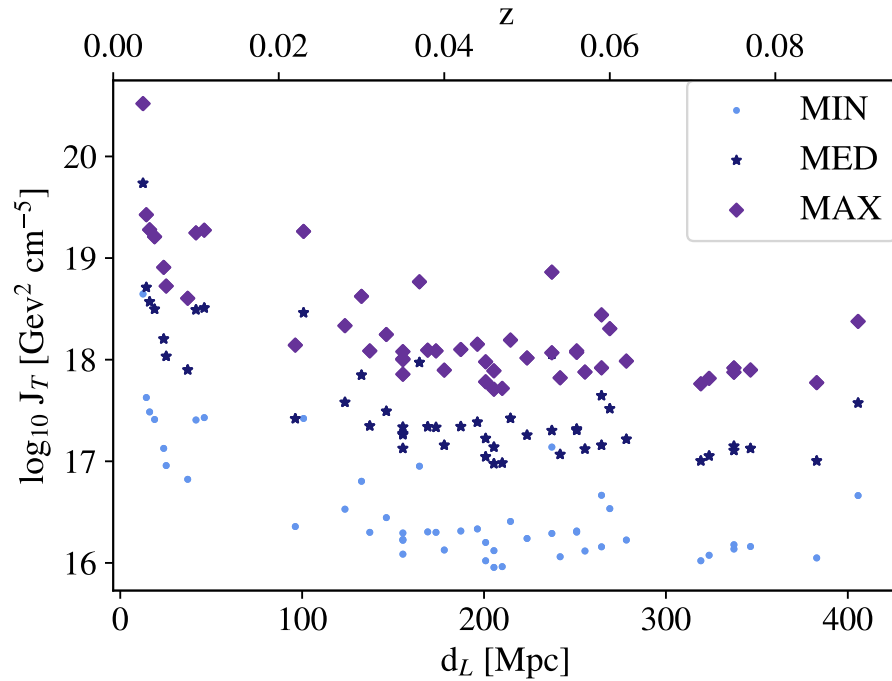
- We define benchmark models to encapsulate the uncertainty on the expected substructure population:

| Model | SRD | α | $c(M)$ | M_{min} | f_{sub} |
|-------|---------------------------------|----------|------------------|---------------------|------------------|
| MIN | - | - | - | - | - |
| MED | VL-II (<i>Diemand+08</i>) | 1.9 | <i>Moliné+17</i> | $10^{-6} M_{\odot}$ | 0.18 |
| MAX | Aquarius (<i>Springer+08</i>) | 2.0 | <i>Moliné+17</i> | $10^{-9} M_{\odot}$ | 0.34 |

- No substructure considered \longrightarrow
- Best guess \longrightarrow
- Educated upper bound \longrightarrow

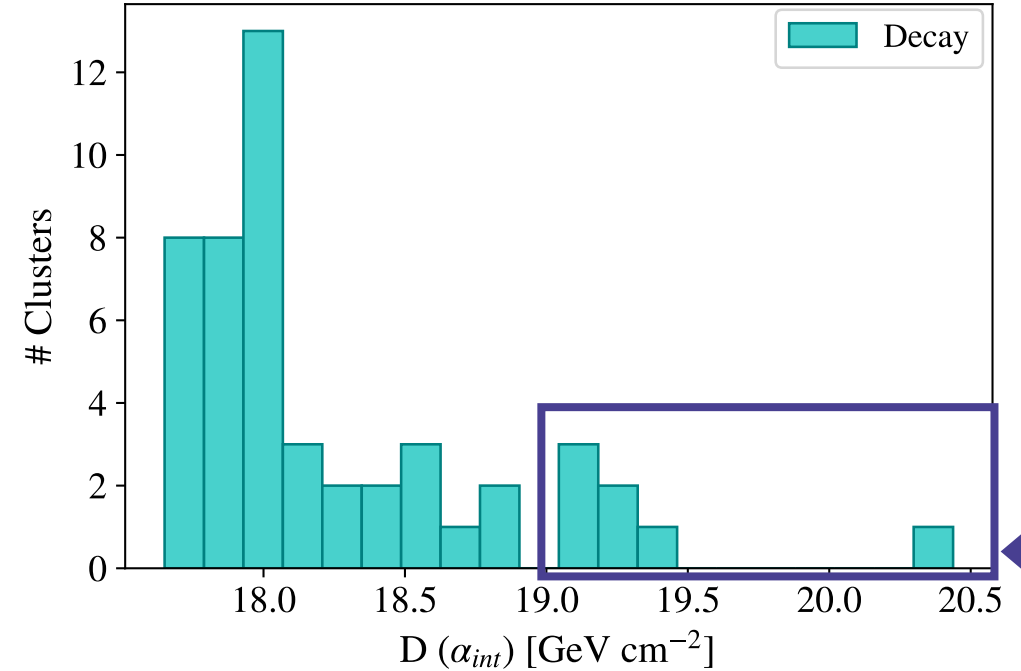
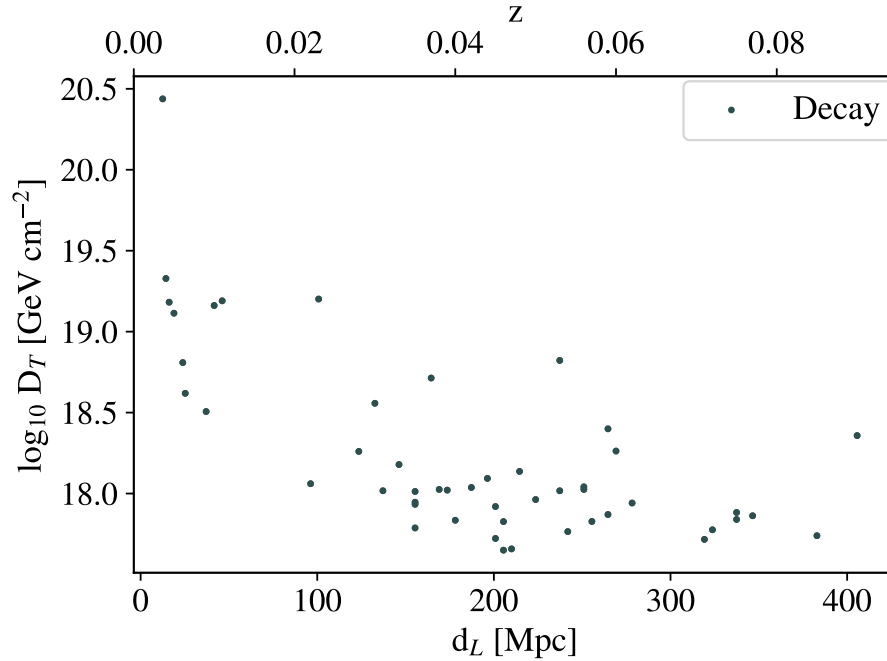
- Will reflect in different levels of contribution to the total J-factor

DM ANNIHILATION FLUXES OF THE SAMPLE



| Cluster | z | M_{200} [$10^{14} M_{\odot}$] | R_{200} [kpc] | θ_{200} [deg] | $\log_{10} J_{MIN}$ [$\text{GeV}^2 \text{cm}^{-5}$] | $\log_{10} J_{MED}$ [$\text{GeV}^2 \text{cm}^{-5}$] | $\log_{10} J_{MAX}$ [$\text{GeV}^2 \text{cm}^{-5}$] | $\log_{10} D$ [GeV cm^{-2}] |
|-----------------|--------|-----------------------------------|-----------------|----------------------|---|---|---|--|
| Virgo | 0.0036 | 5.60 | 1700 | 6.32 | 18.65 | 19.74 | 20.52 | 20.44 |
| NGC 4636 | 0.004 | 0.53 | 777 | 2.61 | 17.63 | 18.71 | 19.43 | 19.33 |
| M49 | 0.0044 | 0.46 | 741 | 2.26 | 17.49 | 18.57 | 19.28 | 19.18 |
| A1060-Hydra | 0.011 | 2.97 | 1376 | 1.70 | 17.43 | 18.51 | 19.27 | 19.19 |
| A1656-Coma | 0.023 | 13.16 | 2260 | 1.35 | 17.42 | 18.46 | 19.26 | 19.20 |
| NGC 1399-Fornax | 0.005 | 0.51 | 763 | 2.05 | 17.41 | 18.50 | 19.21 | 19.11 |
| A3526-Centaurus | 0.01 | 2.27 | 1258 | 1.70 | 17.41 | 18.49 | 19.25 | 19.16 |
| A754 | 0.053 | 25.00 | 2800 | 0.75 | 17.14 | 18.05 | 18.86 | 18.82 |
| NGC 5813 | 0.0064 | 0.27 | 620 | 1.31 | 16.96 | 18.03 | 18.72 | 18.62 |
| A3571 | 0.037 | 10.90 | 2123 | 0.80 | 16.95 | 17.97 | 18.77 | 18.71 |

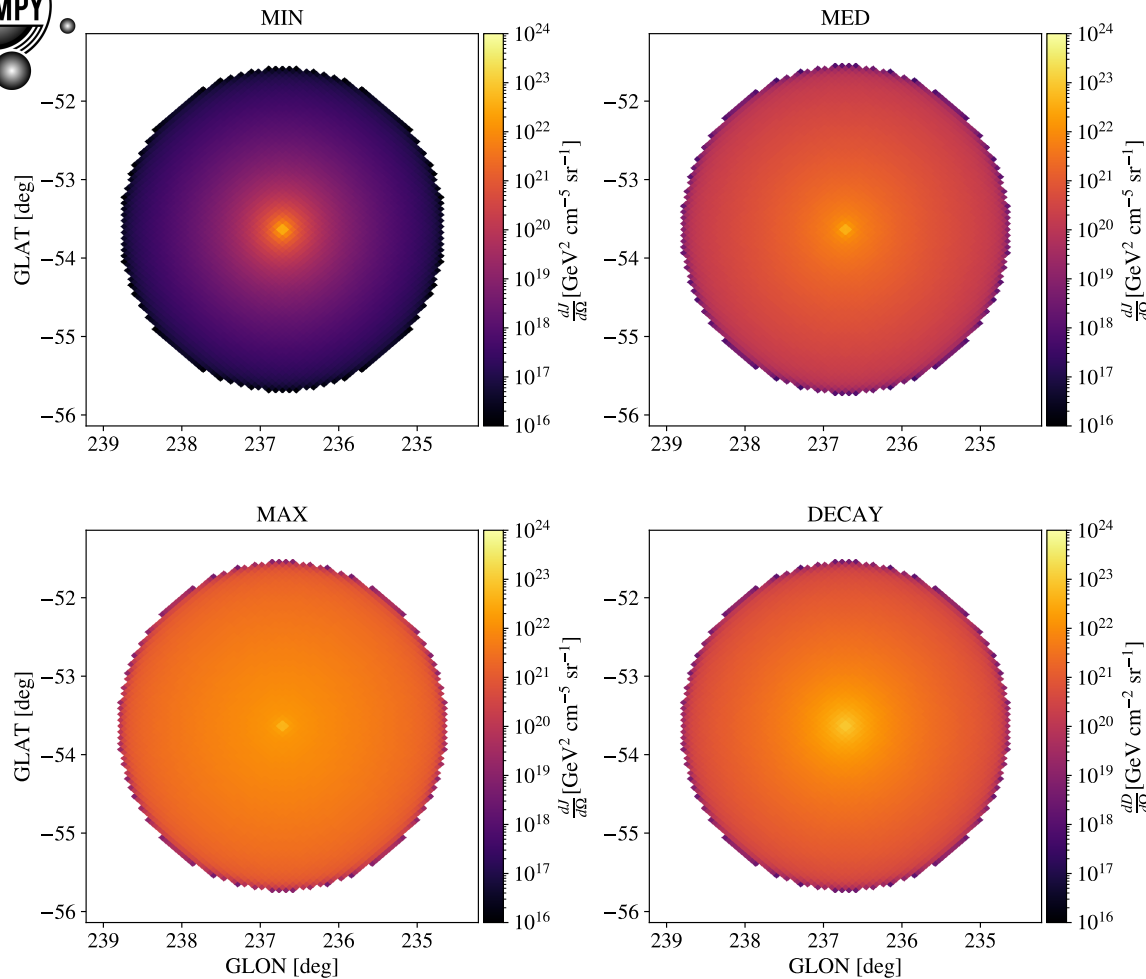
DM DECAY FLUXES OF THE SAMPLE



| Cluster | z | M_{200} [$10^{14} M_{\odot}$] | R_{200} [kpc] | θ_{200} [deg] | $\log_{10} J_{MIN}$ [GeV ² cm ⁻⁵] | $\log_{10} J_{MED}$ [GeV ² cm ⁻⁵] | $\log_{10} J_{MAX}$ [GeV ² cm ⁻⁵] | $\log_{10} D$ [GeV cm ⁻²] |
|-----------------|--------|-----------------------------------|-----------------|----------------------|--|--|--|---------------------------------------|
| Virgo | 0.0036 | 5.60 | 1700 | 6.32 | 18.65 | 19.74 | 20.52 | 20.44 |
| NGC 4636 | 0.004 | 0.53 | 777 | 2.61 | 17.63 | 18.71 | 19.43 | 19.33 |
| M49 | 0.0044 | 0.46 | 741 | 2.26 | 17.49 | 18.57 | 19.28 | 19.18 |
| A1060-Hydra | 0.011 | 2.97 | 1376 | 1.70 | 17.43 | 18.51 | 19.27 | 19.19 |
| A1656-Coma | 0.023 | 13.16 | 2260 | 1.35 | 17.42 | 18.46 | 19.26 | 19.20 |
| NGC 1399-Fornax | 0.005 | 0.51 | 763 | 2.05 | 17.41 | 18.50 | 19.21 | 19.11 |
| A3526-Centaurus | 0.01 | 2.27 | 1258 | 1.70 | 17.41 | 18.49 | 19.25 | 19.16 |
| A754 | 0.053 | 25.00 | 2800 | 0.75 | 17.14 | 18.05 | 18.86 | 18.82 |
| NGC 5813 | 0.0064 | 0.27 | 620 | 1.31 | 16.96 | 18.03 | 18.72 | 18.62 |
| A3571 | 0.037 | 10.90 | 2123 | 0.80 | 16.95 | 17.97 | 18.77 | 18.71 |

DM FLUXES OF THE SAMPLE

Example of skymaps of the differential J/D-factors for NGC 1399-Fornax



- Effects of substructure:
 - Most relevant in outskirts
 - Boost factor:

$$B = J^X / J^{\text{MIN}} - 1$$



$$B_{\text{MED}} = 11 \quad (B \sim 9 - \text{Moliné+17})$$

$$B_{\text{MAX}} = 60 \quad (B \sim 65 - \text{Moliné+17})$$

FERMI-LAT ANALYSIS SET-UP

Baseline set-up

| | |
|--|--------------------|
| Years of <i>Fermi</i> data | 12 |
| IRFs | P8R3_SOURCEVETO_V2 |
| Energy range [GeV] | 0.5 – 1000 |
| Bins per decade | 8 |
| Region of Interest (ROI) [deg ²] | 20 x 20 |
| Pixel size [deg] | 0.08 |
| Catalogue | 4FGL-DR2 |

- Standard template Fermi analysis
 - Combined likelihood:
- +
- $$\log(\mathcal{L}_j(\mu_\chi, \nu_j | \mathcal{D}_j)) = \sum_i \log(\mathcal{L}_{i,j}(\mu_\chi, \nu_{i,j} | \mathcal{D}_{i,j}))$$

$$TS = 2 \ln \frac{\mathcal{L}(\mu, \hat{\nu} | \mathcal{D})}{\mathcal{L}_{null}(\mu = 0, \hat{\nu} | \mathcal{D})}$$

- $TS < 25 \rightarrow$ No signal

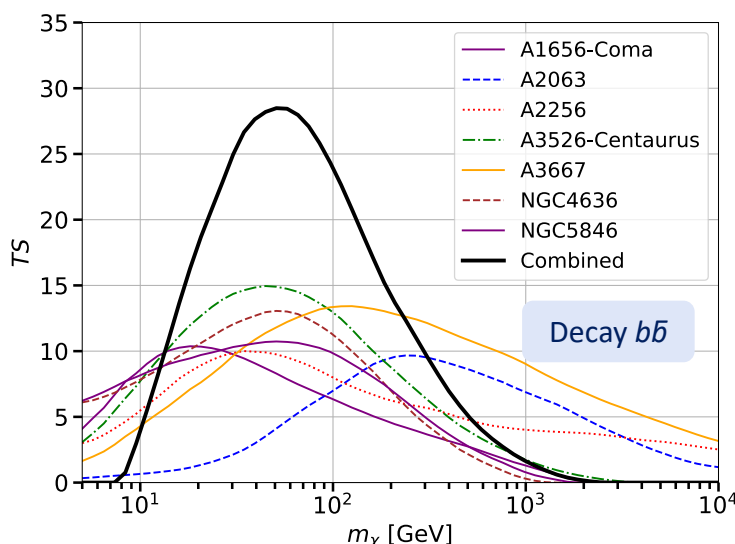
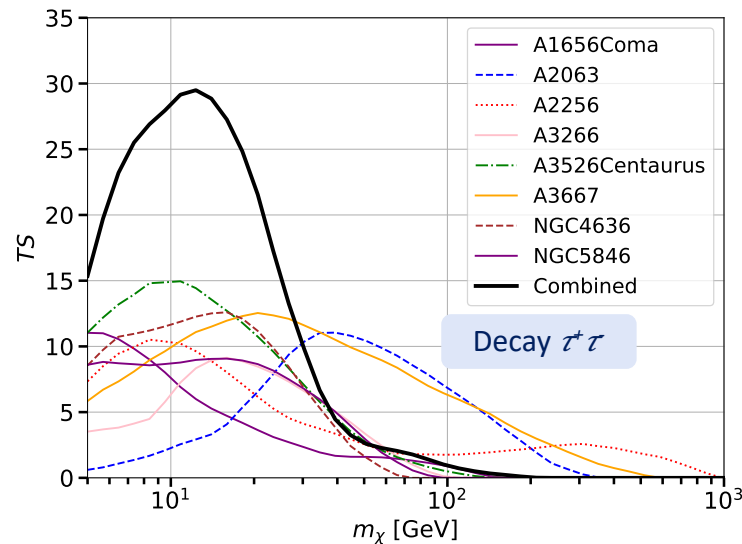
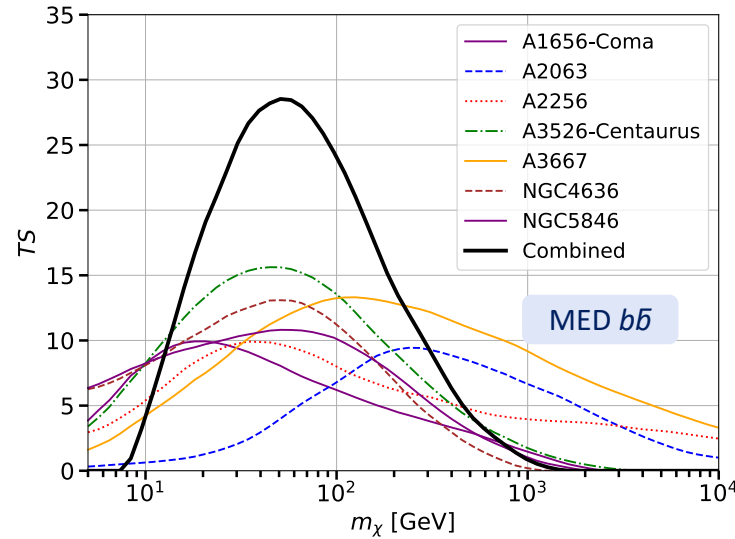
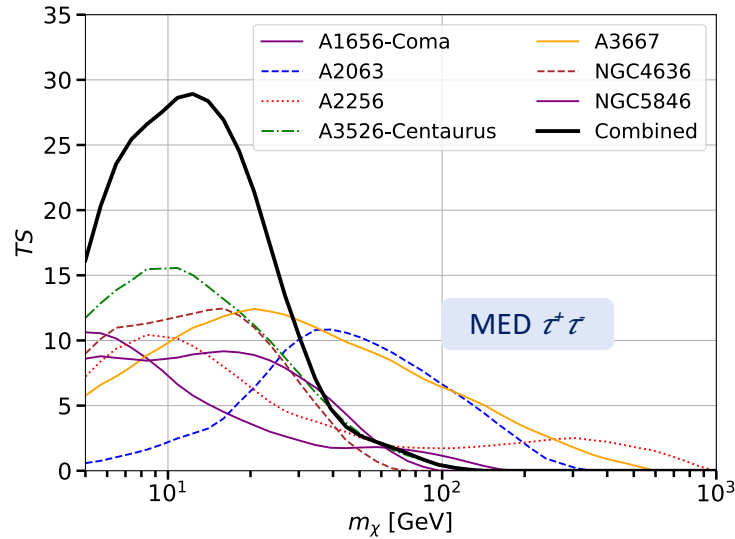
- Tested different set-ups for energy range, Region of Interest (ROI), IRFs and Background (BKG) models

- Background components:

- Individual point-sources from LAT (4FGL-DR2)
- Fermi bubbles
- Loop I + Sun + Moon
- Isotropic emission
- Galactic Interstellar Emission (IEM)

} Divided in: Bremsstrahlung + π^0 + Inverse Compton (CMB + starlight + Infrared)
Ackerman+17 [*Fermi Collab.*]

TS OF THE BENCHMARK MODELS



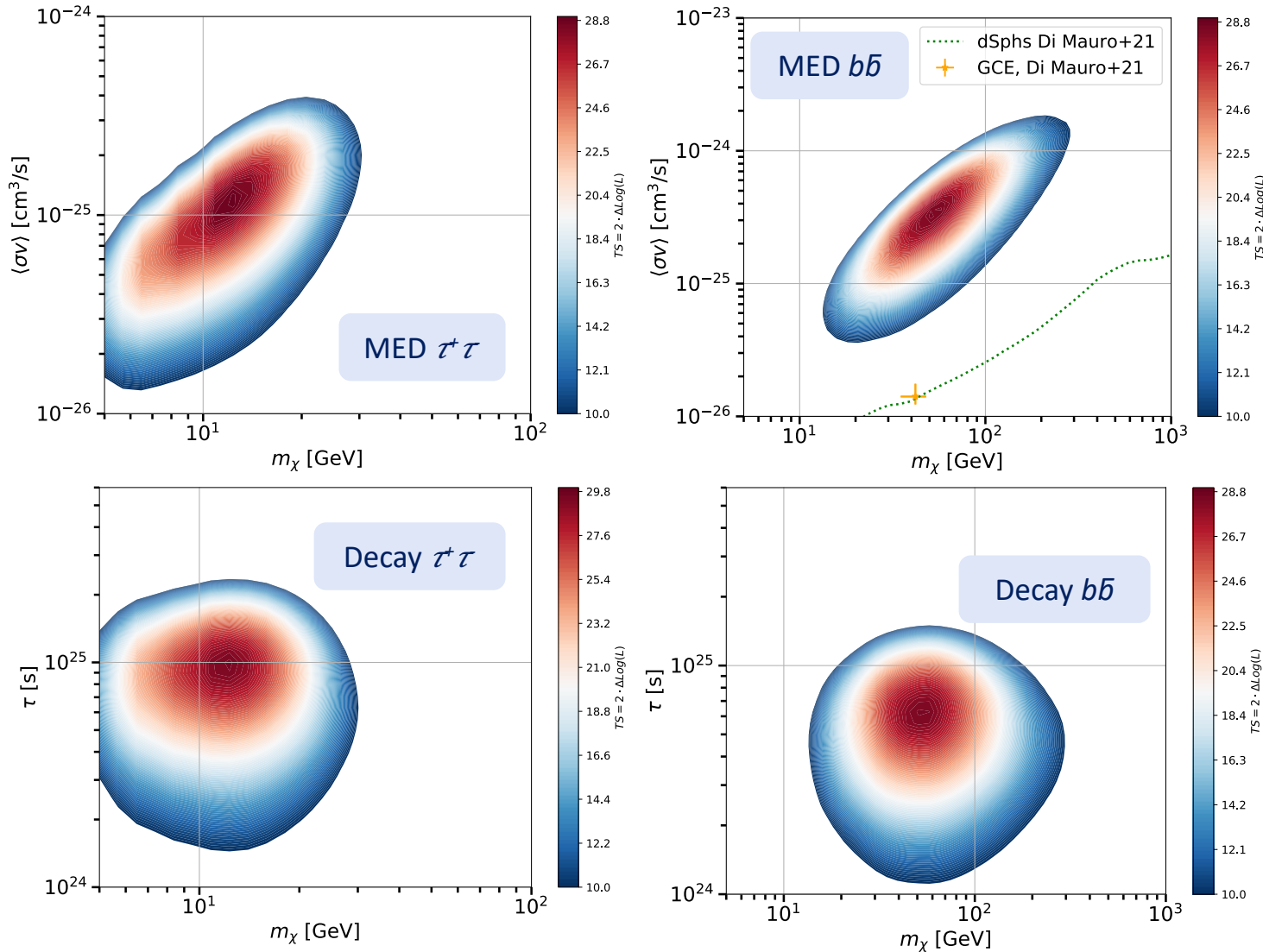
Individual TS

- Highest **A3526-Centaurus** – TS = 15
- A1656-Coma – TS ~10 (Ackermann+17 [Fermi Collab.]

Combined TS

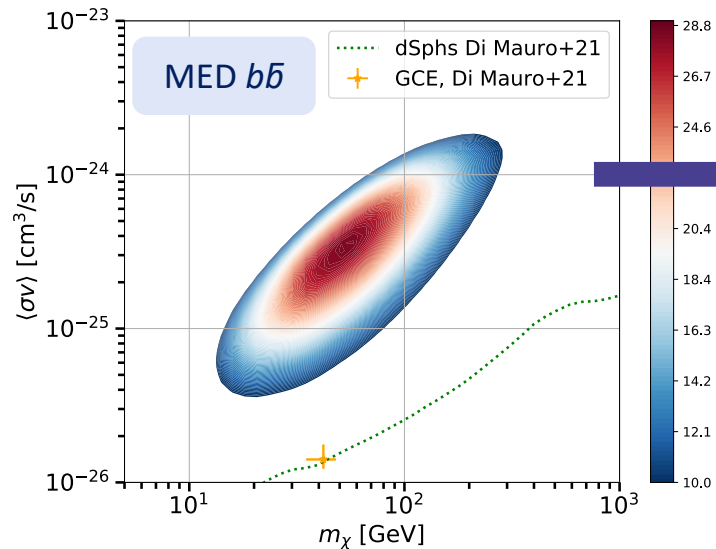
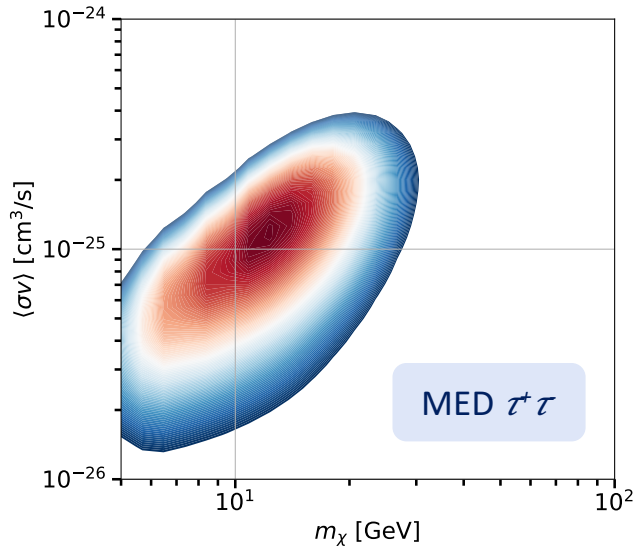
| | |
|-------|---------|
| MIN | No sig. |
| MED | TS = 27 |
| MAX | TS = 23 |
| DECAY | TS = 28 |

TS VALUES INTERPRETED AS DM

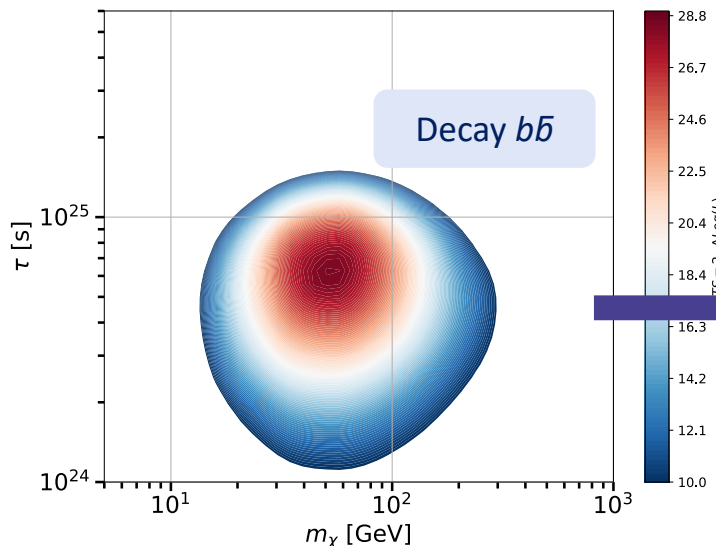
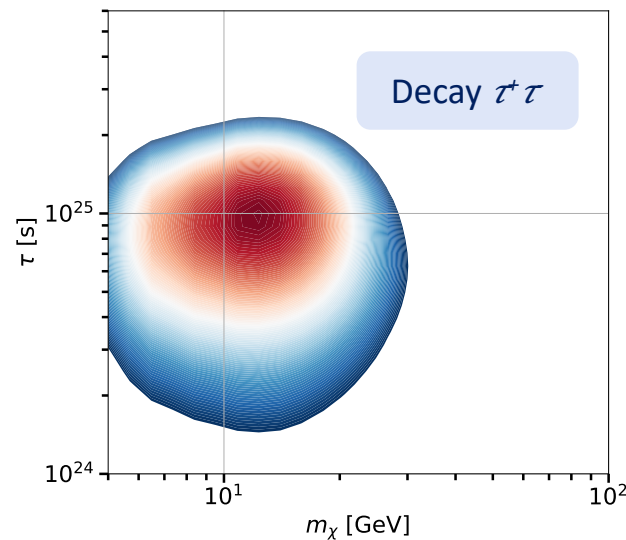


| | $b\bar{b}$ (40 - 60 GeV) | $\tau^+\tau^-$ (8-20 GeV) |
|-------|---|--|
| MED | $2-4 \times 10^{-25} \text{ cm}^3\text{s}^{-1}$ | $8-20 \times 10^{-26} \text{ cm}^3\text{s}^{-1}$ |
| MAX | $4-9 \times 10^{-26} \text{ cm}^3\text{s}^{-1}$ | $1-3 \times 10^{-26} \text{ cm}^3\text{s}^{-1}$ |
| DECAY | $5-8 \times 10^{24} \text{ s}$ | $8-12 \times 10^{24} \text{ s}$ |

TS VALUES INTERPRETED AS DM



- Not compatible with GC excess
- Ruled out by dSphs



- Ruled out by Isotropic γ -ray Background (IGRB) and GC
Blanco&Hooper18, Ando&Ishiwata15, Ackermann+12
[Fermi Collab.]

| | $b\bar{b}$ (40 - 60 GeV) | $\tau^+\tau^-$ (8-20 GeV) |
|-------|---|--|
| MED | $2-4 \times 10^{-25} \text{ cm}^3\text{s}^{-1}$ | $8-20 \times 10^{-26} \text{ cm}^3\text{s}^{-1}$ |
| MAX | $4-9 \times 10^{-26} \text{ cm}^3\text{s}^{-1}$ | $1-3 \times 10^{-26} \text{ cm}^3\text{s}^{-1}$ |
| DECAY | $5-8 \times 10^{24} \text{ s}$ | $8-12 \times 10^{24} \text{ s}$ |

NULL HYPOTHESIS FOR TS DISTRIBUTION

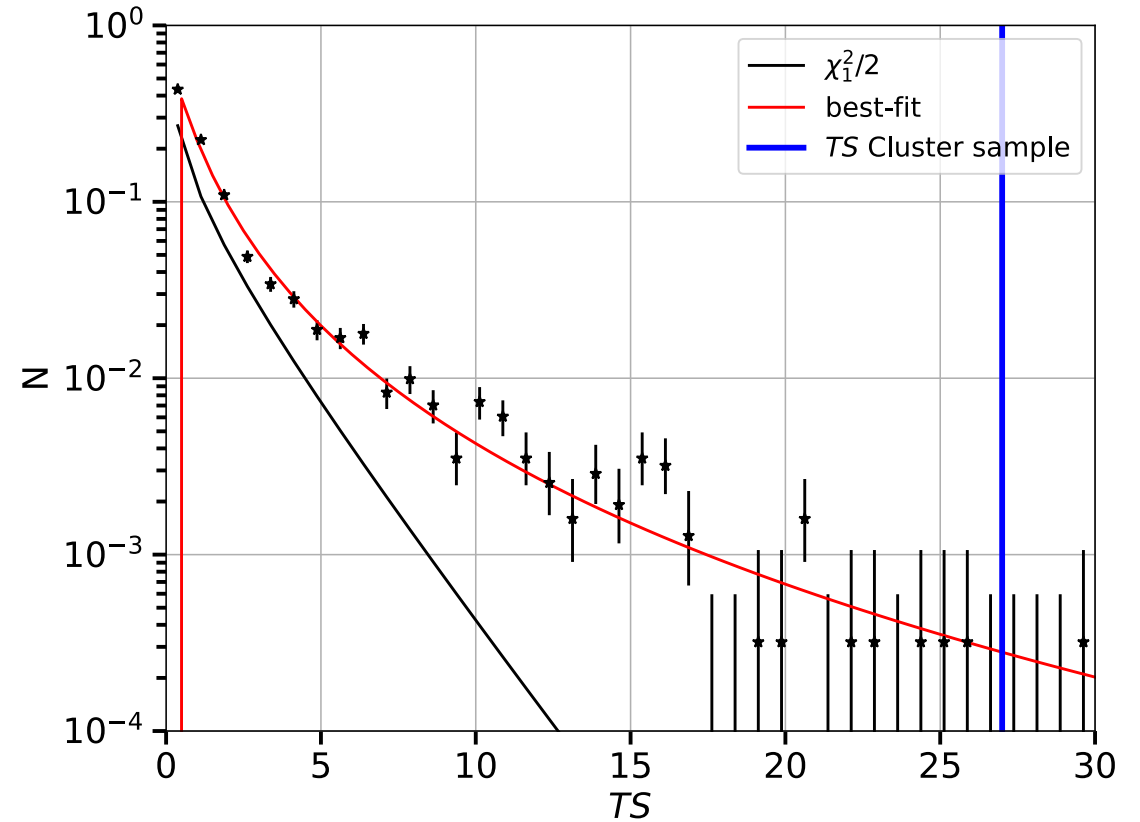
- Ideal knowledge of BKGs \longrightarrow TS distribution described as $\chi_2^2/2$ \longrightarrow BUT \longrightarrow Analysis of real data at low energies for extended sources
Chernoff 54

Analysis of real data at low energies for extended sources

- Build TS distribution using 3100 random blank sky directions
 - Remove directions with $|b| < 20$ deg
 - Farther than 2 deg from known sources
 - Limited to extension of sources and ROI
- For each ROI, fit MED DM template and $b\bar{b}$ annihilation for $m_\chi = 50$ GeV

$$N_{\text{norm}}(TS) = 0.22 \times (TS)^{-1.29 - 0.31 \log(TS/2.55)}$$

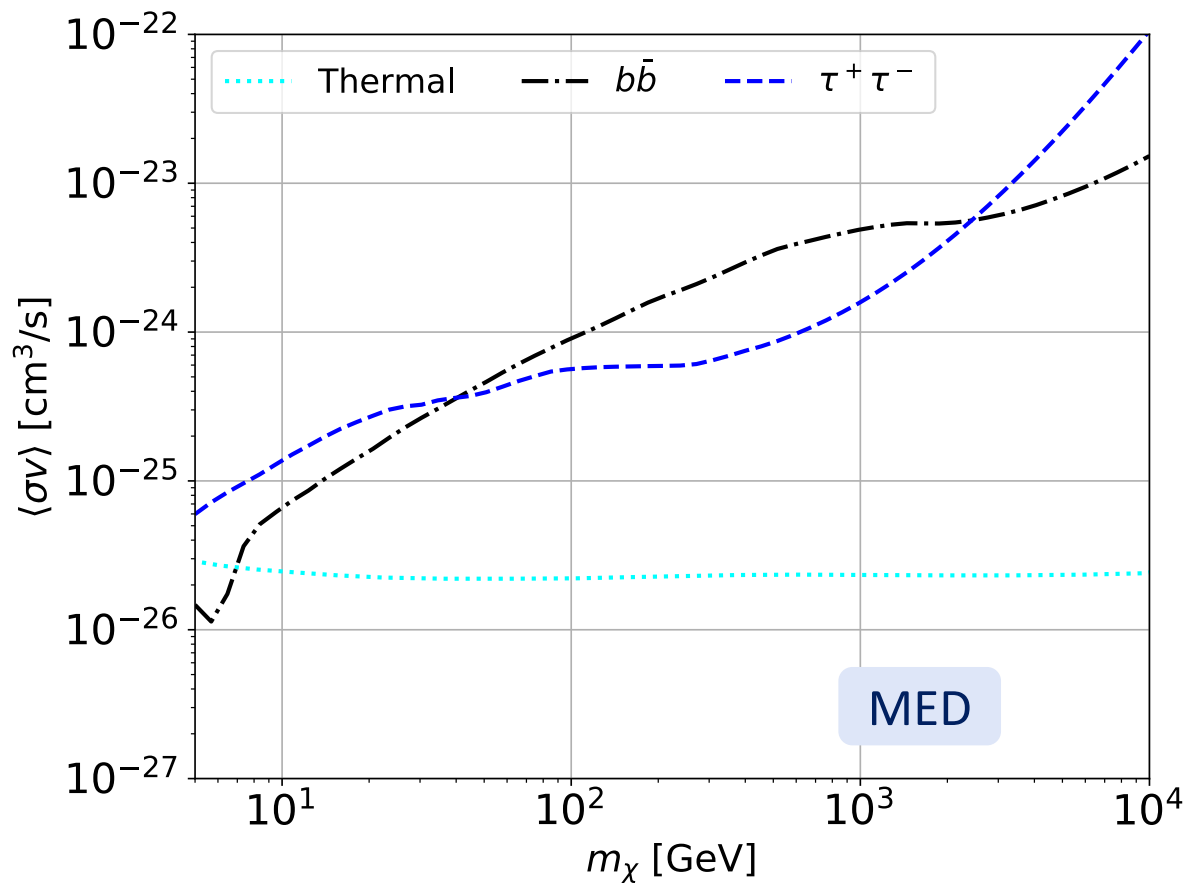
$TS = 27$ for MED \longrightarrow p -value = 3.1×10^{-3} \longrightarrow 2.7σ (local)



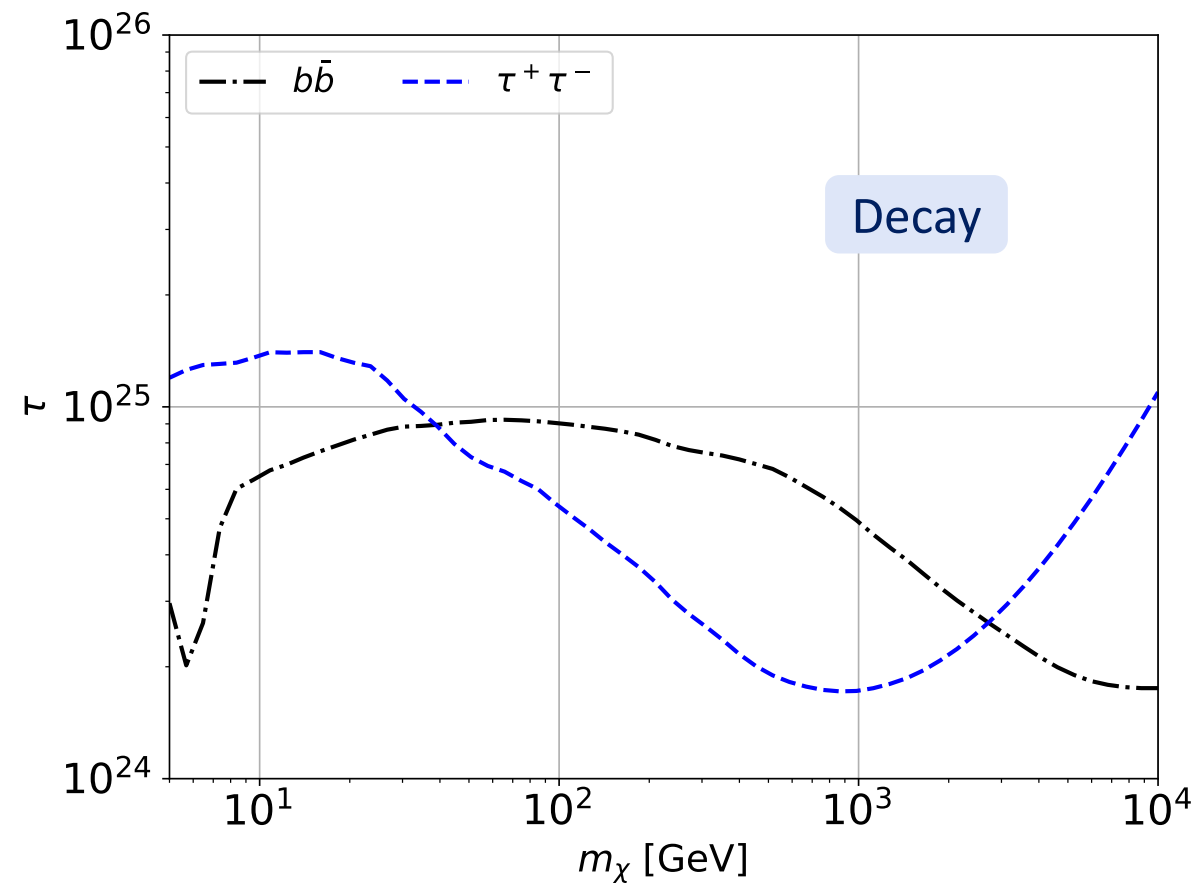
DM CONSTRAINTS FROM COMBINED CLUSTERS ANALYSIS

- The signal is not significant and if interpreted as DM, is not compatible with existing limits

- Annihilation 95% C.L Upper Limits



- Decay 95% C.L Lower Limits

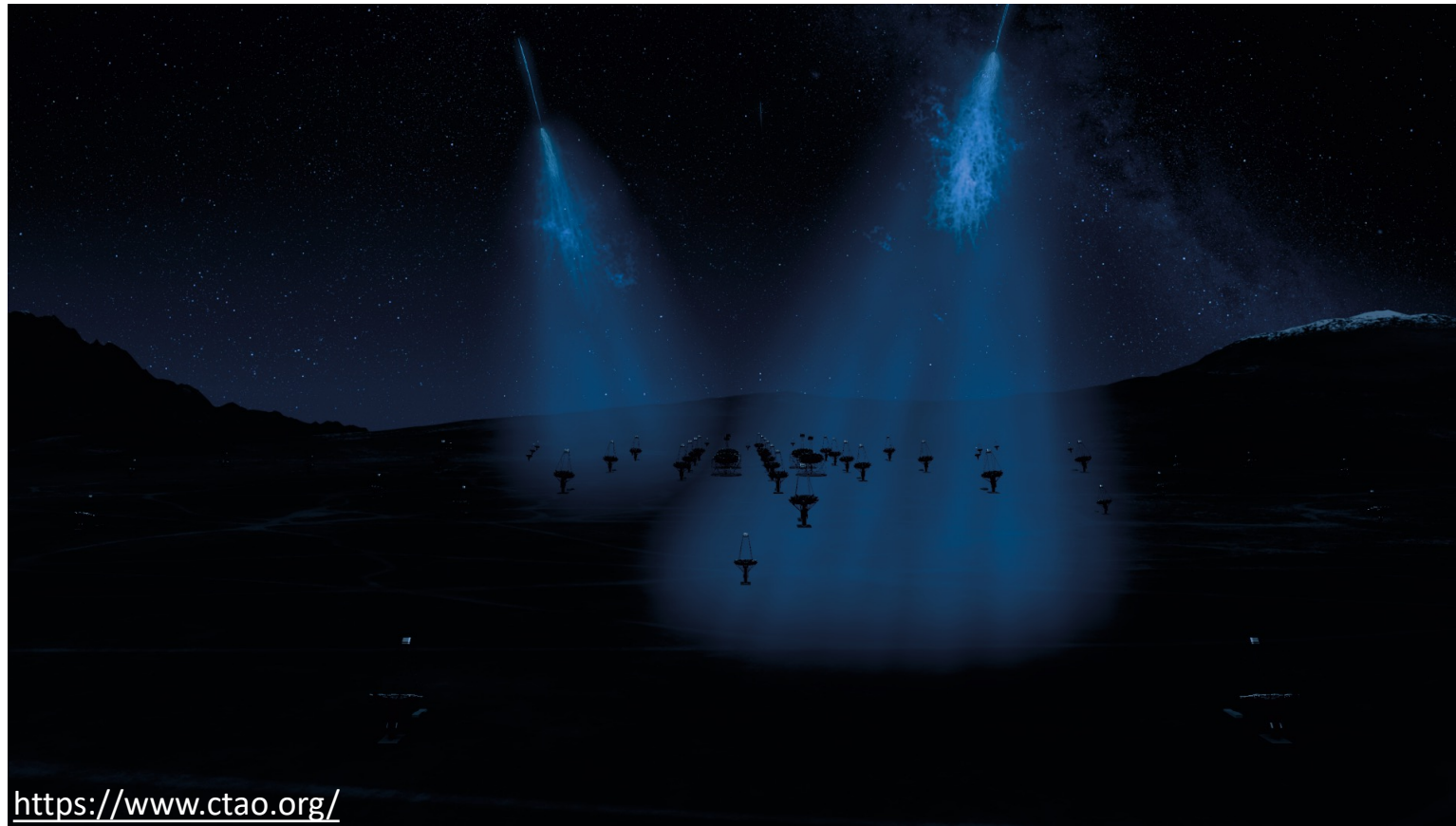


γ -RAY DM SEARCHES FROM THE PERSEUS CLUSTERS WITH CTAO

Prospects for gamma-ray observations of the Perseus galaxy cluster with the Cherenkov Telescope Array

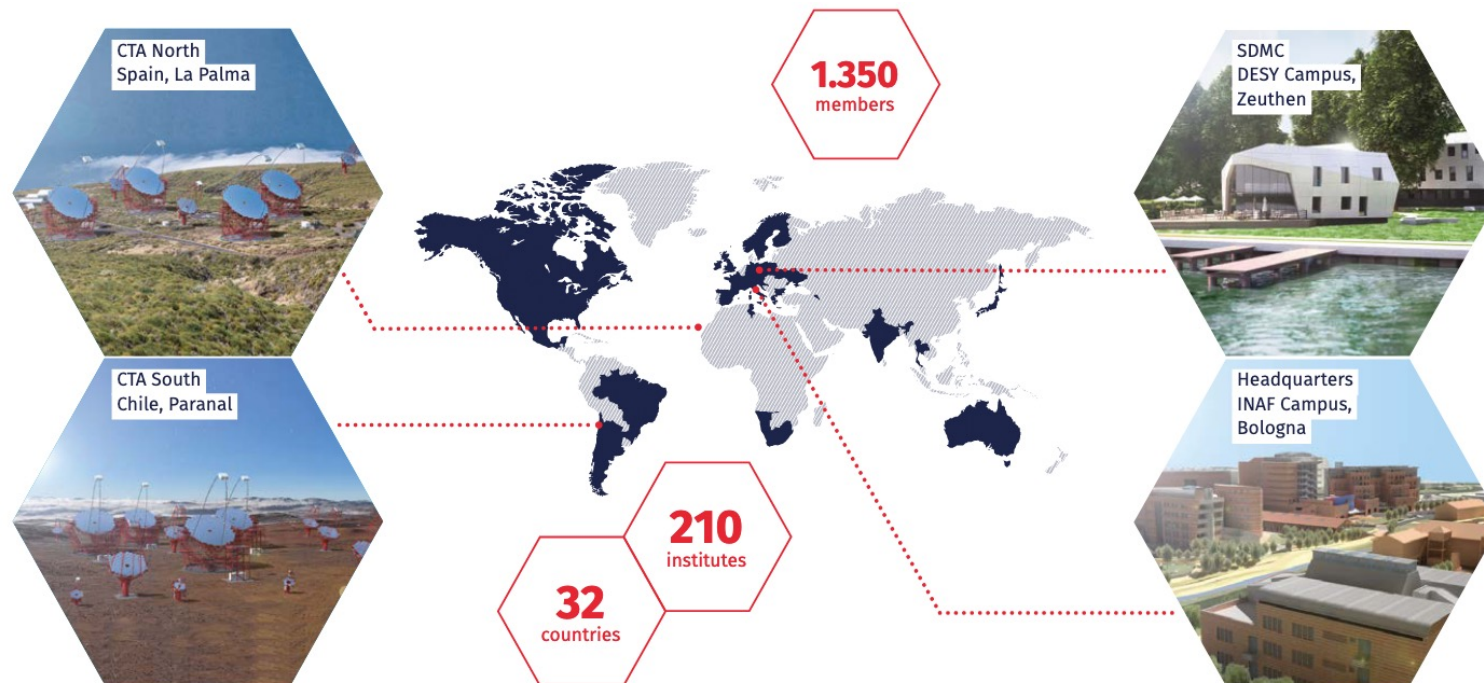
The CTAO Consortium (corresponding authors - alphabetical: R. Adam, M. Hütten, JPR, M. A. Sánchez-Conde, S. Hernández Cadena)

Submitted to JCAP, [[arXiv:2309.03712](https://arxiv.org/abs/2309.03712)]



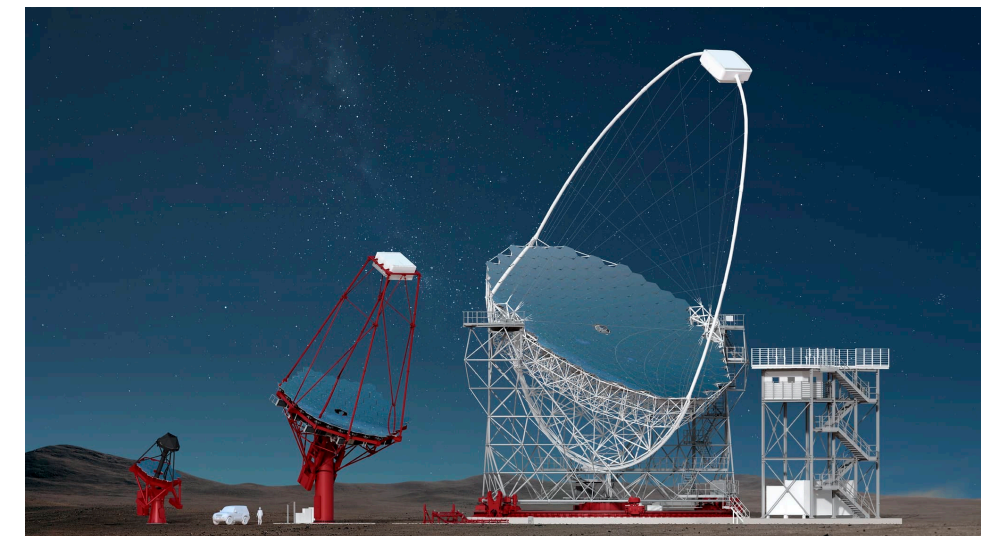
THE CHERENKOV TELESCOPE ARRAY OBSERVATORY (CTAO)

- Future of Imaging Atmospheric Cherenkov Telescopes for very-high-energy (VHE) γ -ray astronomy
- 2 arrays: Northern Array (La Palma, Spain) and Southern Array (Paranal, Chile)
- First telescope already operating



<https://www.ctao.org/>

Energy range 20 GeV - 300 TeV



SST

5 - 300 TeV

$D_{\phi} = 4.3\text{m}$

MST

150 GeV - 5 TeV

$D_{\phi} = 11.5\text{m}$

LST

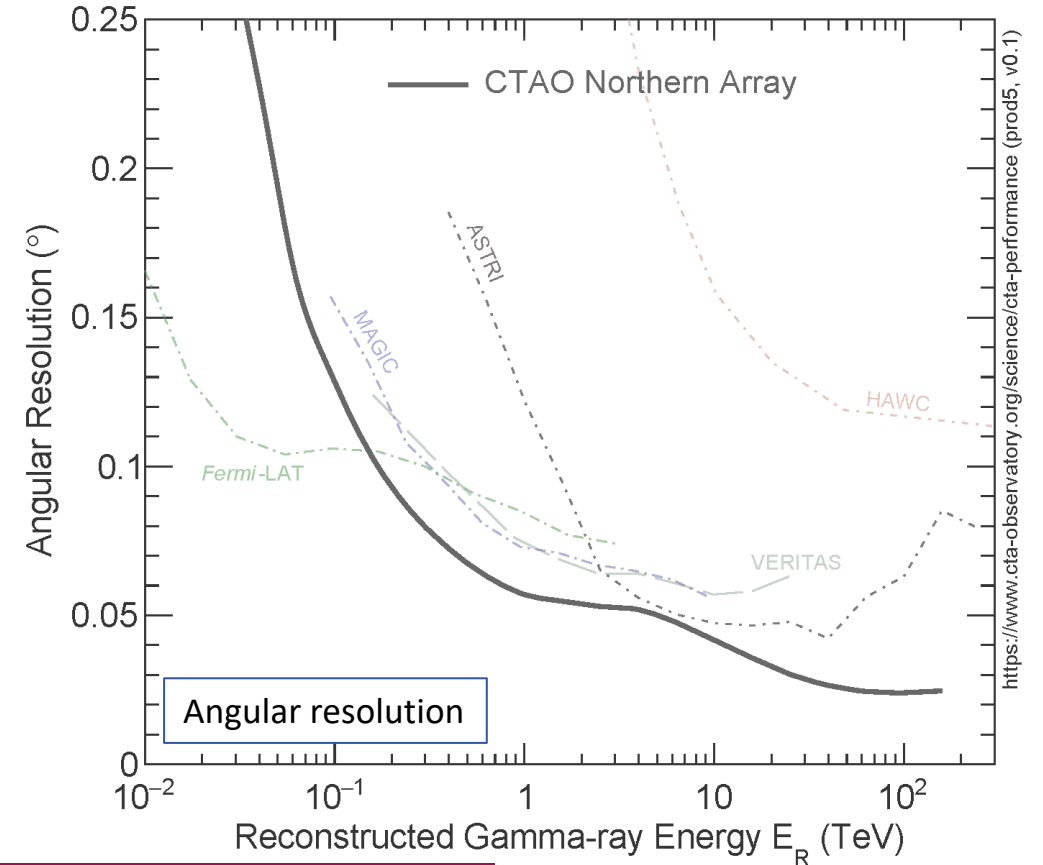
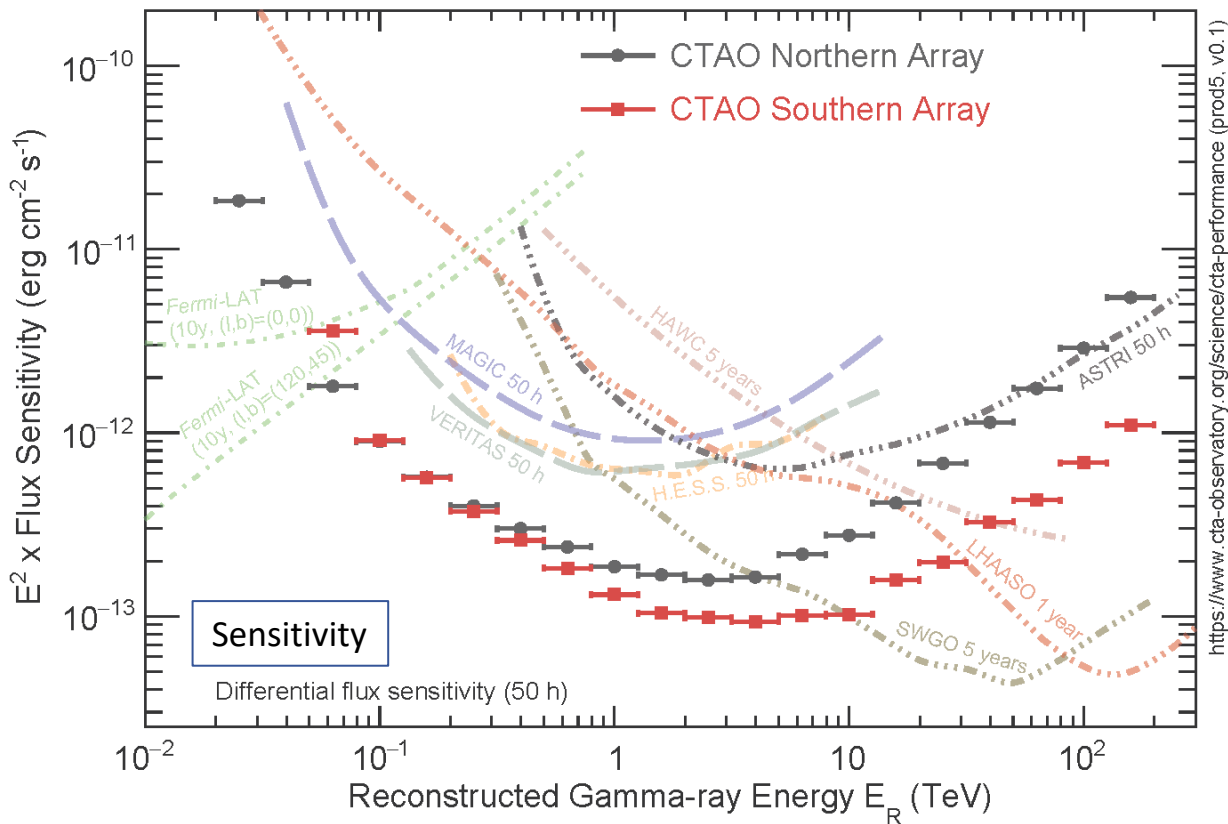
20 - 150 GeV

$D_{\phi} = 23\text{m}$

CTAO PERFORMANCE

Preliminary Performance Capabilities

<https://www.ctao.org/>



CTAO will have superb capabilities for DM γ -ray searches

PERSEUS GALAXY CLUSTER WITH CTAO: A KEY SCIENCE PROJECT

- Among local clusters, Perseus is the brightest in X-ray sky

- Cool-cored, relaxed cluster

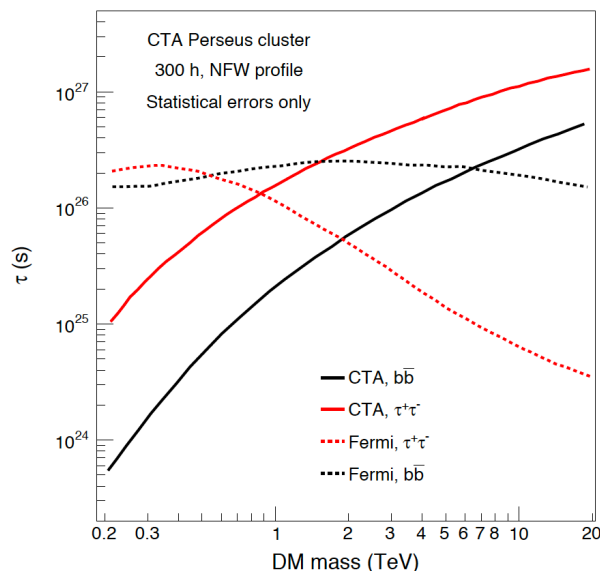
| Object | l [deg] | b [deg] | d_L [Mpc] |
|---------|-----------|-----------|-------------|
| Perseus | 150.57 | -13.26 | 75.01 |

- Hosts two Active Galactic Nuclei (AGN), both variable

| Object | l [deg] | b [deg] |
|---------|-----------|-----------|
| NGC1275 | 150.58 | -13.26 |
| IC310 | 150.18 | -13.74 |

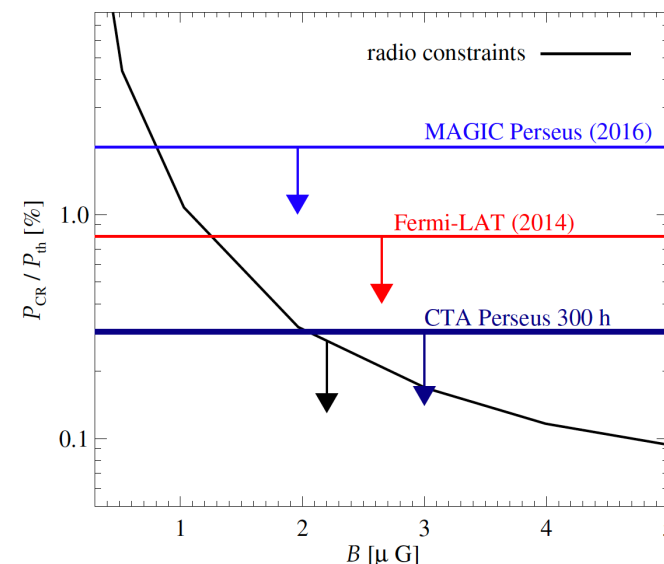
NGC 1275 aligned with X-rays centre

Optimal conditions for observation from the northern array



Prospects of constraints for DM decay

Acharya+17
[CTAO Cons.]



Prospects of constraints for CR models

We use the latest version of the CTAO science tools with the latest IRFs to perform the analysis

PERSEUS DM MODELLING

- Follow similar strategy:
 - I. Model de main halo;
 - II. Model de substructure population defining benchmark models

$$\langle \rho_{\text{tot}} \rangle(r) = \rho_{\text{sm}}(r) + \langle \rho_{\text{subs}} \rangle(r)$$

ρ_{sm} \rightarrow $\rho(r) = \frac{\rho_0}{\left(\frac{r}{r_s}\right) \left(1 + \frac{r}{r_s}\right)^2}$ (NFW) $+$ $(c_{200} - M_{200})$ (Sánchez-Conde & Prada 14)

Navarro+96, Navarro+97

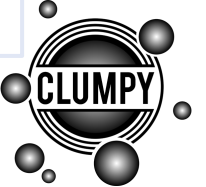
$$\langle \rho_{\text{subs}} \rangle$$

$$\frac{d^3 N}{dV dM dc} = N_{\text{tot}} \frac{d\mathcal{P}_V}{dV}(r) \cdot \frac{d\mathcal{P}_M}{dM}(M) \cdot \frac{d\mathcal{P}_c}{dc}(M, c)$$

- MIN** \rightarrow No substructure considered
- MED** \rightarrow Best guess according to most recent results
- MAX** \rightarrow Educated upper bound

$$J(l.o.s, \Delta\Omega, z) = \int_{\Delta\Omega} \int_{l.o.s} \rho_{DM}^2(r) dr$$

$$D(l.o.s, \Delta\Omega, z) = \int_{\Delta\Omega} \int_{l.o.s} \rho_{DM}(r) dr$$



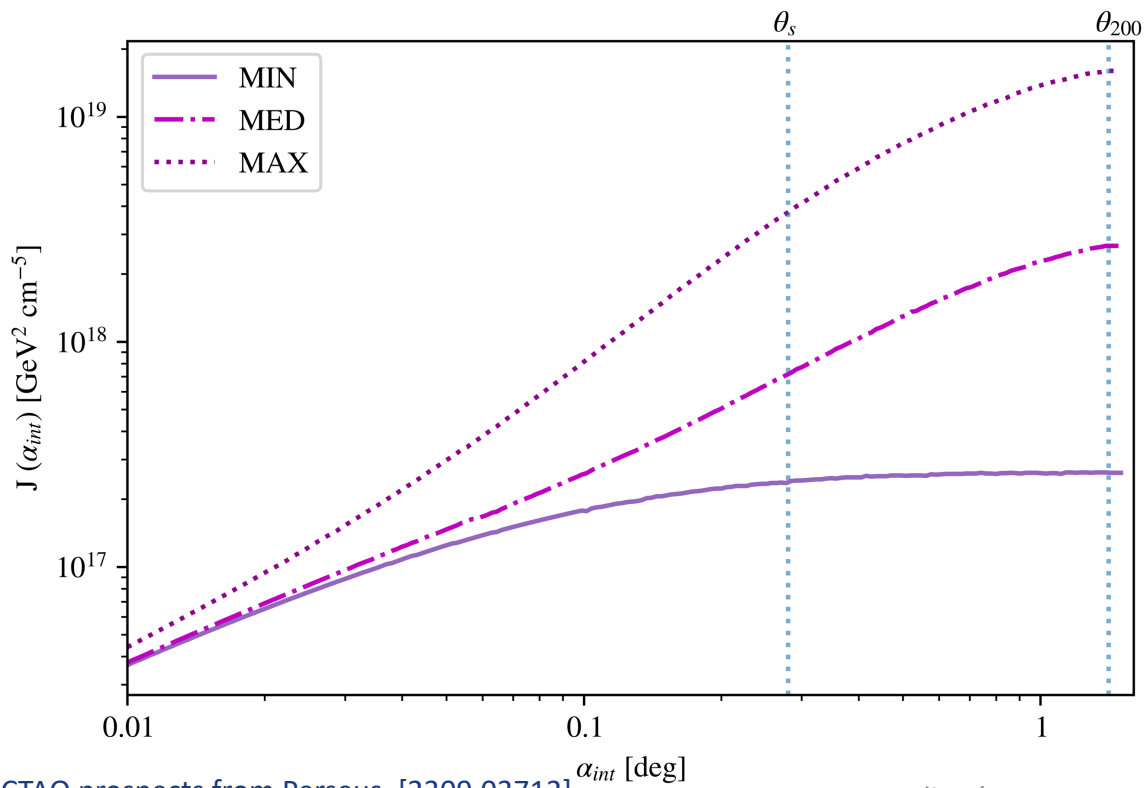
Benchmark models

| Model | SRD | $(c - M)_{sub}$ | α | f_{sub} | M_{min} |
|-------|--|------------------|----------|-----------|---------------------|
| MIN | - | - | - | 0 | - |
| MED | <i>Antibiased</i> VL-II (<i>Diemand+08</i>) | <i>Moliné+17</i> | 1.9 | 0.182 | $10^{-6} M_{\odot}$ |
| MAX | <i>Antibiased</i> VL-II (<i>Diemand+08</i>) | <i>Moliné+17</i> | 2.0 | 0.319 | $10^{-6} M_{\odot}$ |

EXPECTED PERSEUS DM SIGNAL

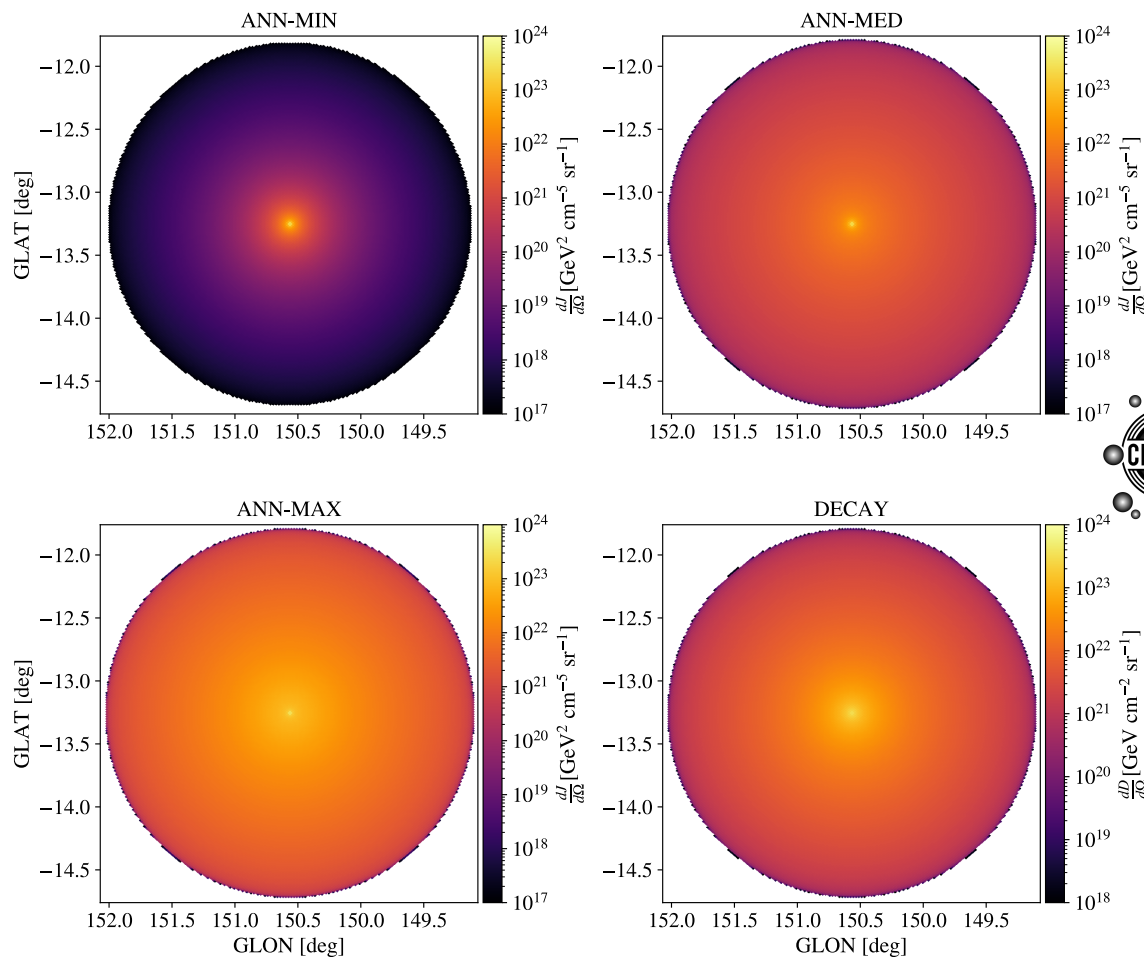
- Accumulated annihilation flux profile

| Annihilation | $\log_{10} J$ [$\text{GeV}^2 \text{cm}^{-5}$] |
|--------------|---|
| MIN | 17.42 |
| MED | 18.43 |
| MAX | 19.20 |
| Decay | $\log_{10} D$ [GeV cm^{-2}] |
| | 19.20 |



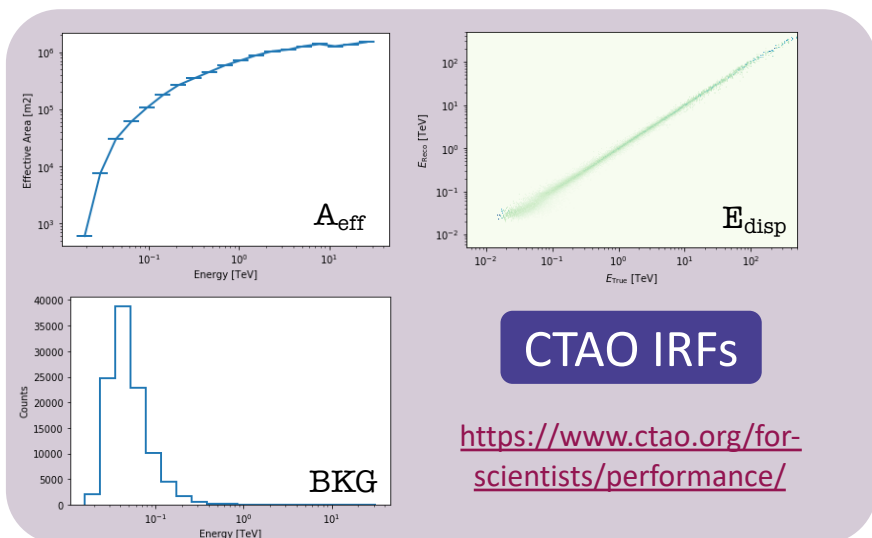
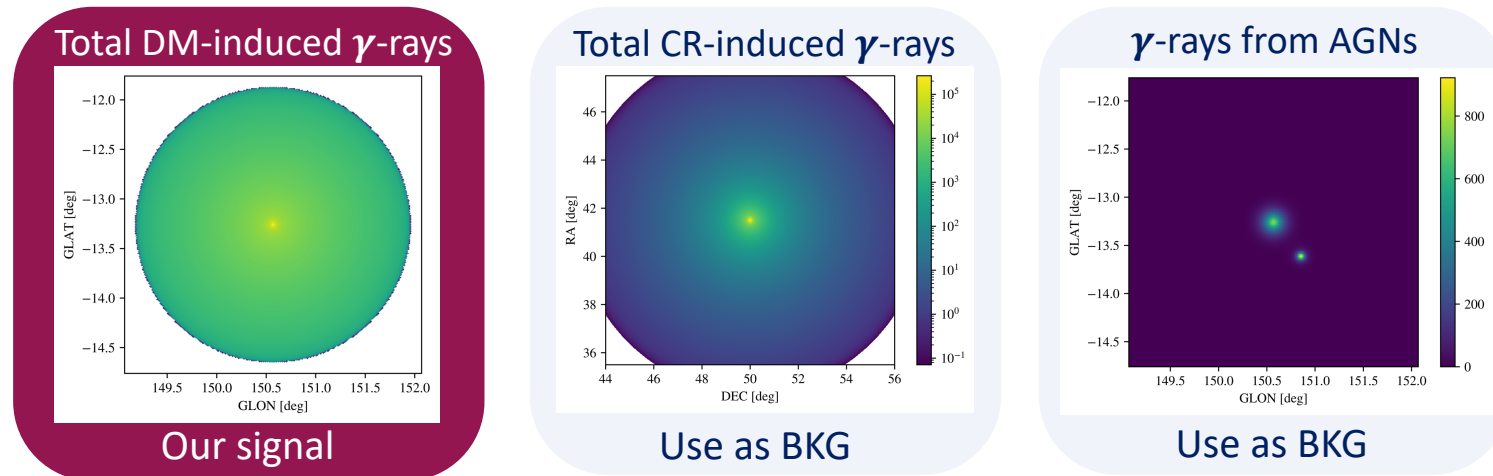
- Skymaps of the differential J/D-factors

$B_{\text{MED}} = 9$ ($B \sim 9$ – Moliné+17)
 $B_{\text{MAX}} = 59$ ($B \sim 72$ – Moliné+17)



CTAO DM ANALYSIS ROADMAP

- Different γ -ray sources in Perseus region:



Observation Simulation

If no signal found

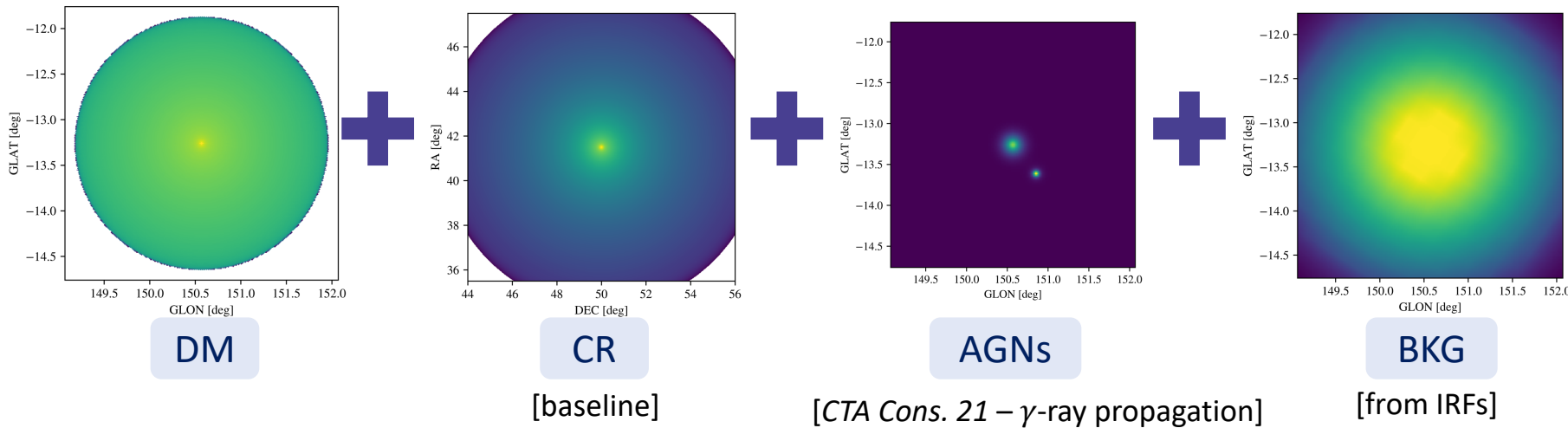
Constraints on DM models

$$\frac{d\Phi_{\chi}^{Ann}}{dE} = \frac{\langle \sigma v \rangle}{8\pi m_{\chi}^2} \frac{dN}{dE} \times J$$

$$\frac{d\Phi_{\chi}^{Decay}}{dE} = \frac{1}{4\pi m_{\chi} \tau_{\chi}} \frac{dN}{dE} \times D$$

CTAO ANALYSIS CONFIGURATION: TEMPLATE FITTING

- Includes all expected γ -ray sources: DM + CRs + AGNs + BKG IRFs



Most realistic physical scenario

- Fitting 8 parameters in total

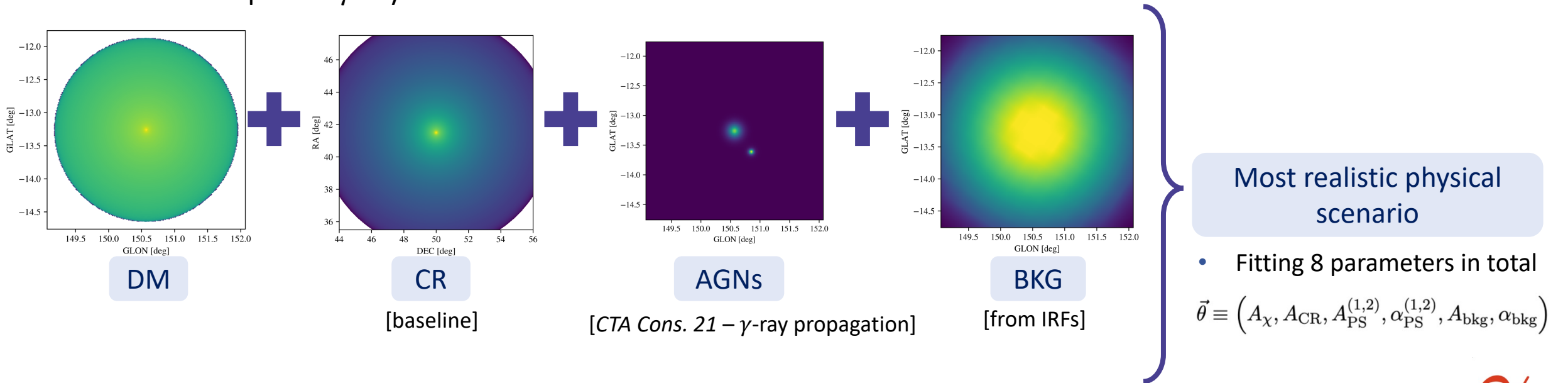
$$\vec{\theta} \equiv (A_{\chi}, A_{\text{CR}}, A_{\text{PS}}^{(1,2)}, \alpha_{\text{PS}}^{(1,2)}, A_{\text{bkg}}, \alpha_{\text{bkg}})$$

- Considers the different morphologies of each emission
- Allows to check correlations between components
- Historically used in *Fermi*-LAT analysis and in a recent CTAO analysis (*Acharyya+20* [CTA Cons.]])

State-of-the-art analysis pipeline

CTAO ANALYSIS CONFIGURATION: TEMPLATE FITTING

- Includes all expected γ -ray sources: DM + CRs + AGNs + BKG IRFs



- Use likelihood ratio test to fit the models to the simulated data:

$$\ln \mathcal{L}(\vec{\theta} | D) = \sum_i \tilde{M}_i(\vec{\theta}) - d_i \ln(\tilde{M}_i(\vec{\theta}))$$

Poissonian likelihood for each parameter

$$TS = 2 \log \left[\frac{\mathcal{L}(A_\chi, \hat{\nu})}{\mathcal{L}_{\text{null}}(A_\chi = 0, \hat{\nu})} \right]$$

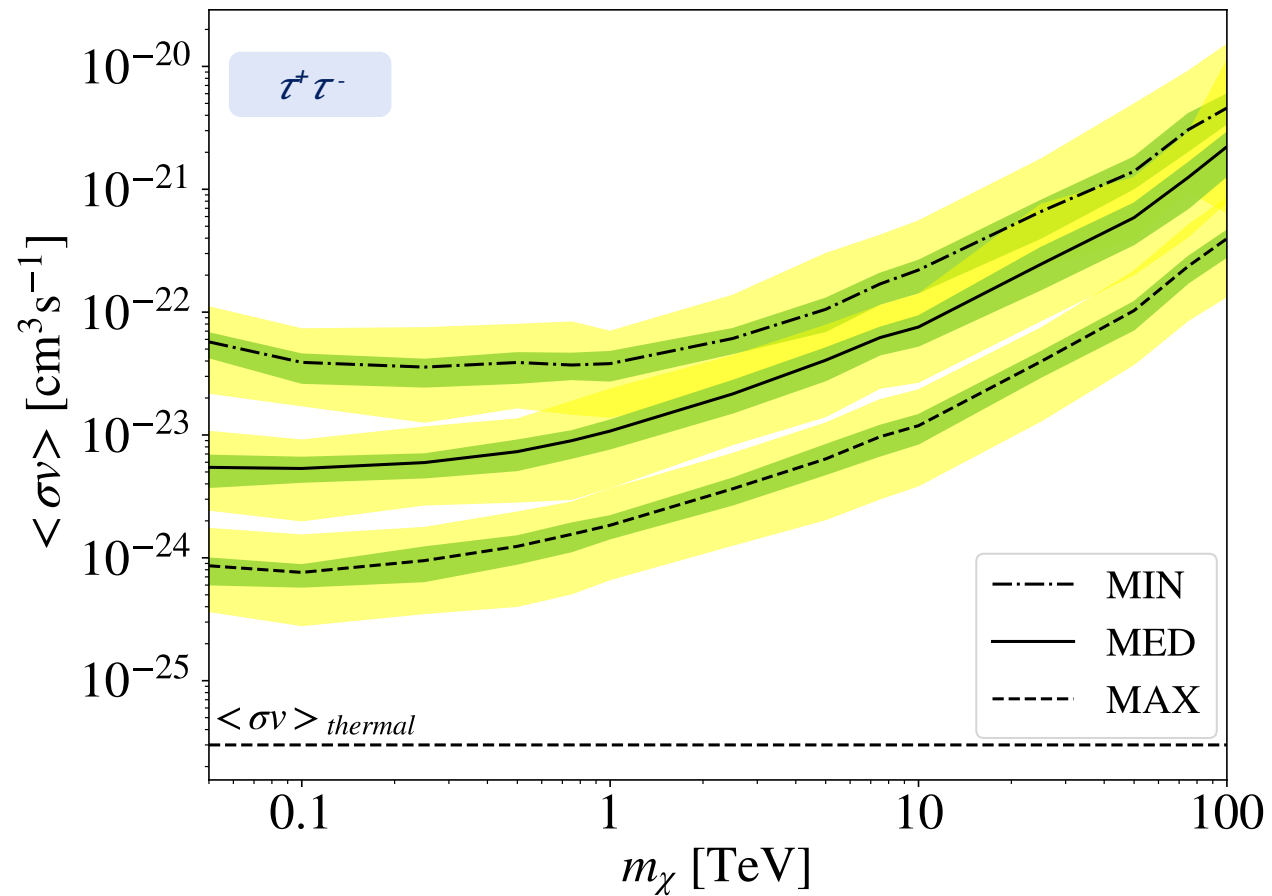
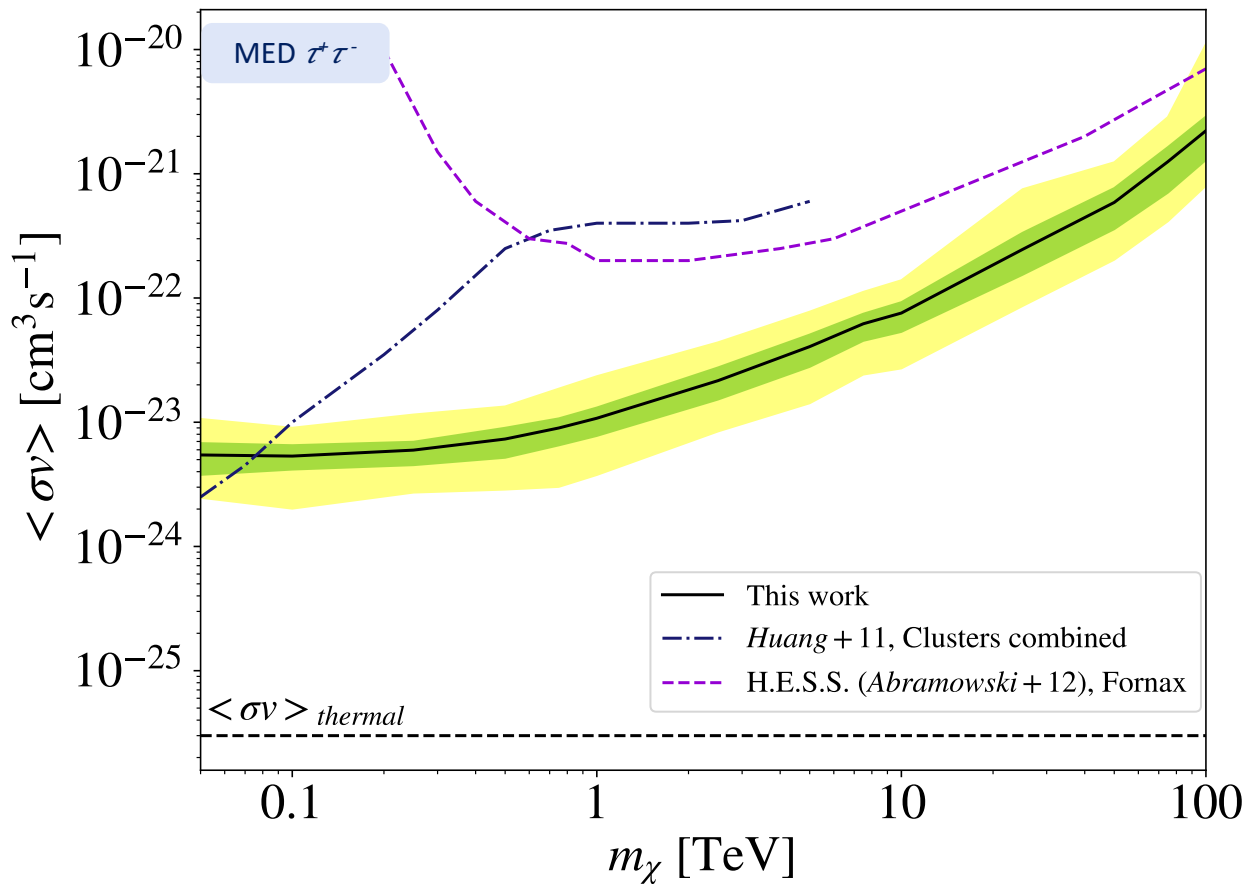
➡ No signal

Donath+23
<https://gammapy.org/> $\gamma\pi$

| | |
|--------------------|----------------------|
| N_{obs} | 100 |
| T_{obs} [h] | 300 |
| IRFs | North_z20_50h, prod5 |
| Energy range [TeV] | 0.03 - 100 |

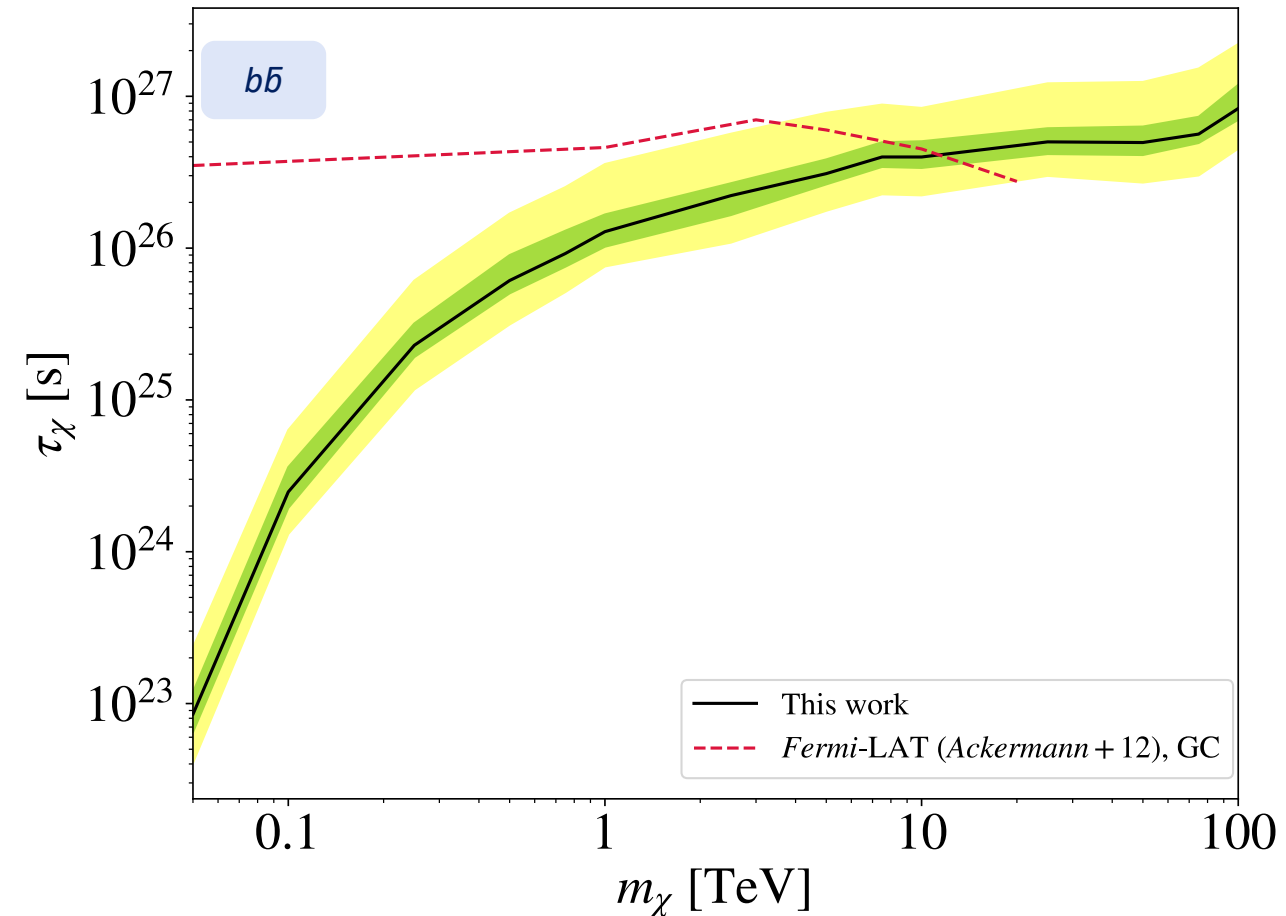
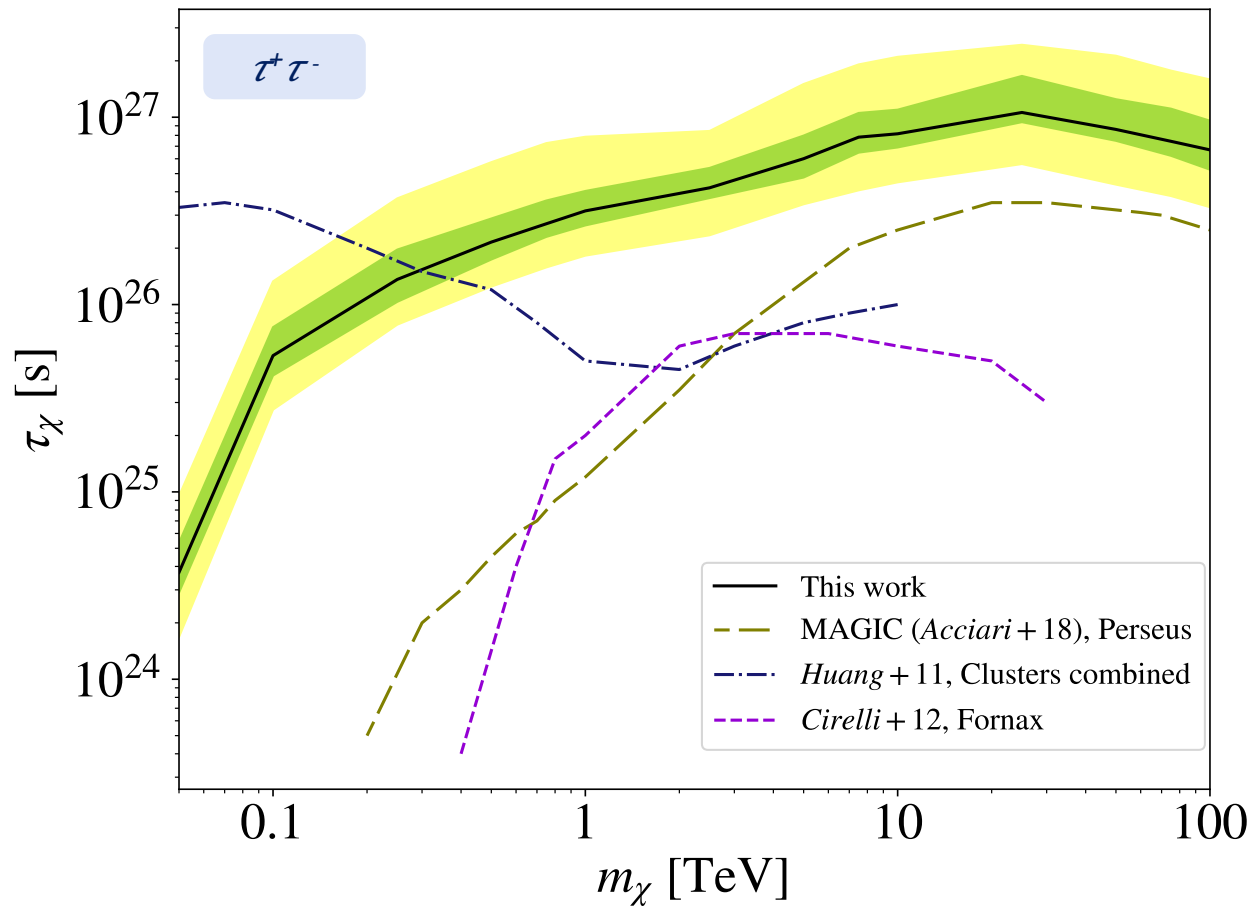
CTAO ANALYSIS: DM PROSPECTS FOR CONSTRAINTS

Annihilation 95% C.L Upper Limits



CTAO ANALYSIS: DM PROSPECTS FOR CONSTRAINTS

Decay 95% C.L. Lower Limits

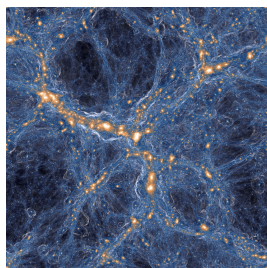


SUMMARY AND CONCLUSIONS

- We have focused on searching for WIMPs through the γ -ray channel
- Galaxy clusters are among the best targets to search for DM-induced γ -ray emission
 - Construction of the sample of best galaxy clusters to search for DM in γ -rays with state-of-the-art modelling of subhalo population
 - Template-fitting analysis using 12 years of LAT data with combined likelihood
 - “Signal” from combined analysis at $m_\chi \sim O(10)$ GeV with $\langle\sigma v\rangle \sim 10^{-25}-10^{-26} \text{cm}^3 \text{s}^{-1}$ or $\tau_\chi \sim 10^{24}$ s
 - Significance $2.5 - 3\sigma$ (pre-trials), uncertain origin
- State-of-the-art DM modelling for Perseus: Decay & Annihilation + subhalo population through benchmark models
- Simulations of CTAO observations: CRs + NGC 1275 + IC 310 + BKG IRFs
- State of the art use of template fitting analysis in IACTs
- DM annihilation: Most constraining results from cluster searches
- DM decay: Most constraining results in the literature

Present: *Fermi*-LAT

Future: CTAO





Thanks for your attention



BACK UP MATERIAL

STRUCTURE FORMATION IN Λ CDM

- **Cosmological principle**

- Isotropy
- Homogeneity

- **Components of the Universe**
- **Metric**



Friedman Equations

$$H^2(a) = H_0^2 (\Omega_{r,0}(1+z)^4 + \Omega_{m,0}(1+z)^3 + \Omega_{k,0}(1+z)^2 + \Omega_{\Lambda,0})$$

BUT



Need inhomogeneities to form structures

- **Inflation**

- Seeds of perturbation in the field
- Create curvature perturbation
- Matter falls, creating **density perturbations**

$$\delta(\vec{x}, t) = \frac{\rho(\vec{x}, t) - \bar{\rho}(t)}{\bar{\rho}(t)}$$

If $\delta \ll 1$

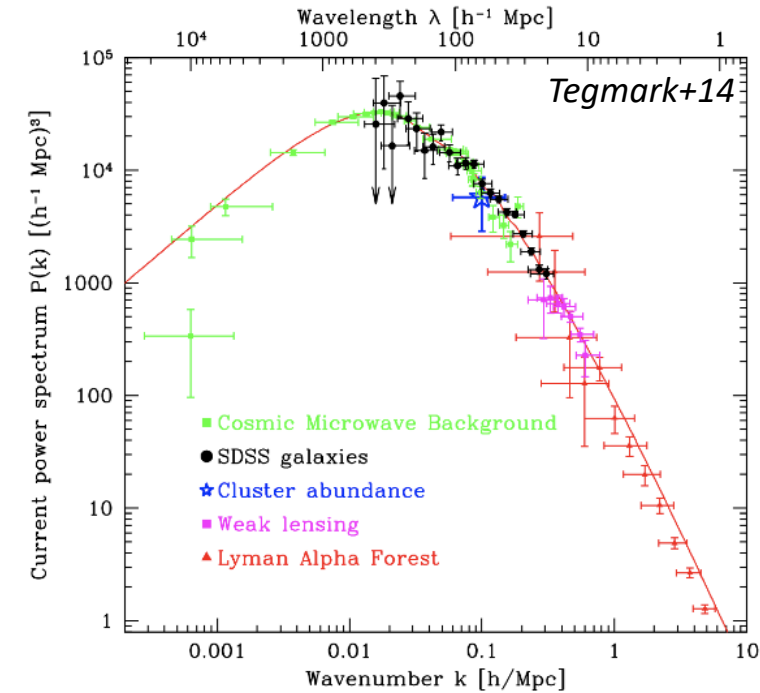
Linear perturbation theory

CDM

Halos and subhalos

Matter power spectrum

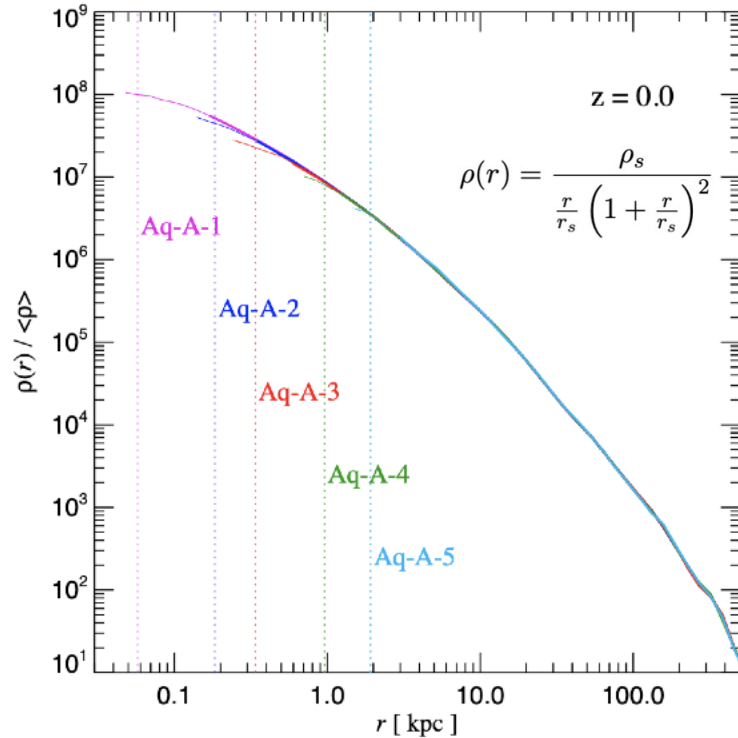
- dominant component is collisionless, non-relativistic dark matter
- gathers gravitationally on small scales
- seeds of larger structures by hierarchical clustering



HALO AND SUBHALO PROPERTIES

Main halos

- Fundamental non-linear units of cosmic structures
- Inner density profile



- Mass distribution

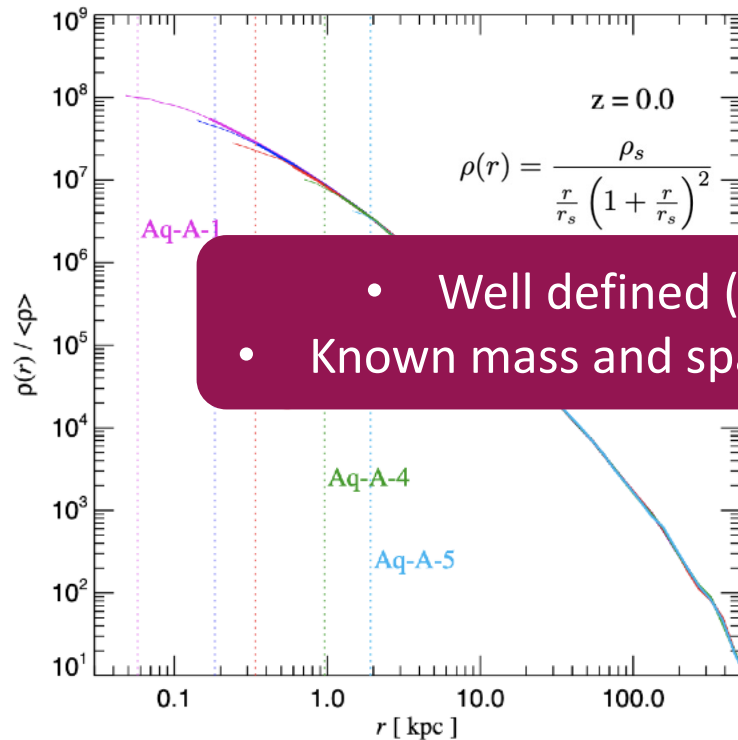
$$\frac{dn}{dM} \propto M^\alpha$$

- Concentration
 $c(M)$

HALO AND SUBHALO PROPERTIES

Main halos

- Fundamental non-linear units of cosmic structures
- Inner density profile



- Mass distribution

$$dn \propto M^\alpha$$

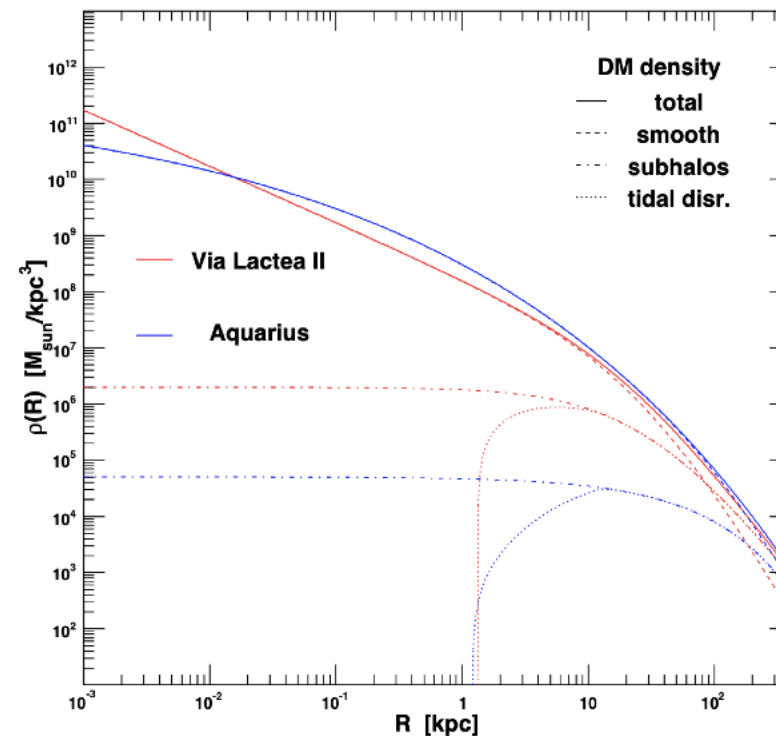
- Well defined (M_{200}, R_{200})
- Known mass and spatial distribution

- Concentration

$$c(M)$$

Subhalos

- The later halos that do not get to merge with the rest
- Fall in the potential wells of main halos



- Mass distribution

$$\frac{dn_{sub}}{dM_{sub}} \propto M_{sub}^\alpha$$

$$\alpha \in [1.9, 2.0]$$

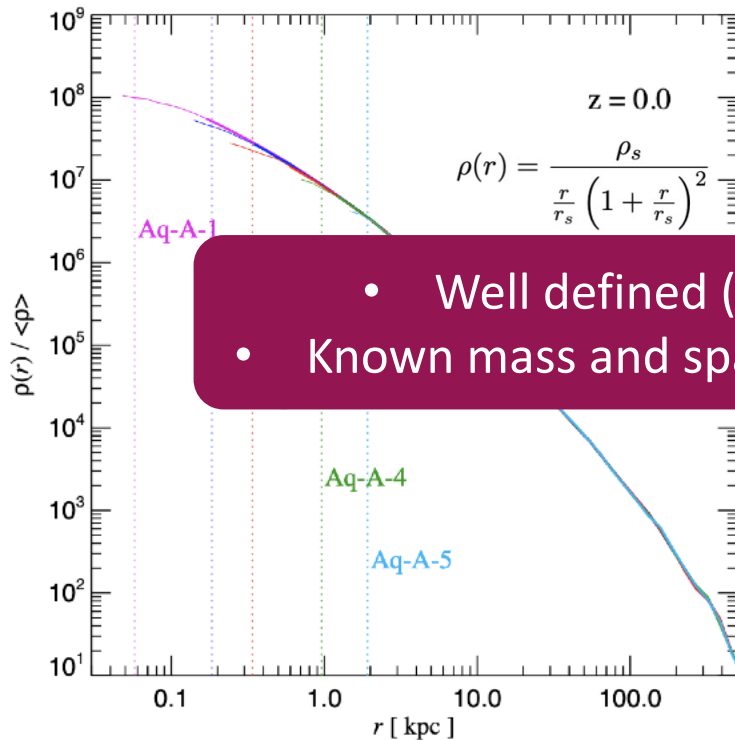
- Concentration

$$c_{sub}(M_{sub}, r_{sub})$$

HALO AND SUBHALO PROPERTIES

Main halos

- Fundamental non-linear units of cosmic structures
- Inner density profile



- Mass distribution

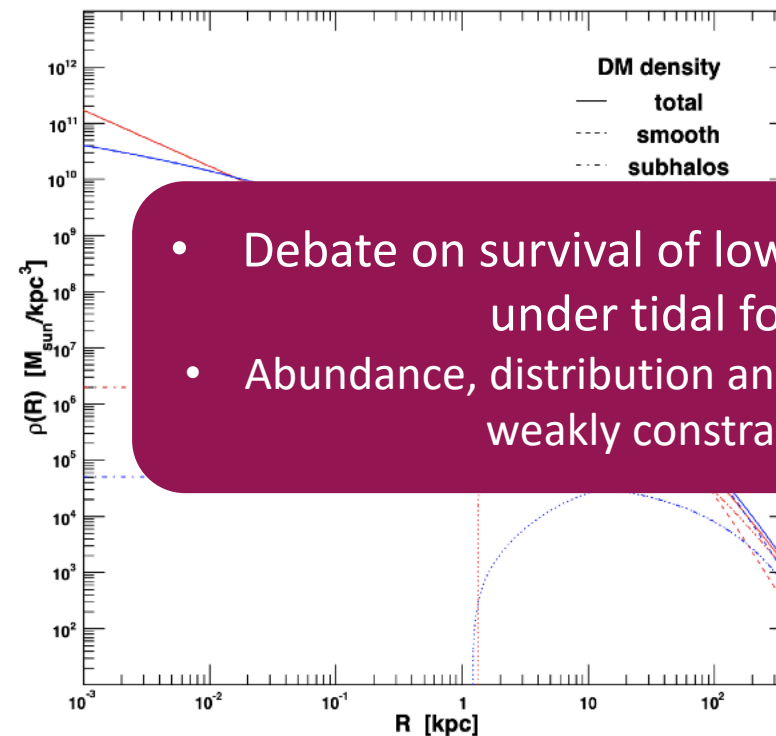
$$dn \propto M^\alpha$$

- Well defined (M_{200}, R_{200})
- Known mass and spatial distribution

- Concentration $c(M)$

Subhalos

- The later halos that do not get to merge with the rest
- Fall in the potential wells of main halos



- Mass distribution

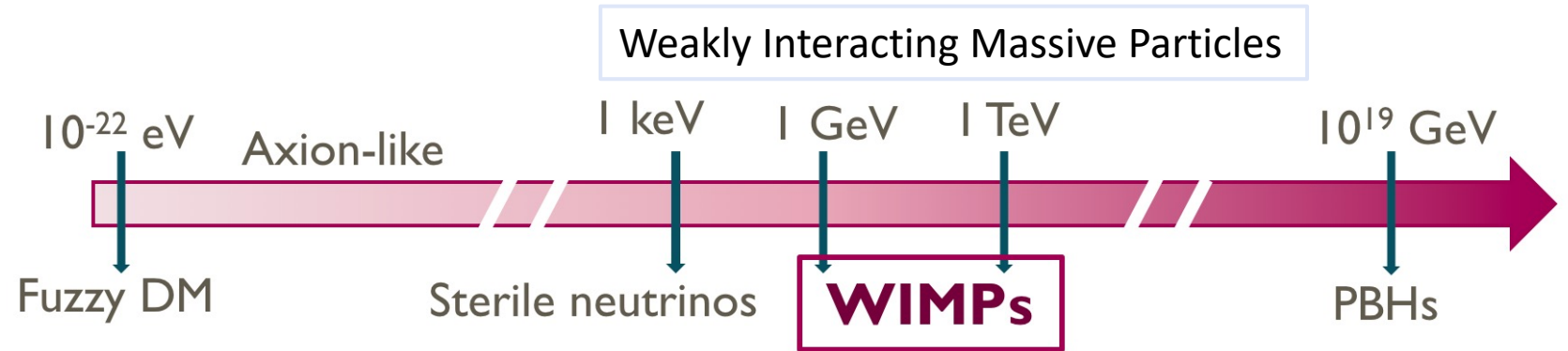
- Debate on survival of low mass subhalos under tidal forces
- Abundance, distribution and inner structure weakly constrained

$$c_{sub}(M_{sub}, r_{sub})$$

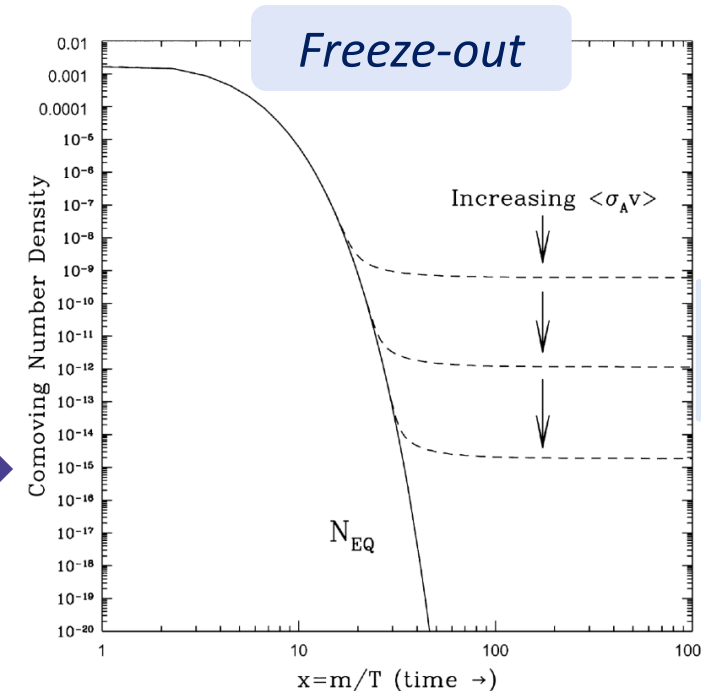
PARTICLE MODELS FOR DM: WIMPS

- Different DM candidates:

- Non-baryonic
- Electrically neutral
- Non-relativistic & collisionless
- Long-lived



- Only interact via weak nuclear force with standard matter
- To be stable, usually assigned as lightest member of dark sector carrying conserved quantum number
- Produced as a thermal relic: their cosmological abundance is set by thermal production in the early Universe

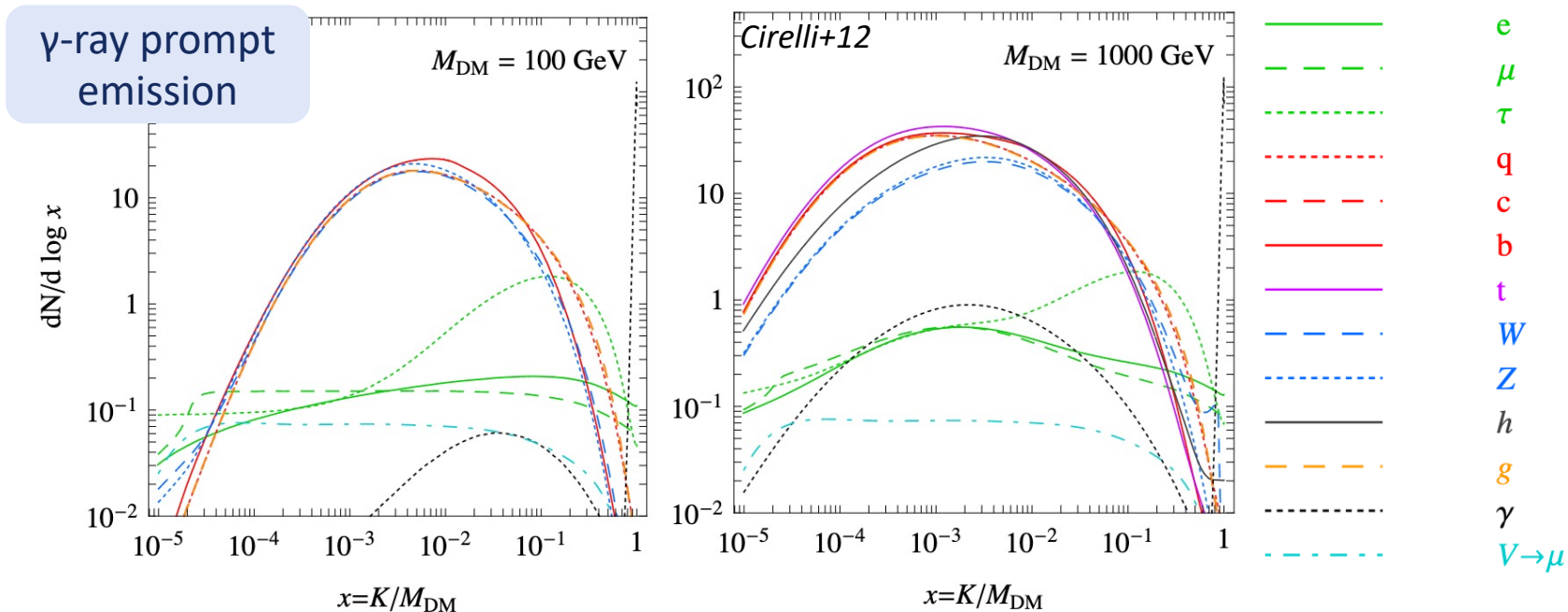


WIMP miracle

$$\Omega_\chi h^2 = \frac{10^{-27} \text{ cm}^3 \text{ s}^{-1}}{\langle \sigma v \rangle}$$

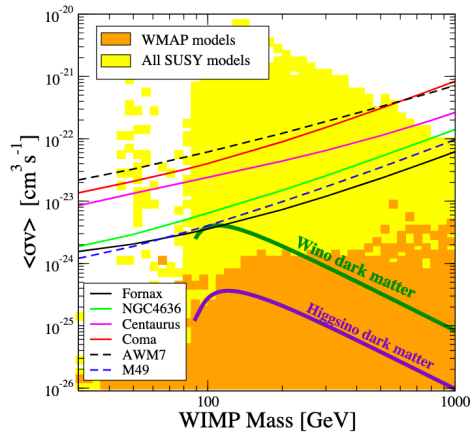
PARTICLE MODELS FOR DM: WIMPS

- DM production at source: *Cirelli+12* (EW corrections)
 - includes electroweak radiation effects, specially important for the flux of γ and e^\pm for energies around m_χ
 - s-wave non-relativistic DM-DM annihilation/decay
 - annihilation/decay into primary channel + photon radiation off quarks and leptons, as well as photon branching into quark or lepton pairs
 - γ -ray fluxes only include prompt emission and not the secondary radiation (e.g. Inverse Compton)

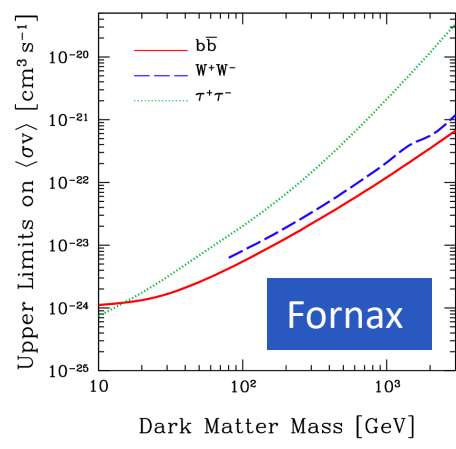


PREVIOUS γ -RAY DM SEARCHES IN GALAXY CLUSTERS

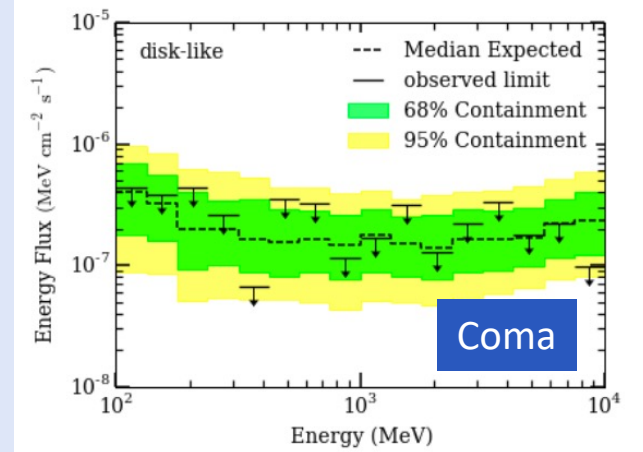
Fermi-LAT - Annihilation



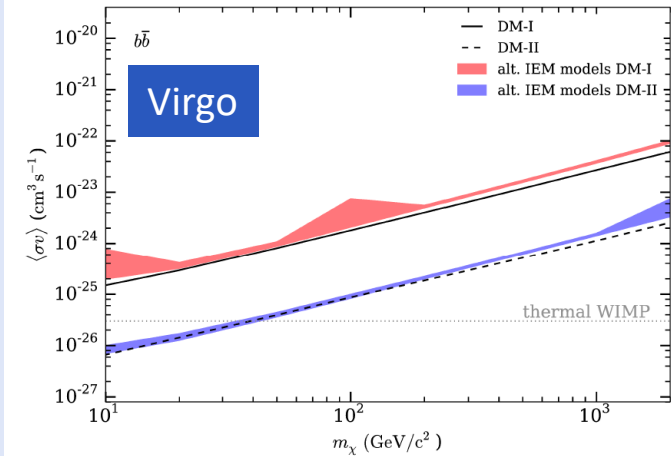
Ackermann+10 [Fermi-LAT Collab.]



Ando&Nagai12



Ackermann+16 [Fermi-LAT Collab.]

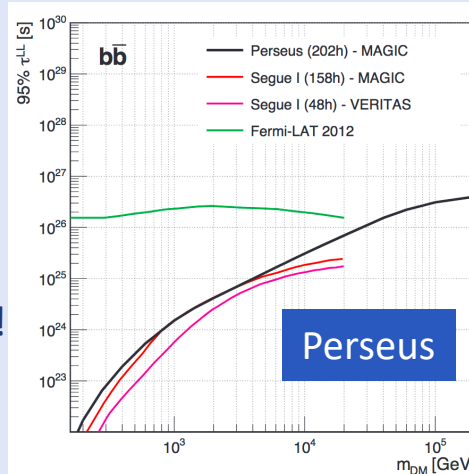


Ackermann+15 [Fermi-LAT Collab.]

- Last word about gamma-ray searches in a big sample of galaxy clusters: CR focused (Ackermann+14 [Fermi-LAT Collab.]

MAGIC - Decay

Best constraints so far!



Acciari+18 [MAGIC Collab.]

OBTENTION OF DM MODEL PARAMETERS

- State-of-the-art parametrization of the DM in galaxy clusters: $\langle \rho_{\text{tot}} \rangle(r) = \rho_{\text{sm}}(r) + \langle \rho_{\text{subs}} \rangle(r)$

- Assume a DM profile

$$\rho(r) = \frac{\rho_0}{\left(\frac{r}{r_s}\right)\left[1 + \frac{r}{r_s}\right]^2} \quad \text{NFW}$$

- Assume a concentration-mass relation ($c_{200} - M_{200}$): *Sánchez-Conde&Prada14*

$$c_{200}(M_{200}, z = 0) = \sum_{i=0}^5 c_i \times \left[\ln \left(\frac{M_{200}}{h^{-1} M_{\odot}} \right) \right]^i$$

- Assume spherical collapse from an overdensity $\Delta = 200$ over the critical density

$$\Delta_{200} = \frac{3M_{200}}{4\pi R_{200}^3 \rho_{\text{crit}}}$$

- Compute remaining parameters

Scale density

$$\rho_0 = \frac{2\Delta_{200}\rho_{\text{crit}}c_{200}}{3F(c_{200})}$$

Scale radius

$$c_{200} = \frac{R_{200}}{r_s}$$

Angular extension

$$\theta_{200} = \tan \left(\frac{R_{200}}{d_L} \right)$$

with

$$F(c_{200}) = \frac{2}{c_{200}^2} \left(\ln(1 + c_{200}) - \frac{c_{200}}{1 + c_{200}} \right)$$

MAIN UNCERTAINTY: DM DENSITY PROFILES

- To model the DM density profile in the objects, we split the contributions:

$$\langle \rho_{\text{tot}} \rangle(r) = \rho_{\text{sm}}(r) + \langle \rho_{\text{subs}} \rangle(r) \longrightarrow \text{Subhalo population (if any)}$$

Main halo

- Cuspy-like,
from N-body simulations

$$\rho_{\text{NFW}}(r) = \frac{\rho_0}{\left(\frac{r}{r_s}\right) \left(1 + \frac{r}{r_s}\right)^2}$$

$$\rho_{\text{Ein}}(r) = \rho_s \exp\left(-\frac{2}{\alpha} \left[\left(\frac{r}{r_s}\right)^\alpha - 1\right]\right)$$

$$\rho_{\text{Bur}}(r) = \frac{\rho_c r_c^3}{(r + r_c)(r^2 + r_c^2)}$$

- Cored-like,
phenomenologically motivated

- Fit the profiles either:

- Rotational curves (spiral galaxies, dwarf irregular galaxies)
- Velocity dispersion measurements (dSphs)
- Normalize to the measured mass (galaxy clusters) \longrightarrow

$$M_\Delta = \int_0^{R_\Delta} \rho(r) r^2 dr d\Omega$$

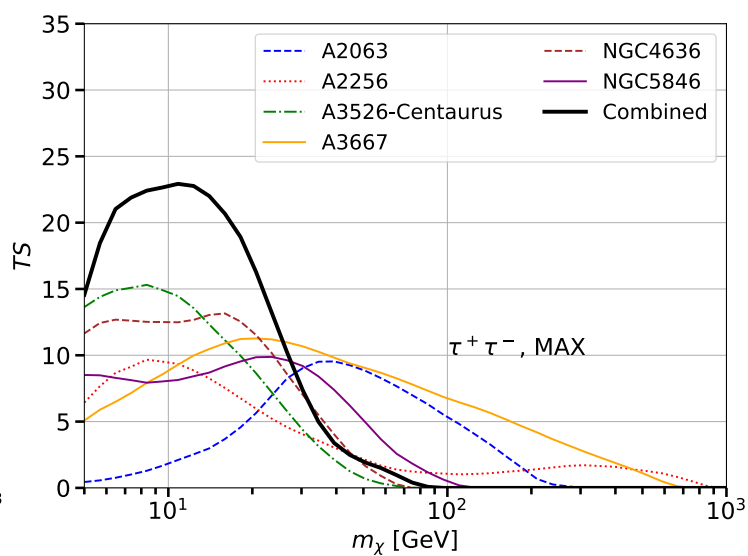
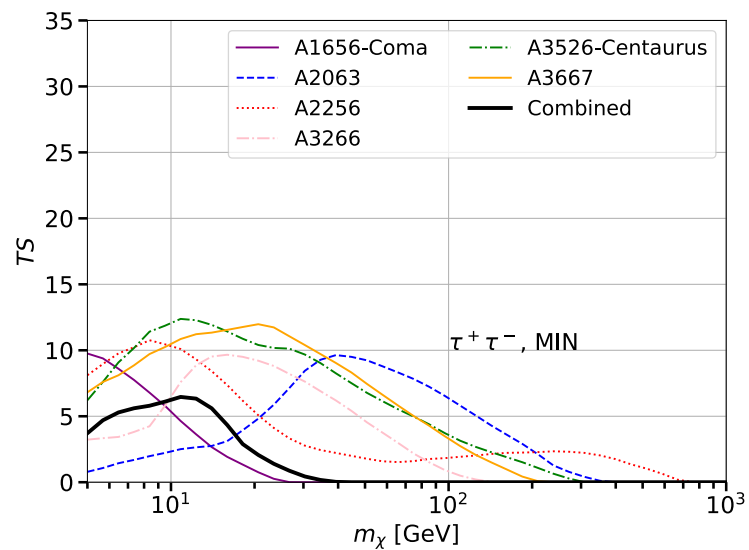
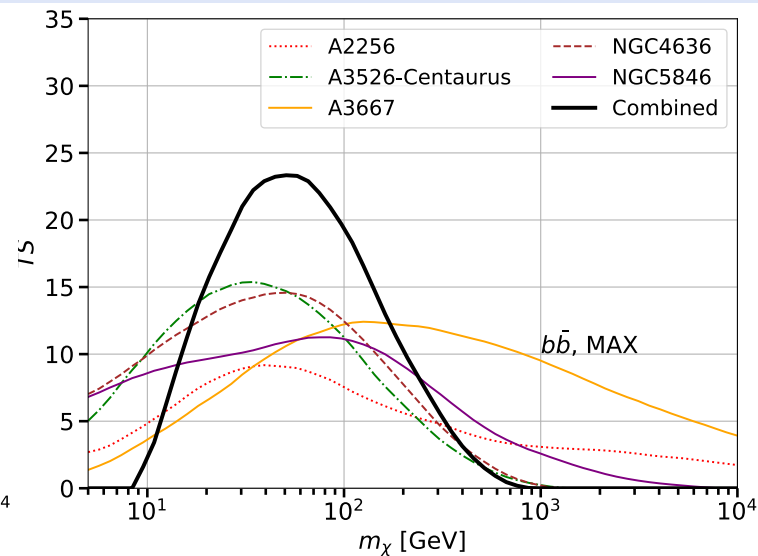
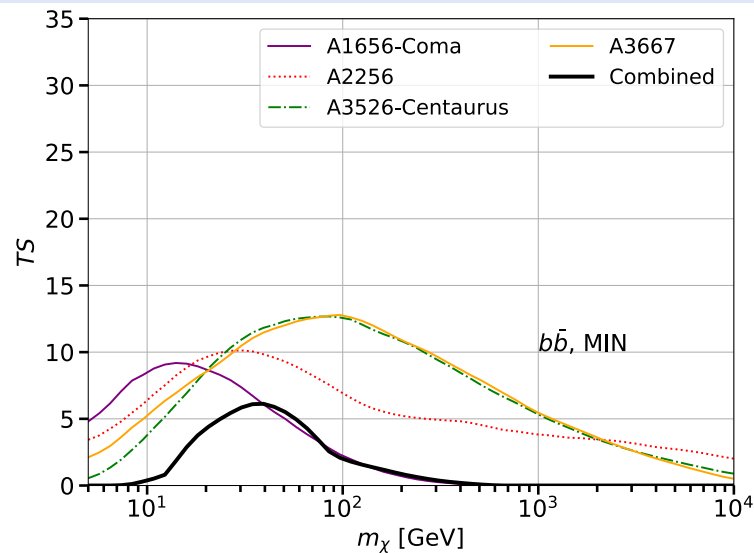
CLUSTERS SAMPLE

| Cluster | d_L | M_{200} | c_{200} | ρ_s | r_s | R_{200} | θ_{200} | $\log_{10} J_{MIN}$ | $\log_{10} J_{MED}$ | B_{MED} | $\log_{10} J_{MAX}$ | B_{MAX} | $\log_{10} D$ | TS |
|----------|--------|-----------------------|-----------|----------------------------|--------|-----------|----------------|----------------------------------|----------------------------------|-----------|----------------------------------|-----------|--------------------------|-------|
| | [Mpc] | [$10^{14} M_\odot$] | | [M_\odot/kpc^3] | [kpc] | [kpc] | [deg] | [$\text{GeV}^2\text{cm}^{-5}$] | [$\text{GeV}^2\text{cm}^{-5}$] | | [$\text{GeV}^2\text{cm}^{-5}$] | | [GeV cm^{-2}] | |
| A478 | 387.29 | 6.08 | 5.06 | 303795 | 345.37 | 1747.71 | 0.30 | 16.05 | 17.00 | 9.03 | 17.77 | 52.90 | 17.74 | 0.00 |
| A399 | 320.39 | 4.03 | 5.14 | 314222 | 296.58 | 1523.16 | 0.31 | 16.02 | 17.00 | 9.54 | 17.76 | 54.90 | 17.72 | 5.69 |
| A2065 | 325.13 | 4.73 | 5.10 | 309802 | 314.87 | 1607.11 | 0.33 | 16.08 | 17.05 | 9.46 | 17.82 | 55.00 | 17.78 | 4.94 |
| A1736 | 203.92 | 1.45 | 5.40 | 352863 | 200.77 | 1084.70 | 0.33 | 15.96 | 16.98 | 10.50 | 17.71 | 56.70 | 17.65 | 4.89 |
| A1644 | 208.50 | 1.55 | 5.38 | 349910 | 205.81 | 1107.83 | 0.33 | 15.96 | 16.98 | 10.50 | 17.72 | 56.70 | 17.66 | 1.90 |
| A401 | 339.38 | 5.92 | 5.06 | 304380 | 342.03 | 1732.25 | 0.34 | 16.14 | 17.11 | 9.34 | 17.88 | 54.90 | 17.84 | 8.07 |
| A2029 | 348.92 | 6.59 | 5.05 | 302105 | 355.64 | 1795.26 | 0.34 | 16.16 | 17.13 | 9.21 | 17.90 | 54.40 | 17.86 | 0.26 |
| Hydra-A | 240.76 | 2.60 | 5.24 | 328469 | 251.56 | 1317.25 | 0.35 | 16.06 | 17.07 | 10.20 | 17.82 | 57.70 | 17.76 | 3.74 |
| ZwCl1215 | 339.38 | 6.54 | 5.05 | 302272 | 354.58 | 1790.34 | 0.35 | 16.18 | 17.15 | 9.32 | 17.92 | 55.00 | 17.88 | 0.00 |
| MKW3S | 199.34 | 1.66 | 5.36 | 346794 | 211.39 | 1133.45 | 0.36 | 16.02 | 17.05 | 10.60 | 17.78 | 57.60 | 17.72 | 0.00 |
| A133 | 254.68 | 3.35 | 5.18 | 319842 | 276.74 | 1432.35 | 0.36 | 16.12 | 17.12 | 10.10 | 17.88 | 57.70 | 17.83 | 2.46 |
| A3158 | 263.99 | 3.97 | 5.14 | 314620 | 295.06 | 1516.19 | 0.37 | 16.16 | 17.16 | 9.99 | 17.92 | 57.70 | 17.87 | 5.39 |
| A4059 | 203.92 | 2.19 | 5.28 | 334997 | 235.56 | 1244.13 | 0.38 | 16.12 | 17.14 | 10.50 | 17.89 | 58.90 | 17.83 | 0.06 |
| A1795 | 278.01 | 5.17 | 5.09 | 307558 | 325.36 | 1655.37 | 0.38 | 16.23 | 17.22 | 9.81 | 17.99 | 57.50 | 17.94 | 0.42 |
| A2657 | 176.55 | 1.69 | 5.36 | 345942 | 212.97 | 1140.70 | 0.40 | 16.13 | 17.16 | 10.80 | 17.90 | 58.90 | 17.84 | 4.53 |
| A2147 | 153.91 | 1.17 | 5.47 | 363492 | 184.45 | 1009.48 | 0.40 | 16.09 | 17.13 | 11.00 | 17.86 | 58.70 | 17.79 | 5.72 |
| A3376 | 199.34 | 2.58 | 5.24 | 328779 | 250.74 | 1313.53 | 0.41 | 16.20 | 17.23 | 10.60 | 17.98 | 59.90 | 17.92 | 0.84 |
| A3562 | 222.29 | 3.53 | 5.16 | 318132 | 282.44 | 1458.40 | 0.41 | 16.24 | 17.26 | 10.40 | 18.02 | 59.70 | 17.96 | 0.03 |
| A85 | 250.04 | 5.09 | 5.09 | 307918 | 323.62 | 1647.33 | 0.42 | 16.30 | 17.31 | 10.10 | 18.07 | 59.00 | 18.03 | 0.31 |
| A3391 | 236.13 | 4.51 | 5.11 | 311034 | 309.49 | 1582.37 | 0.43 | 16.29 | 17.30 | 10.30 | 18.07 | 59.90 | 18.02 | 0.11 |
| A3667 | 250.04 | 5.30 | 5.08 | 306940 | 328.42 | 1669.45 | 0.43 | 16.31 | 17.32 | 10.10 | 18.09 | 59.50 | 18.04 | 13.31 |
| A2052 | 153.91 | 1.63 | 5.37 | 347614 | 209.89 | 1126.58 | 0.45 | 16.22 | 17.26 | 11.00 | 18.00 | 60.10 | 17.93 | 0.03 |
| 2A0335 | 153.91 | 1.66 | 5.36 | 346659 | 211.64 | 1134.59 | 0.45 | 16.23 | 17.27 | 11.00 | 18.01 | 60.20 | 17.95 | 5.44 |
| A2589 | 185.64 | 2.99 | 5.20 | 323540 | 265.28 | 1379.98 | 0.46 | 16.31 | 17.34 | 10.70 | 18.10 | 61.20 | 18.04 | 0.13 |
| EXO0422 | 172.01 | 2.49 | 5.25 | 330093 | 247.36 | 1298.09 | 0.47 | 16.30 | 17.33 | 10.80 | 18.09 | 61.30 | 18.02 | 0.18 |

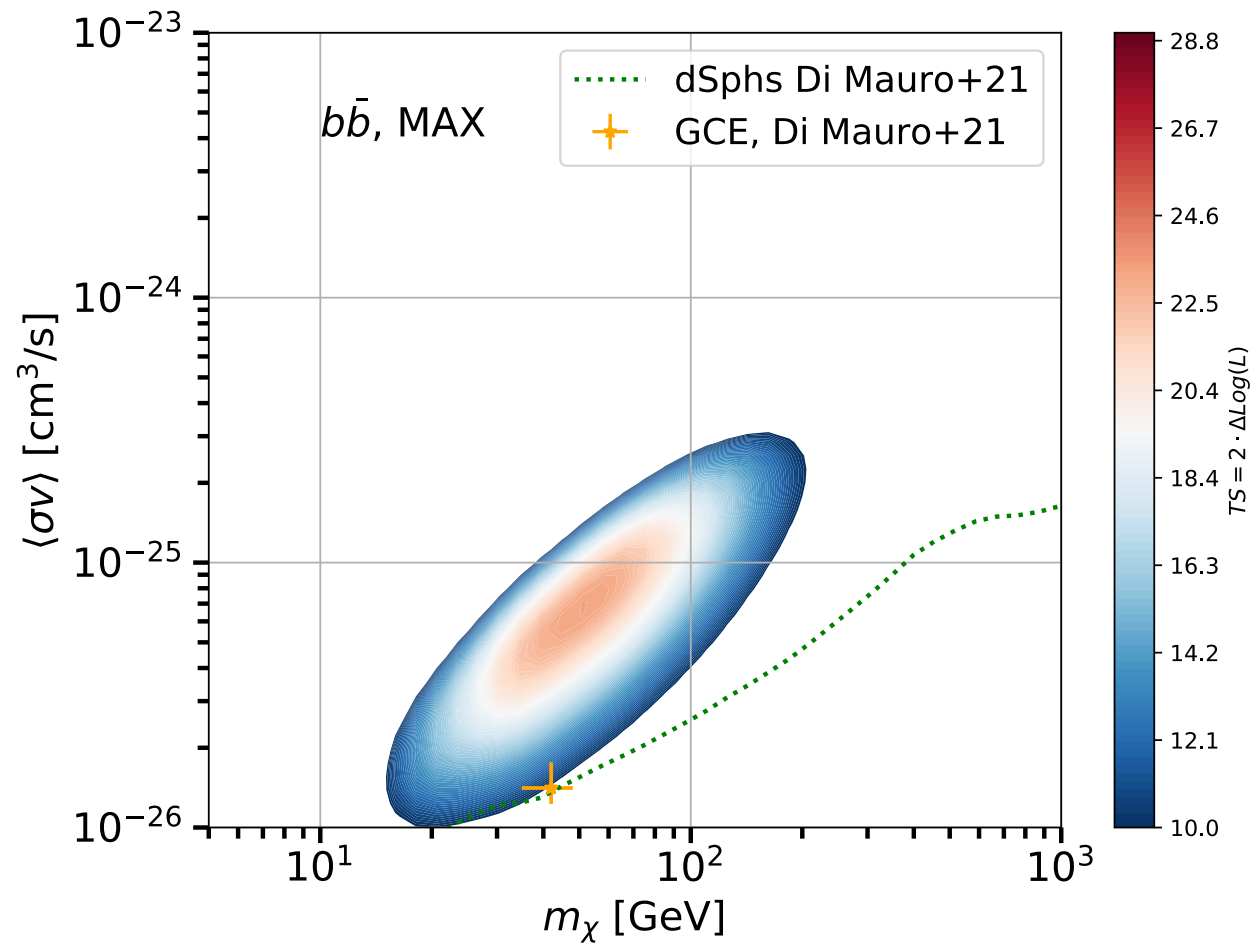
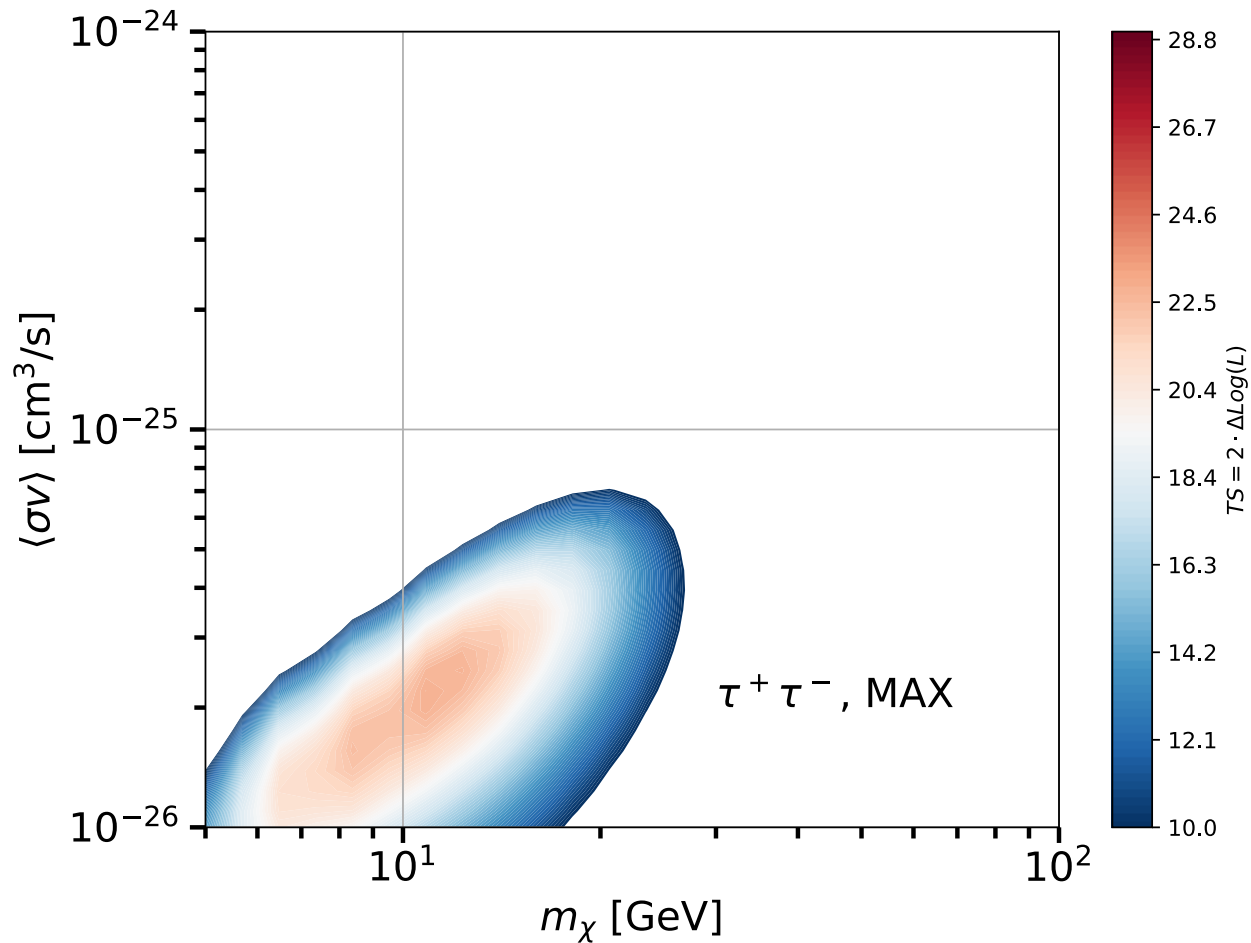
CLUSTERS SAMPLE

| Cluster | d_L | M_{200} | c_{200} | ρ_s | r_s | R_{200} | θ_{200} | $\log_{10} J_{MIN}$ | $\log_{10} J_{MED}$ | B_{MED} | $\log_{10} J_{MAX}$ | B_{MAX} | $\log_{10} D$ | TS |
|-----------------|--------|-------------------------|-----------|------------------------------|--------|-----------|----------------|-----------------------------------|-----------------------------------|-----------|-----------------------------------|-----------|--------------------------|-------|
| | [Mpc] | [$10^{14} M_{\odot}$] | | [M_{\odot}/kpc^3] | [kpc] | [kpc] | [deg] | [$\text{GeV}^2 \text{cm}^{-5}$] | [$\text{GeV}^2 \text{cm}^{-5}$] | | [$\text{GeV}^2 \text{cm}^{-5}$] | | [GeV cm^{-2}] | |
| A576 | 167.47 | 2.37 | 5.26 | 331959 | 242.73 | 1276.91 | 0.47 | 16.31 | 17.34 | 10.90 | 18.09 | 61.30 | 18.03 | 0.99 |
| A2063 | 153.91 | 1.97 | 5.31 | 339288 | 226.15 | 1201.08 | 0.48 | 16.29 | 17.34 | 11.00 | 18.08 | 61.00 | 18.01 | 9.44 |
| A3558 | 213.09 | 4.89 | 5.10 | 308961 | 318.70 | 1624.70 | 0.48 | 16.41 | 17.42 | 10.30 | 18.19 | 60.90 | 18.14 | 0.35 |
| A2142 | 411.48 | 28.03 | 4.97 | 291172 | 585.57 | 2908.46 | 0.48 | 16.66 | 17.57 | 8.15 | 18.38 | 51.70 | 18.36 | 0.00 |
| A119 | 194.77 | 3.96 | 5.14 | 314731 | 294.64 | 1514.28 | 0.49 | 16.33 | 17.39 | 11.20 | 18.15 | 65.60 | 18.09 | 8.49 |
| A2634 | 135.92 | 1.55 | 5.38 | 349762 | 206.07 | 1109.02 | 0.50 | 16.30 | 17.35 | 11.20 | 18.09 | 60.90 | 18.02 | 4.31 |
| A2256 | 268.66 | 10.17 | 4.99 | 294929 | 415.33 | 2074.55 | 0.50 | 16.53 | 17.52 | 9.65 | 18.31 | 59.10 | 18.26 | 9.91 |
| A496 | 144.90 | 2.56 | 5.24 | 329080 | 249.96 | 1309.96 | 0.55 | 16.45 | 17.49 | 11.10 | 18.25 | 63.50 | 18.18 | 0.00 |
| A3266 | 263.99 | 13.44 | 4.97 | 292052 | 457.72 | 2276.43 | 0.55 | 16.67 | 17.65 | 9.57 | 18.44 | 59.60 | 18.40 | 8.19 |
| A1367 | 95.81 | 0.88 | 5.57 | 379136 | 164.49 | 916.83 | 0.57 | 16.36 | 17.42 | 11.50 | 18.14 | 60.80 | 18.06 | 0.99 |
| A4038 | 122.49 | 2.23 | 5.28 | 334336 | 237.08 | 1251.09 | 0.62 | 16.53 | 17.58 | 11.30 | 18.33 | 64.00 | 18.26 | 0.71 |
| A754 | 236.13 | 25.00 | 4.96 | 290649 | 564.09 | 2799.56 | 0.75 | 17.14 | 18.05 | 8.23 | 18.86 | 52.70 | 18.82 | 0.28 |
| A2199 | 131.44 | 5.07 | 5.09 | 308030 | 323.08 | 1644.84 | 0.76 | 16.80 | 17.85 | 11.10 | 18.62 | 66.00 | 18.56 | 1.86 |
| A3571 | 162.95 | 10.90 | 4.99 | 294084 | 425.60 | 2123.16 | 0.80 | 16.95 | 17.97 | 10.50 | 18.77 | 65.20 | 18.71 | 0.00 |
| NGC 5044 | 38.81 | 0.41 | 5.88 | 428317 | 121.16 | 711.87 | 1.07 | 16.82 | 17.90 | 11.90 | 18.60 | 60.50 | 18.51 | 0.00 |
| NGC 5813 | 27.55 | 0.27 | 6.06 | 460583 | 102.21 | 619.60 | 1.31 | 16.96 | 18.03 | 11.80 | 18.72 | 58.30 | 18.62 | 4.10 |
| A1656-Coma | 100.24 | 13.16 | 4.97 | 292223 | 454.37 | 2260.40 | 1.35 | 17.42 | 18.46 | 11.00 | 19.26 | 69.60 | 19.20 | 9.93 |
| NGC 5846 | 26.25 | 0.38 | 5.91 | 434293 | 117.22 | 692.90 | 1.53 | 17.13 | 18.20 | 11.90 | 18.91 | 60.40 | 18.81 | 10.81 |
| A1060-Hydra | 47.51 | 2.97 | 5.20 | 323860 | 264.34 | 1375.66 | 1.70 | 17.43 | 18.51 | 12.00 | 19.27 | 70.00 | 19.19 | 5.41 |
| A3526-Centaurus | 43.16 | 2.27 | 5.27 | 333726 | 238.51 | 1257.60 | 1.70 | 17.41 | 18.49 | 12.10 | 19.25 | 69.20 | 19.16 | 15.62 |
| NGC 1399-Fornax | 21.50 | 0.51 | 5.79 | 413641 | 131.82 | 762.97 | 2.05 | 17.41 | 18.50 | 12.20 | 19.21 | 62.60 | 19.11 | 4.01 |
| M49 | 18.91 | 0.46 | 5.82 | 419644 | 127.27 | 741.24 | 2.26 | 17.49 | 18.57 | 12.10 | 19.28 | 62.00 | 19.18 | 0.00 |
| NGC 4636 | 17.18 | 0.53 | 5.77 | 409991 | 134.72 | 776.79 | 2.61 | 17.63 | 18.71 | 12.20 | 19.43 | 63.00 | 19.33 | 13.09 |
| VIRGO | 15.46 | 5.60 | 5.07 | 305646 | 335.10 | 1700.27 | 6.32 | 18.65 | 19.74 | 12.30 | 20.52 | 74.80 | 20.44 | 1.05 |

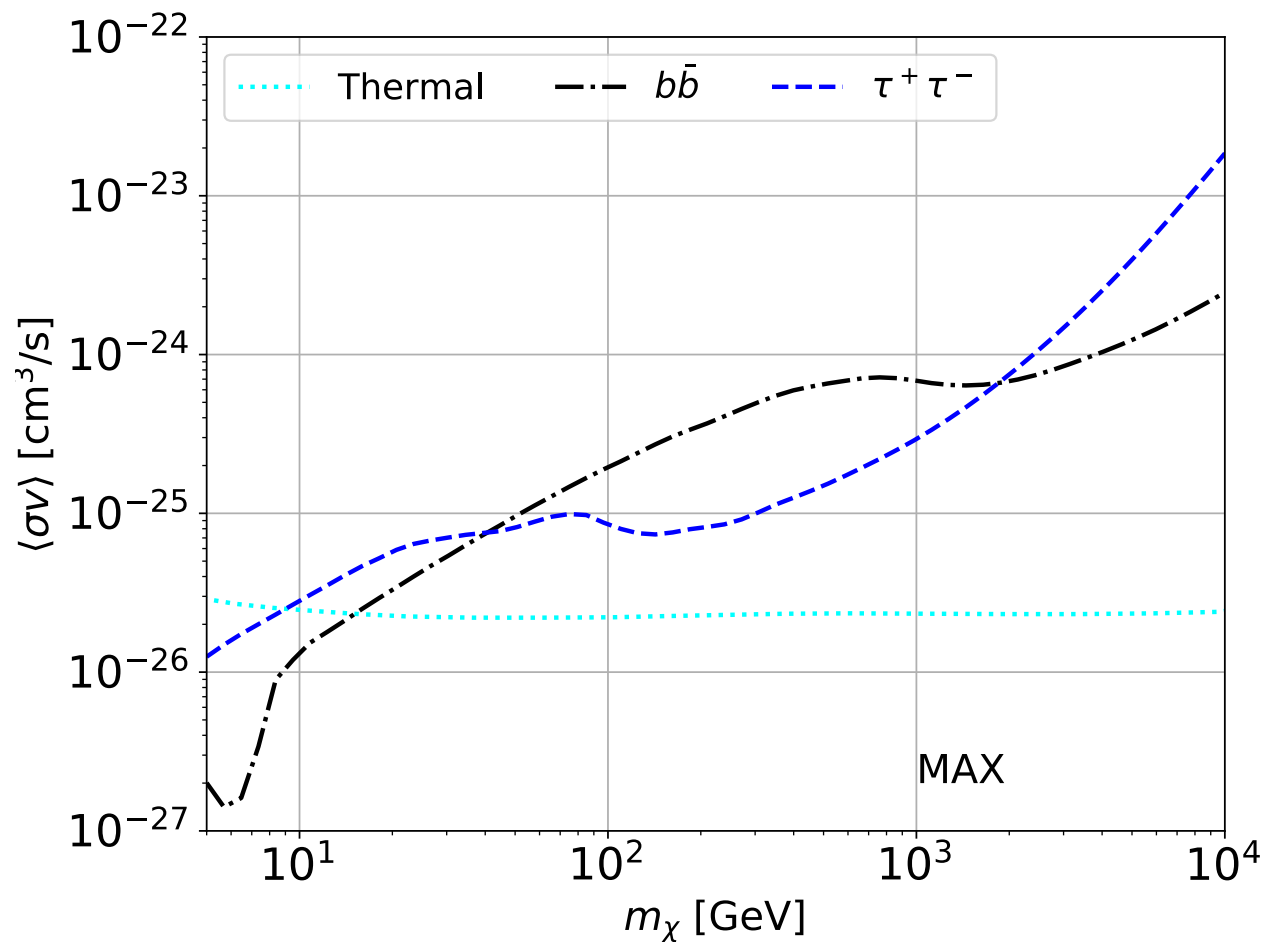
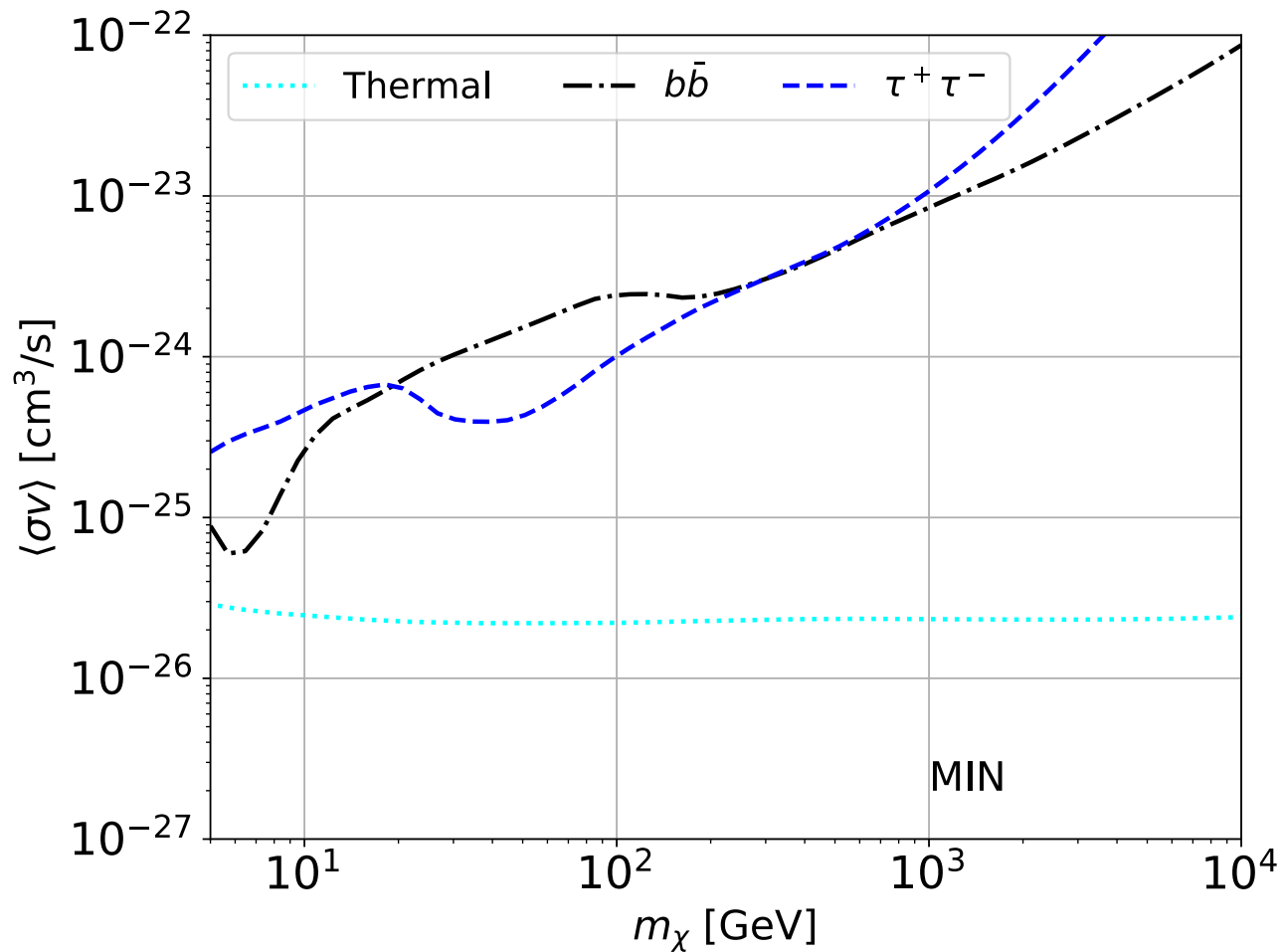
INSIGHT RESULTS: OTHER CHANNELS & MODELS



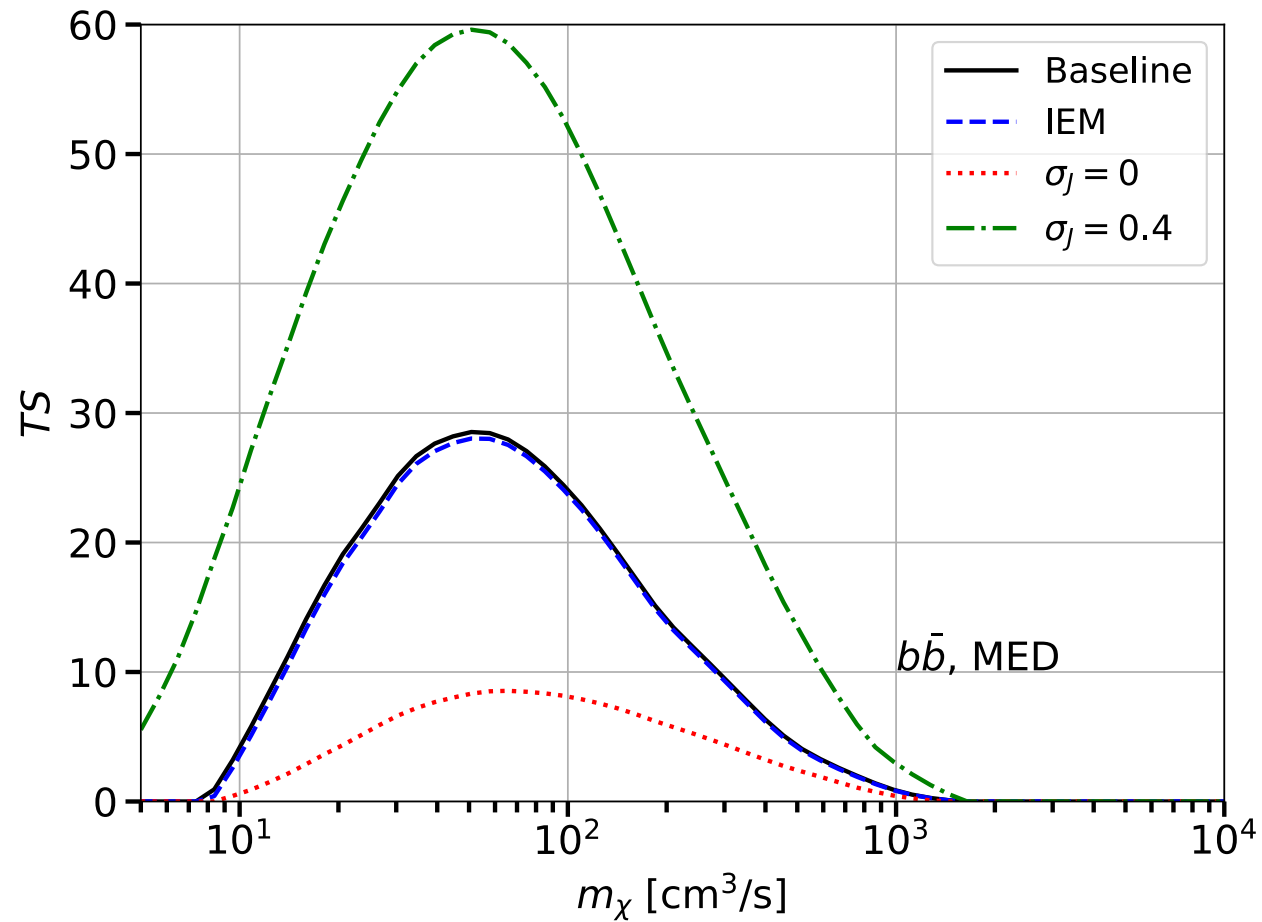
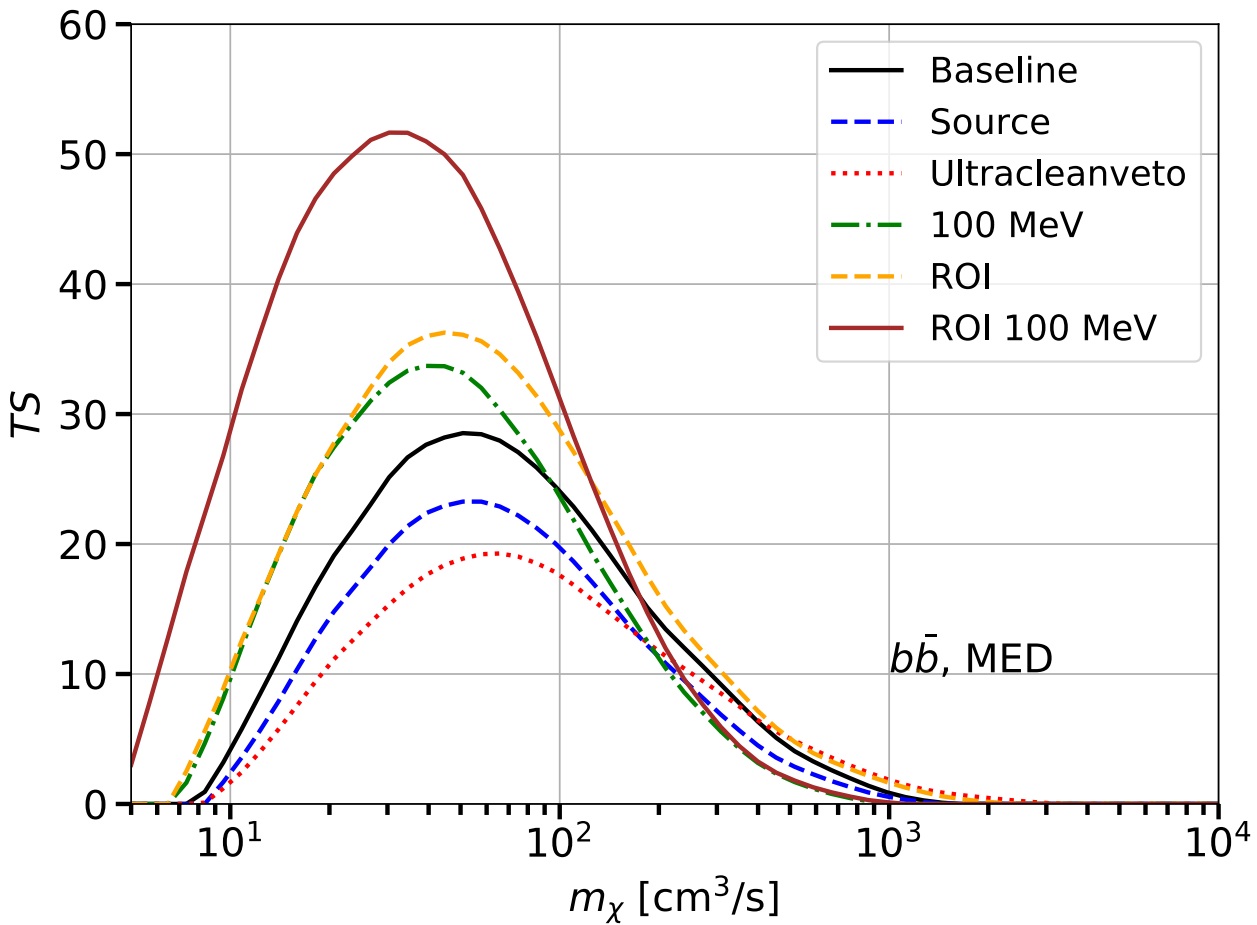
INSIGHT RESULTS: OTHER CHANNELS & MODELS



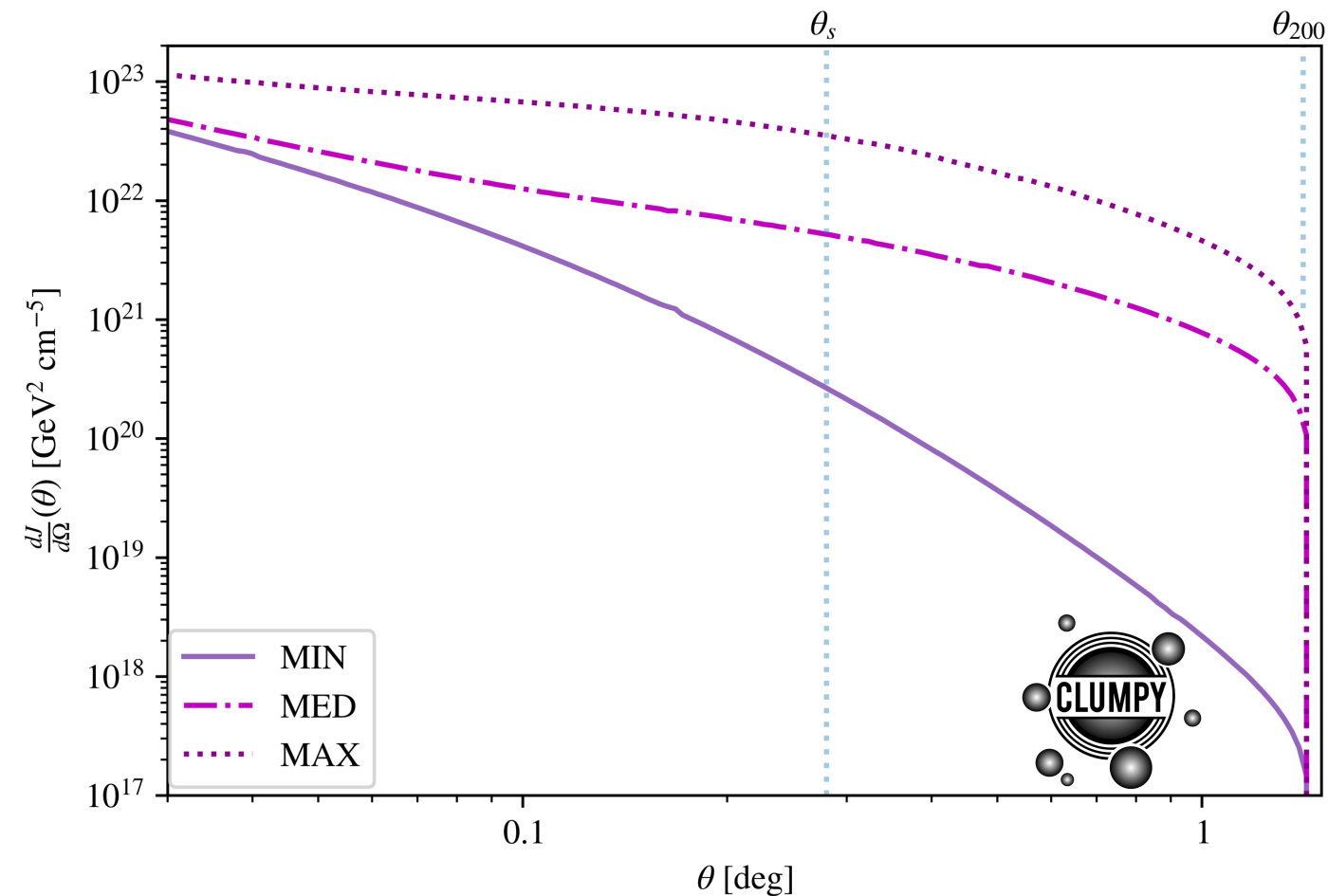
INSIGHT RESULTS: OTHER CHANNELS & MODELS



INSIGHT RESULTS: OTHER ANALYSIS SET-UPS



PERSEUS DIFFERENTIAL ANNIHILATION FLUX PROFILE



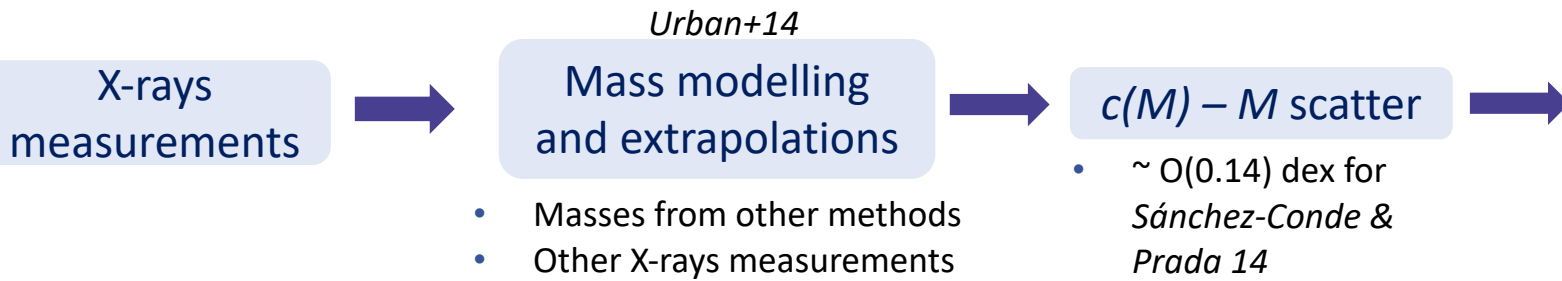
General parameters

| | | | | |
|-------------------------------------|-----------|---------------------------------|----------------|---------------------------------|
| <i>Hitomi Coll.18</i> | z | 0.017284 | l, b | 150.58 deg, -13.26 deg |
| <i>Urban+14</i> | M_{200} | $7.52 \times 10^{14} M_{\odot}$ | R_{200} | 1865.0 kpc |
| <i>Sánchez-Conde & Prada 14</i> | c_{200} | 5.03 | θ_{200} | 1.42 deg |
| | r_s | 370.82 kpc | θ_s | 0.28 deg |
| Flat Λ CDM | d_L | 75.01 Mpc | ρ_s | $299581 M_{\odot}/\text{kpc}^3$ |

| | |
|--------------|---|
| Annihilation | $\log_{10} J [\text{GeV}^2 \text{cm}^{-5}]$ |
| MIN | 17.42 |
| MED | 18.43 |
| MAX | 19.20 |
| Decay | $\log_{10} D [\text{GeV cm}^{-2}]$ |
| | 19.20 |

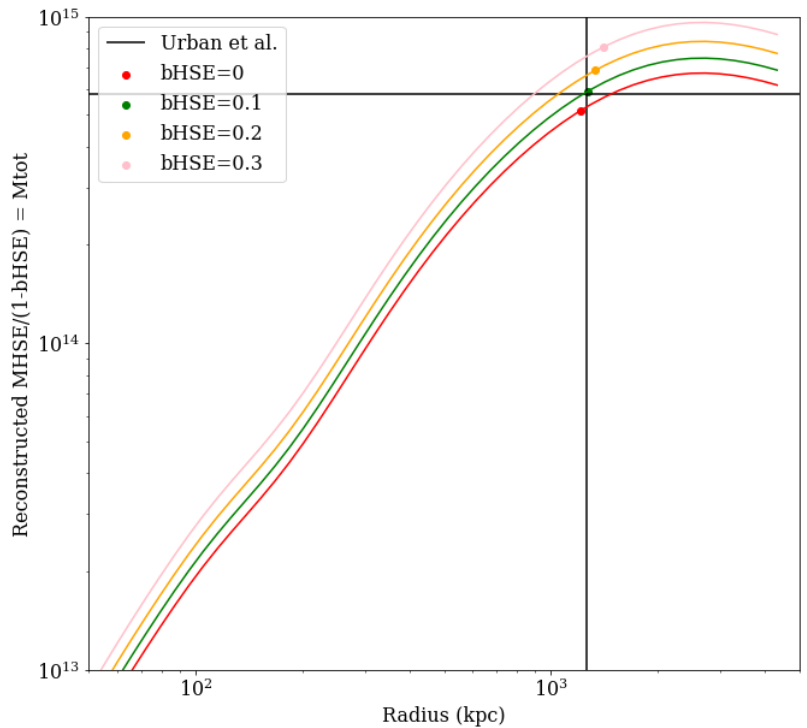
UNCERTAINTIES FOR CLUSTER'S DM MODELS

- Uncertainties in the J/D-factor enter through:



| | σ_J | σ_D |
|-------------------------|------------|------------|
| $M_{min} + c_{200,min}$ | 0.2 | 0.003 |
| M_{min} | 0.002 | 0.0 |
| M_{max} | 0.005 | 0.0 |
| $M_{max} + c_{200,max}$ | 0.2 | 0.0 |

- $\sim O(0.14)$ dex for *Sánchez-Conde & Prada 14*



$$\mathcal{J}(J | J_{obs}, \sigma_J) = \frac{1}{\ln(10) J_{obs} \sqrt{2\pi} \sigma_J} \times e^{-\left(\log_{10}(J) - \log_{10}(J_{obs})\right)^2 / 2\sigma_J^2}$$

Gaussian prior in J-factor uncertainty

CHARACTERISTICS OF THE SIMULATIONS

Background models:

CR baseline model



NGC1275
&
IC310



CTAO IRFs instrumental

- From simulations by *Pinzke&Pfrommer 2010*:
 π^0 decay + Inverse Compton

- Quiescent states

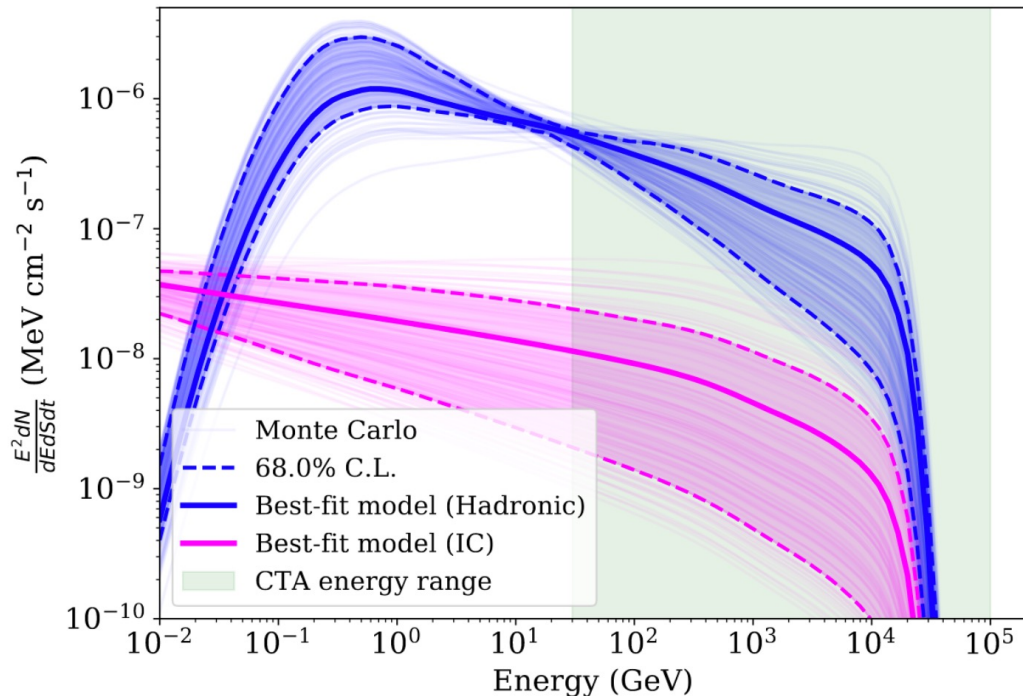
- NGC 1275 (*Ahnen+16*)

$$\frac{dN}{dEdSdt} = 2.1 \times 10^{-11} \left(\frac{E}{200 \text{ GeV}} \right)^{-3.6} \text{ cm}^{-2} \text{ s}^{-1} \text{ TeV}^{-1}$$

- IC 310 (*Alecksic+14*)

$$\frac{dN}{dEdSdt} = 0.741 \times 10^{-12} \left(\frac{E}{1 \text{ TeV}} \right)^{-1.81} \text{ cm}^{-2} \text{ s}^{-1} \text{ TeV}^{-1}$$

| Model | X_{500} (%) | α_{CRp} | η_{CRp} | $F_{500, E_\gamma > 150 \text{ GeV}}^{(\text{had})}$ | $F_{500, E_\gamma > 150 \text{ GeV}}^{(\text{IC})} [10^{-14} \text{ cm}^{-2} \text{ s}^{-1}]$ |
|----------|-----------------------------|-----------------------|---------------------|--|---|
| | reference value, [min, max] | | | | |
| Baseline | 1.0, [0.0, 20.0] | 2.30, [2.0, 3.0] | 1.0, [0.0, 1.5] | 70.2, [0, 11373.8] | 2.1, [0, 625.4] |



CHARACTERISTICS OF THE SIMULATIONS

• Input models:

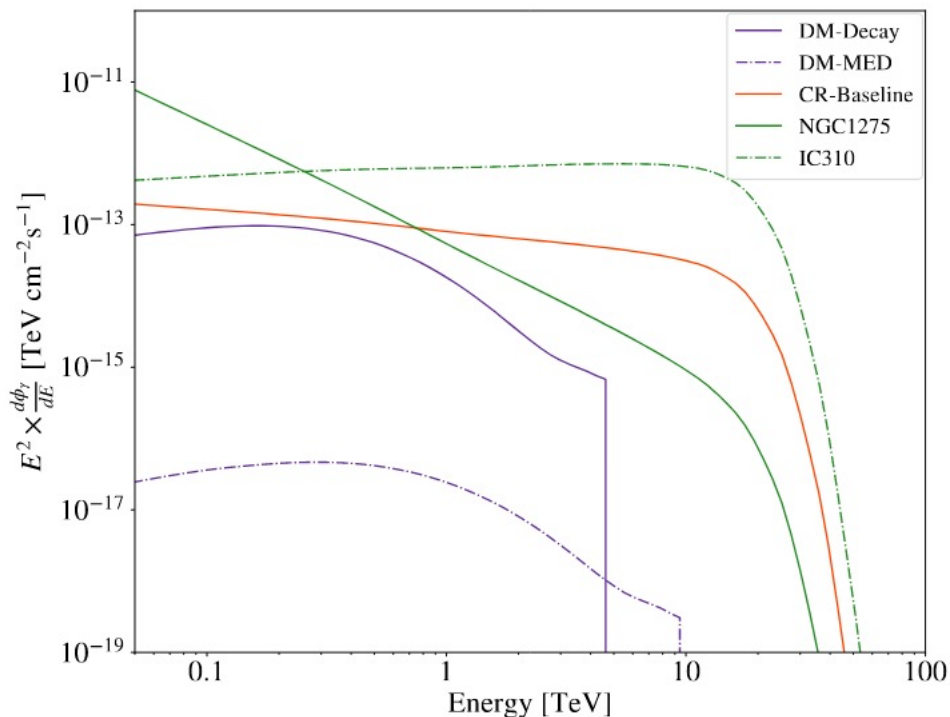
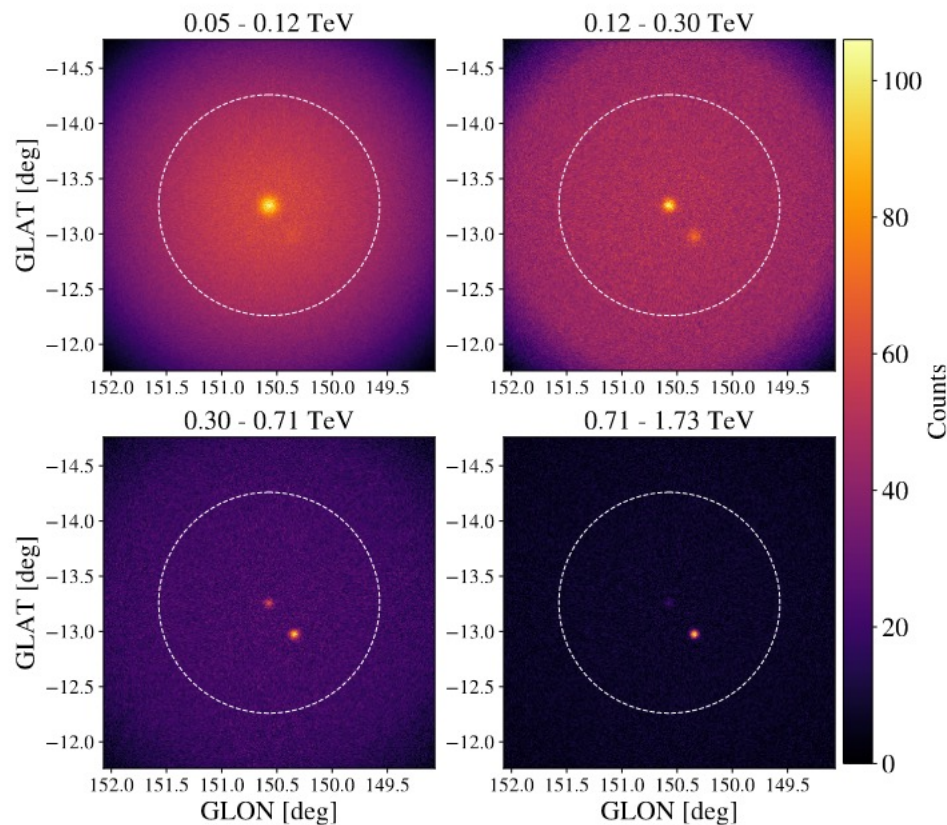
DM Annihilation (thermal cross-section)
 DM Decay ($\tau_\chi = 10^{27}s$)
 $m_\chi = 10$ TeV
 b \bar{b}

CR baseline model

NGC1275
 &
 IC310

EBL

Domínguez+11



CTA ANALYSIS ELEMENTS

- https://docs.gammapy.org/0.19/stats/fit_statistics.html

- Likelihood ratio test:

$$TS = 2 \log \left[\frac{\mathcal{L}(A_\chi, \hat{\nu})}{\mathcal{L}_{\text{null}}(A_\chi = 0, \hat{\nu})} \right]$$

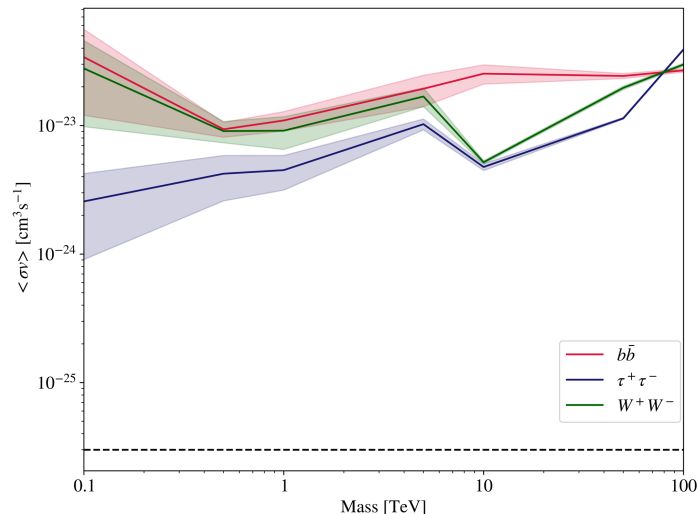
- $TS < 25 \rightarrow$ No signal

Template fitting: Poisson likelihood for each component, *Cash* statistics (*Cash 79*)

$$\ln \mathcal{L}(\vec{\theta} | D) = \sum_i \tilde{M}_i(\vec{\theta}) - d_i \ln(\tilde{M}_i(\vec{\theta})) \quad \vec{\theta} \equiv (A_\chi, A_{\text{CR}}, A_{\text{PS}}^{(1,2)}, \alpha_{\text{PS}}^{(1,2)}, A_{\text{bkg}}, \alpha_{\text{bkg}})$$

ON-OFF analysis: Poisson likelihood for signal and background, *Wstat* statistics (*XSpec manual*)

$$\mathcal{L}(A_\chi | D) = \prod_{ij} \frac{(N_{ij}^S + \kappa_{ij} N_{ij}^B)^{N_{ij}^{ON}}}{N_{ij}^{ON}!} e^{-(N_{ij}^S + \kappa_{ij} N_{ij}^B)} \times \frac{(N_{ij}^B)^{N_{ij}^{OFF}}}{N_{ij}^{OFF}!} e^{-N_{ij}^B}$$

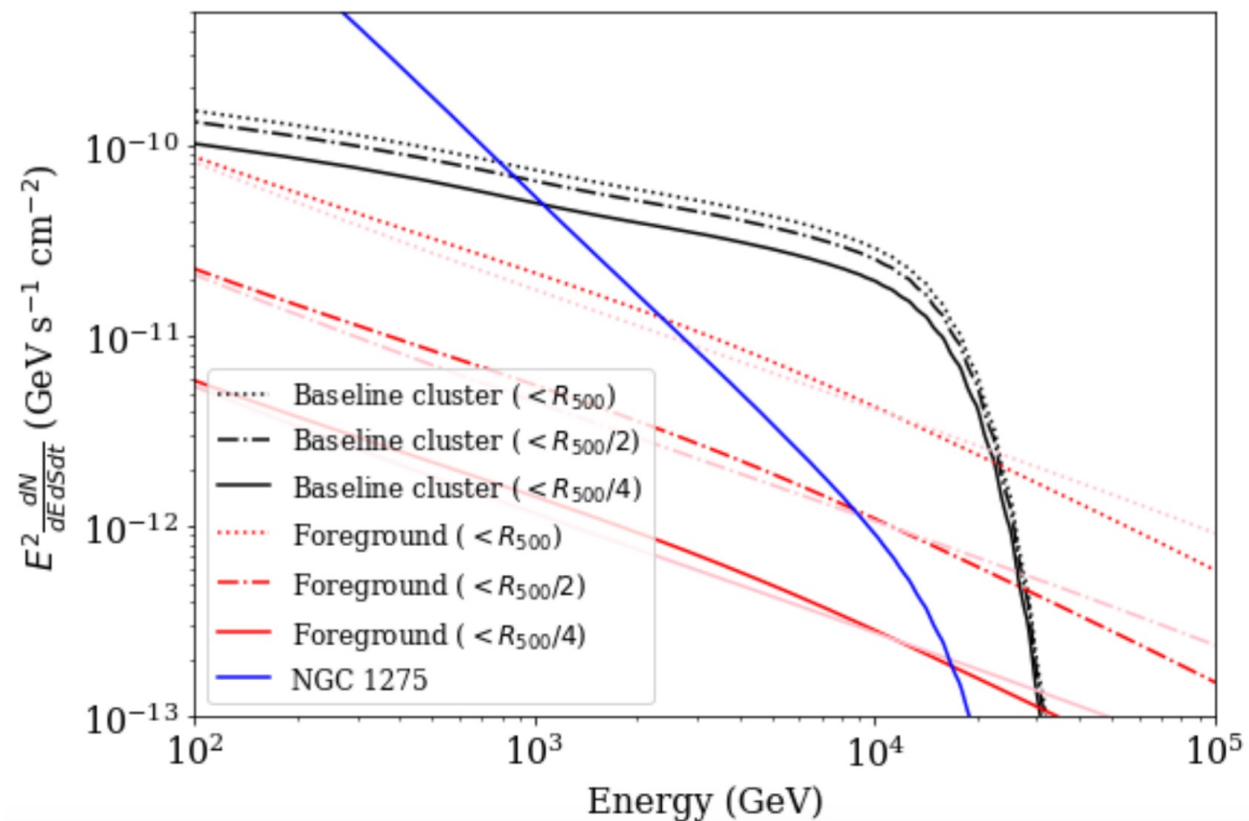


Caveat

- Since WStat takes into account background estimation uncertainties and makes no assumption such as a background model, it usually gives larger statistical uncertainties on the fitted parameters. If a background model exists, to properly compare with parameters estimated using the Cash statistics, one should include some systematic uncertainty on the background model.
- Note also that at very low counts, WStat is known to result in biased estimates. This can be an issue when studying the high energy behaviour of faint sources. When performing spectral fits with WStat, it is recommended to randomize observations and check whether the resulting fitted parameters distributions are consistent with the input values.

CTA ANALYSIS ELEMENTS

- Role of the Galactic diffuse emission:
 - Perseus is located “close” to the galactic plane (150.57, -13.26) deg
 - Baseline model for the galactic diffuse emission provided by D. Gaggero & P. de la Torre Luque
 - Integrated up to different radius and compared to CR baseline model
 - Worst case scenario, still factor ~few 10 below the expected CR emission



CTA ANALYSIS APPROACHES: DMTOOLS

- Most DM projects within CTA with same needs in terms of analysis tools and statistical treatment



Common set of tools

- Unified definitions, methodology
- Avoids repetition of same coding
- Allows easy comparison of results.
- Everyone can potentially contribute

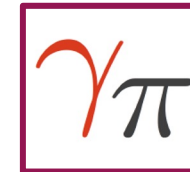
- Creation & coordination of *DMTools Task Force* within CTA
- Gammapy beta-testing and software development



Since v-0.8 to v-1.0
(15 versions)



- Gammmapy embedded functions:
 - `DarkMatterAnnihilationSpectralModel`
- GitHub repository:
 - `Gammmapy-DMTools`
https://github.com/peroju/dmtools_gammmapy
- Gammmapy coding sprints



CTA ANALYSIS APPROACHES: DMTOOLS

ON-OFF/Wobble Analysis

Standard for IACTs

Point-like

- Lowest complexity
- Most constraining results

Extended

- More complex and realistic than point-like approach
- Benefits from CTA large FoV and angular resolution

Template fitting

State-of-the-art pipeline

Minuit

- Already embedded in `Gammapy`
- Historically used fitter (`iminuit`) and very well documented (stability)

MCMC

- Flexible definition of likelihood and priors
- Easy analysis of correlations

CTA ANALYSIS APPROACHES: DMTOOLS

Basic functioning of the pipelines

Input DM model

- Spectral (based on Cirelli+12)
- Spatial (point-like, analytical, FITS files)



Combine with observation set-up

- IRFs
- Observation time
- Backgrounds



- Simulated Observation (Poisson realization)
- Observation

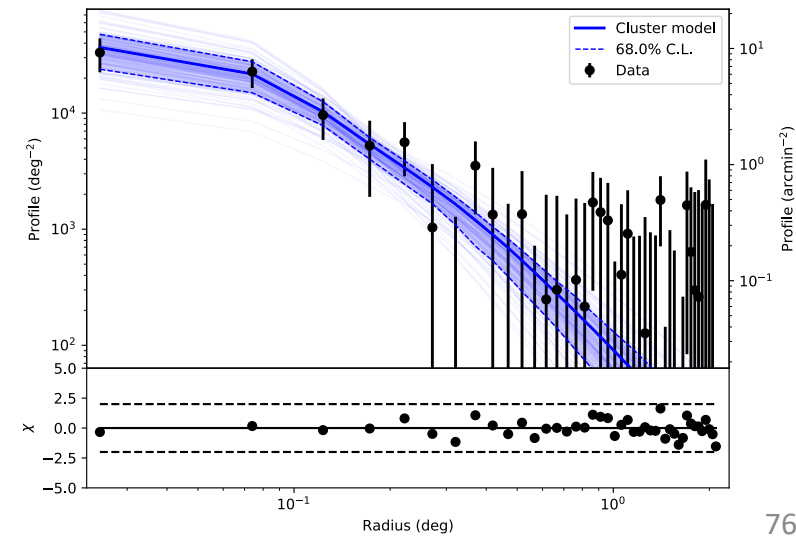
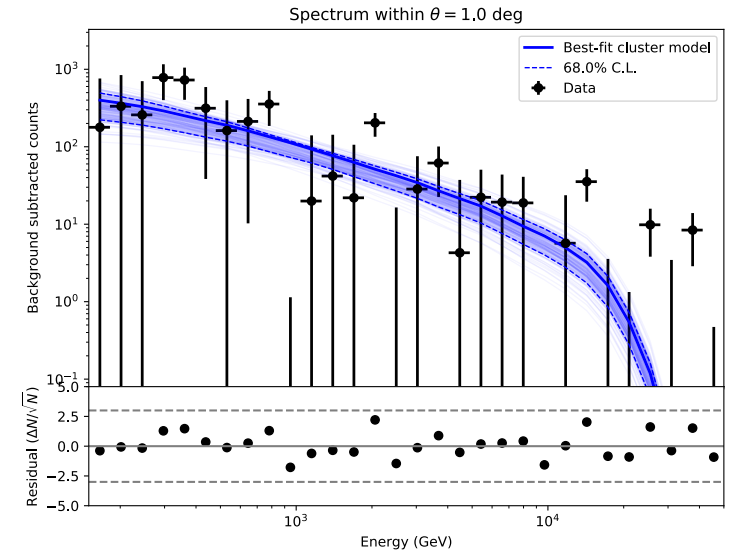
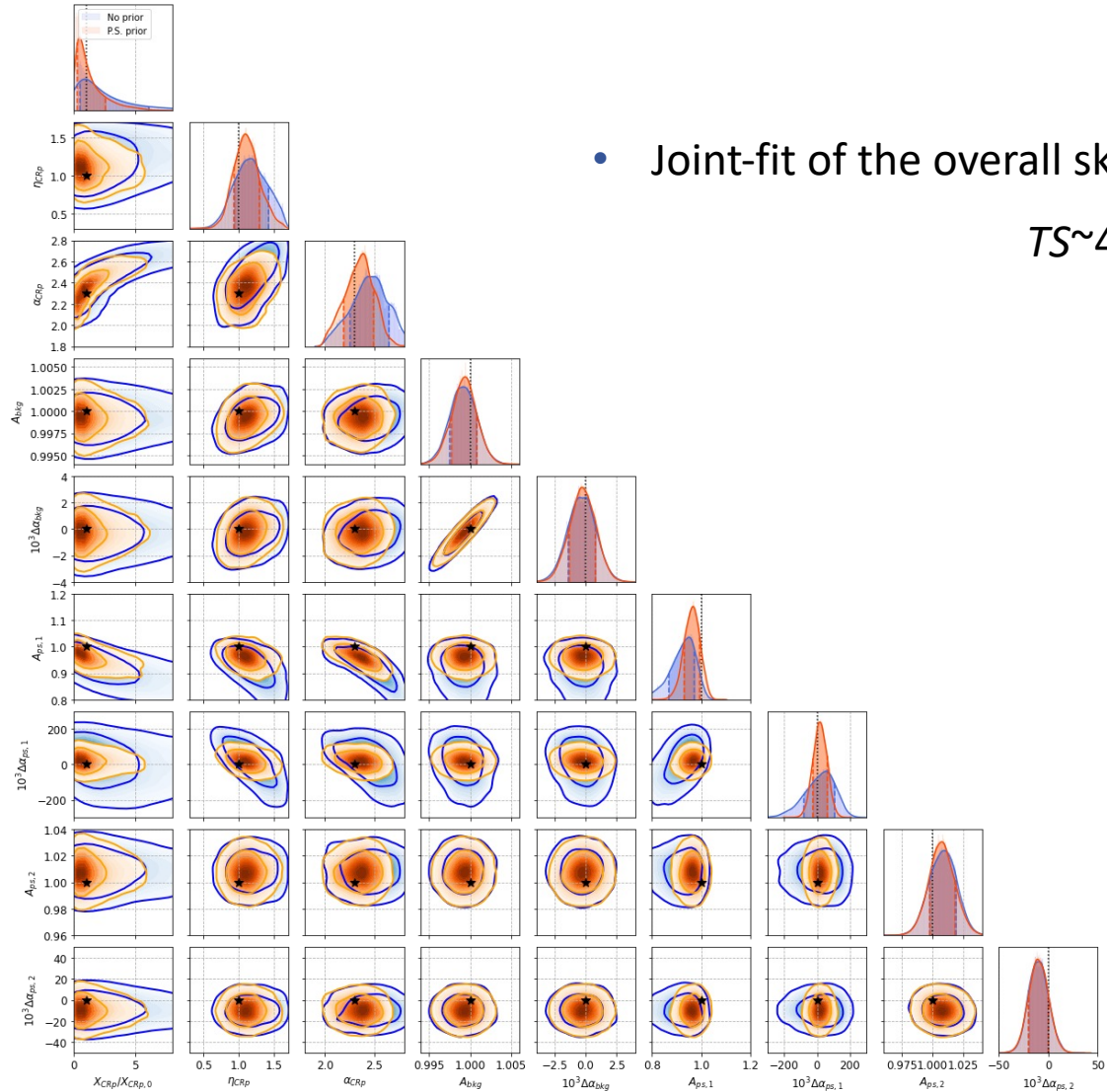
Enter the DM fit loop

1. For each realization, consider a list of channels and for each, a list of DM masses
2. Perform a likelihood fit to this specific model
3. Check $TS(H_{null}) \geq 25$
4. Compute $\langle \sigma v \rangle$ upper limits with $TS(H_{\text{best-fit}}) = 2.71$

INSIGHT RESULTS: CR ANALYSIS SUMMARY

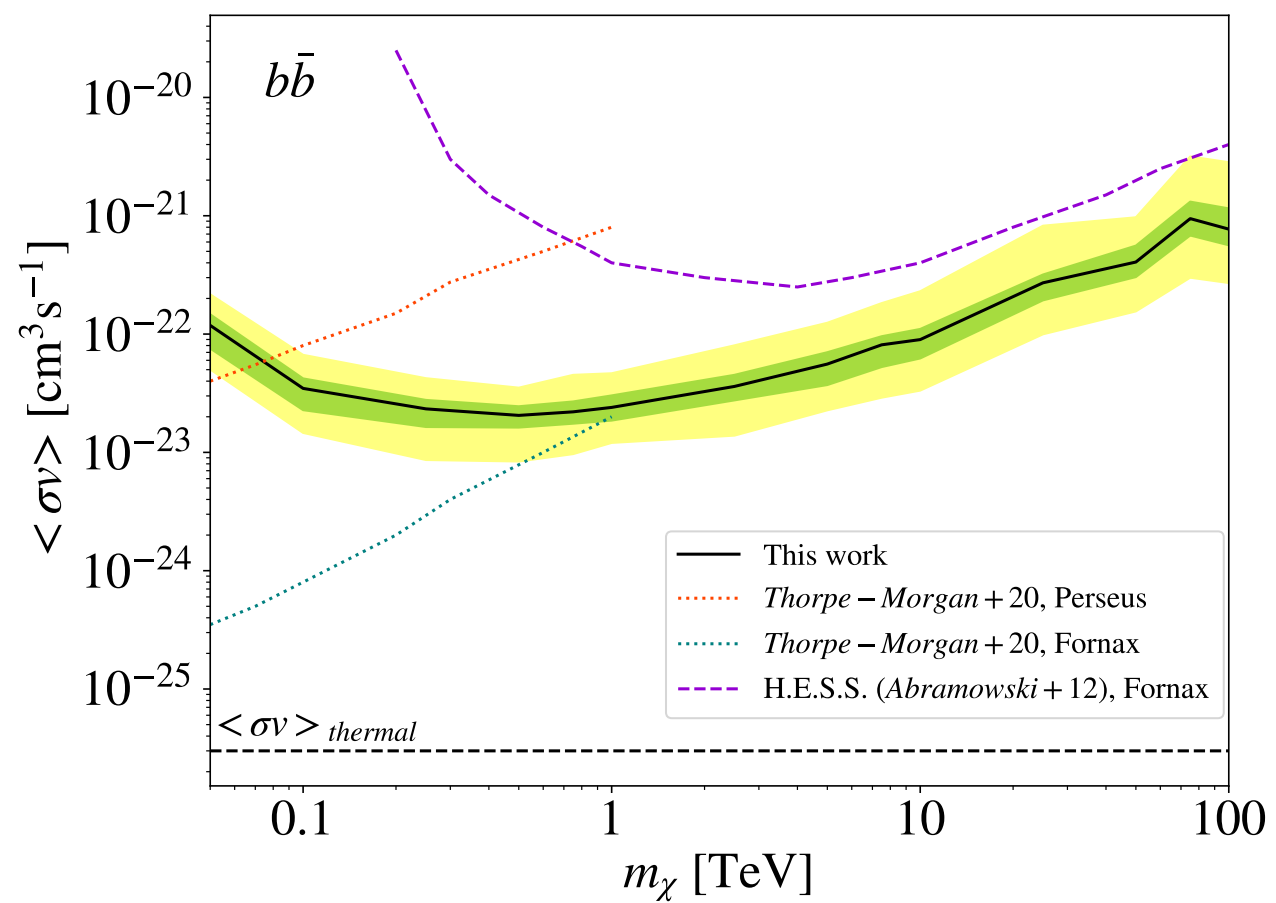
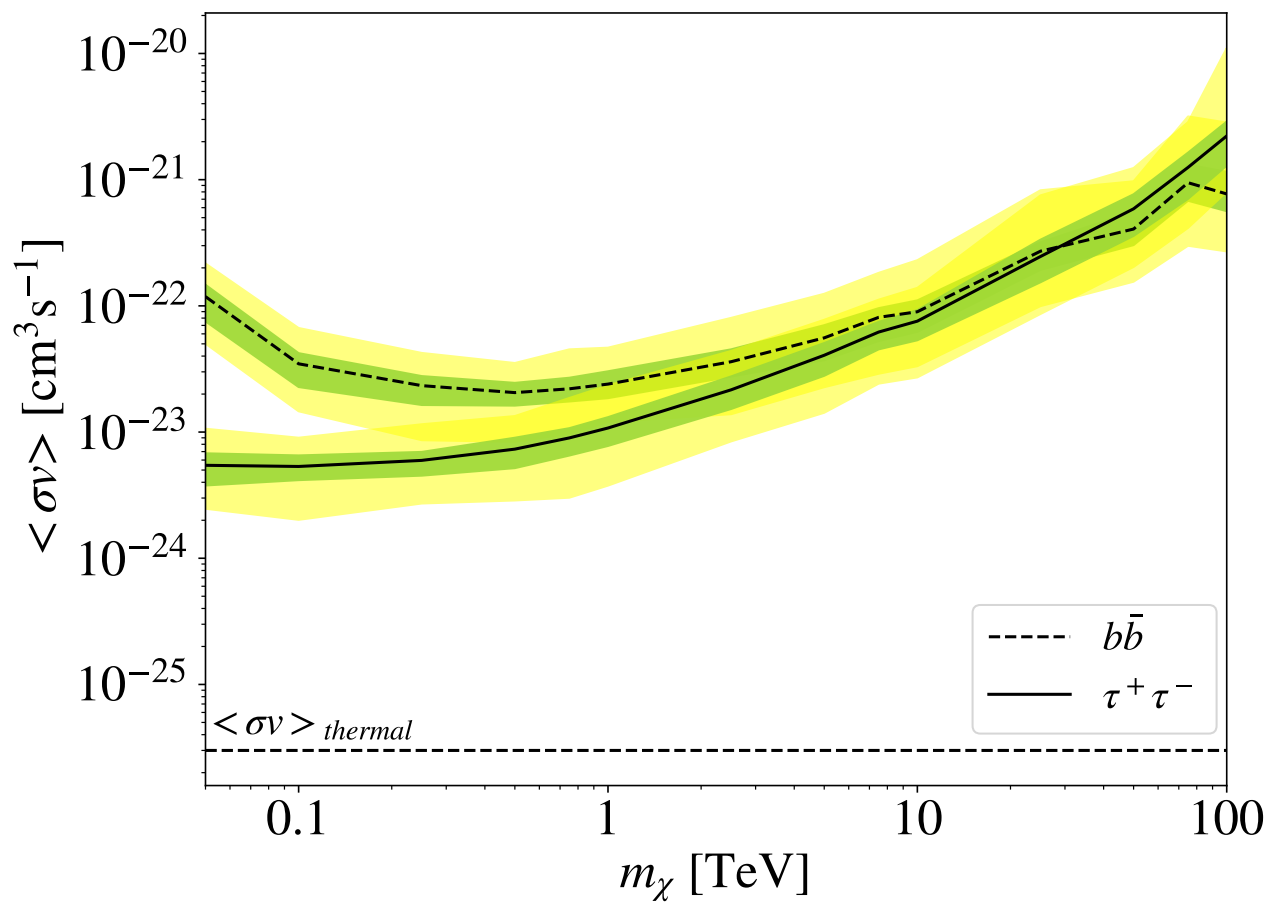
- Joint-fit of the overall sky model simultaneously

$TS \sim 42$



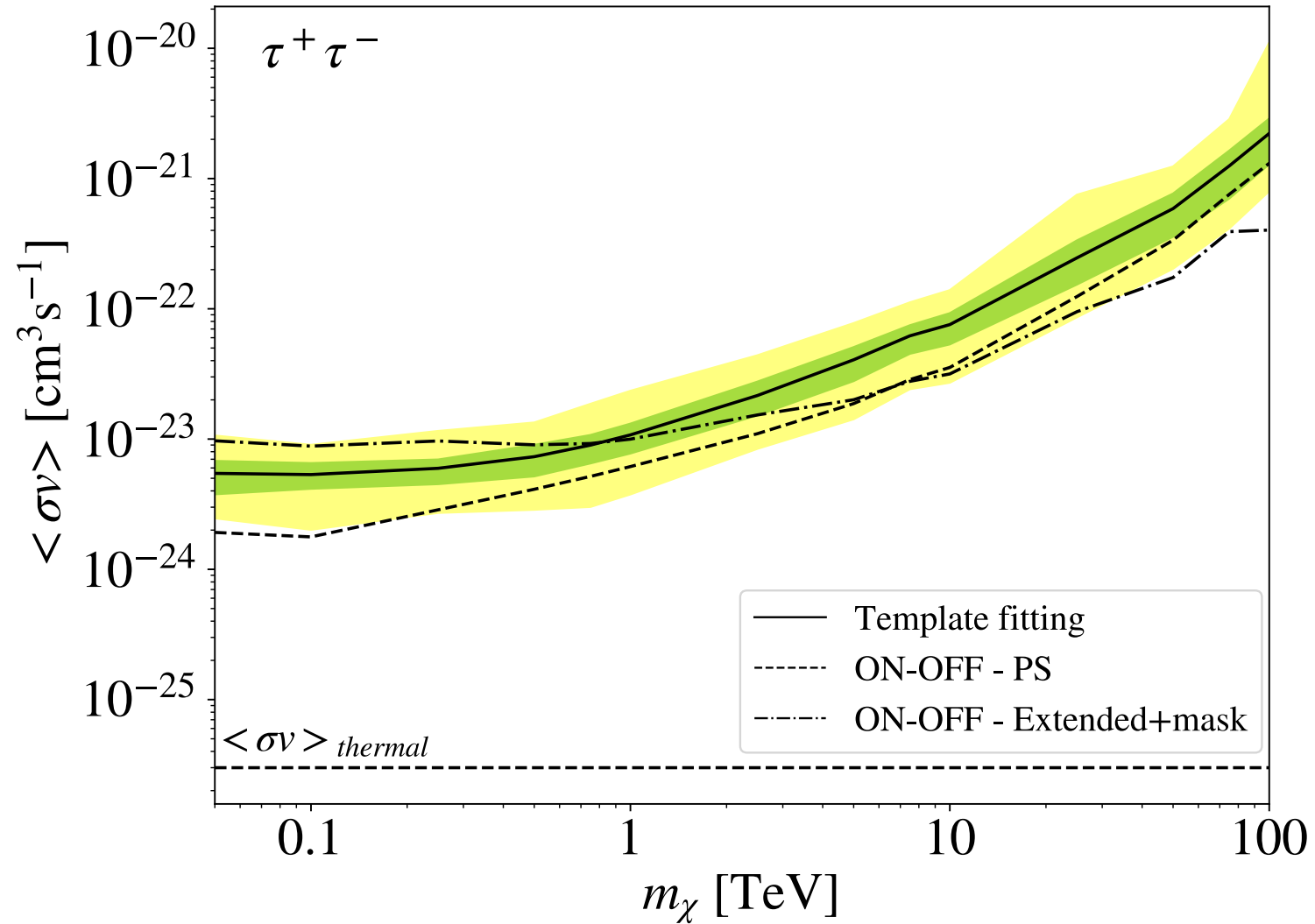
INSIGHT RESULTS: DM CONSTRAINTS

Annihilation (MED)



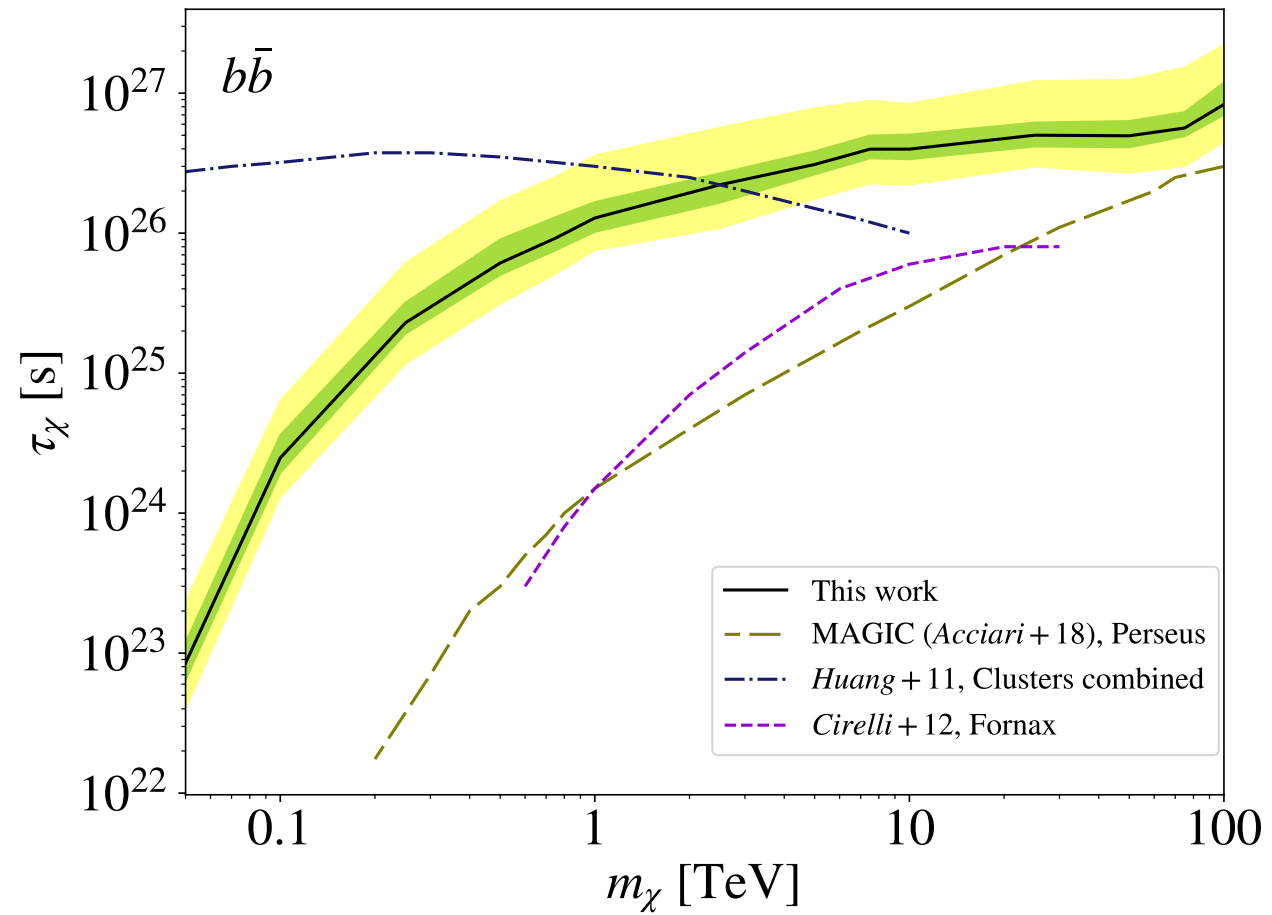
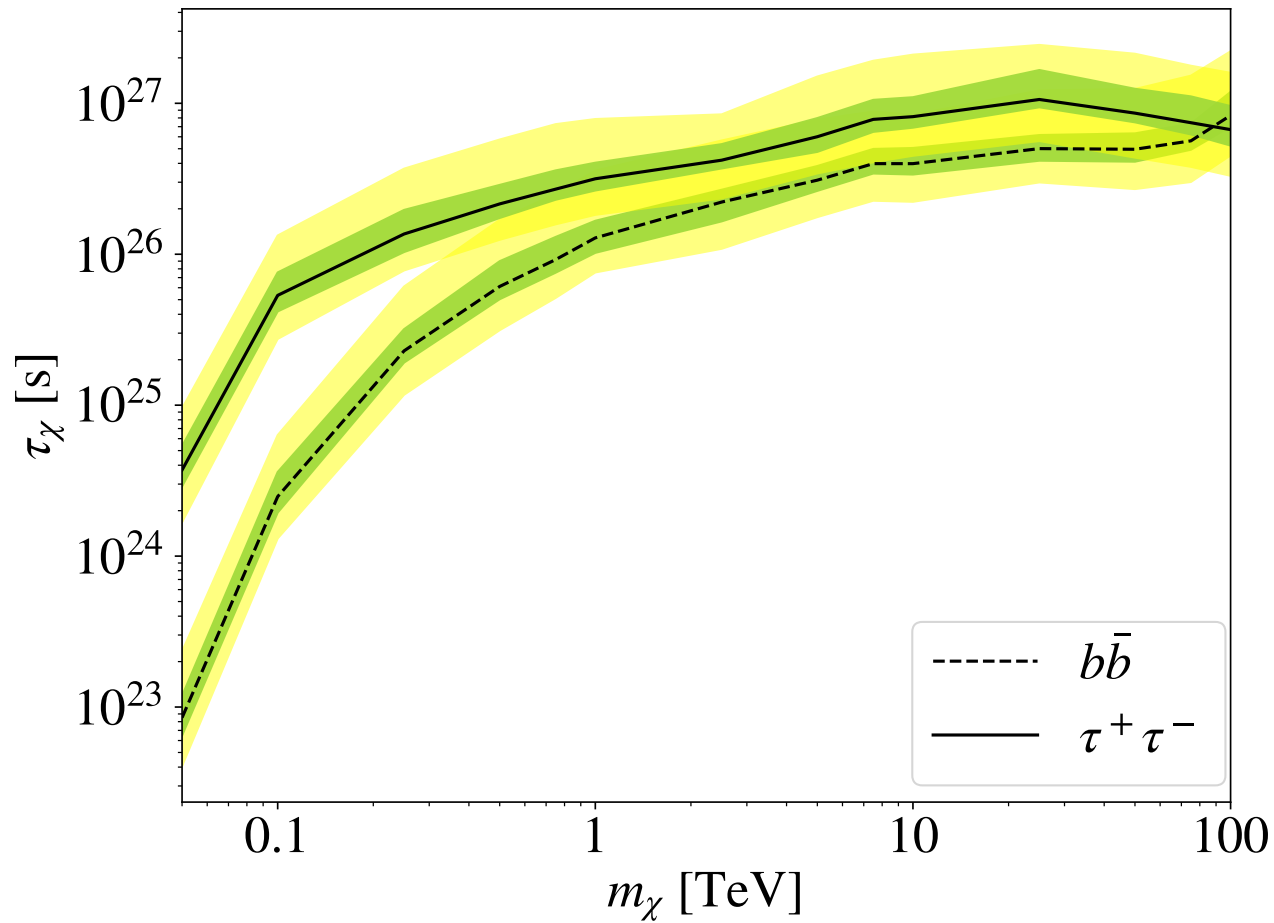
INSIGHT RESULTS: DM CONSTRAINTS

Annihilation (MED)



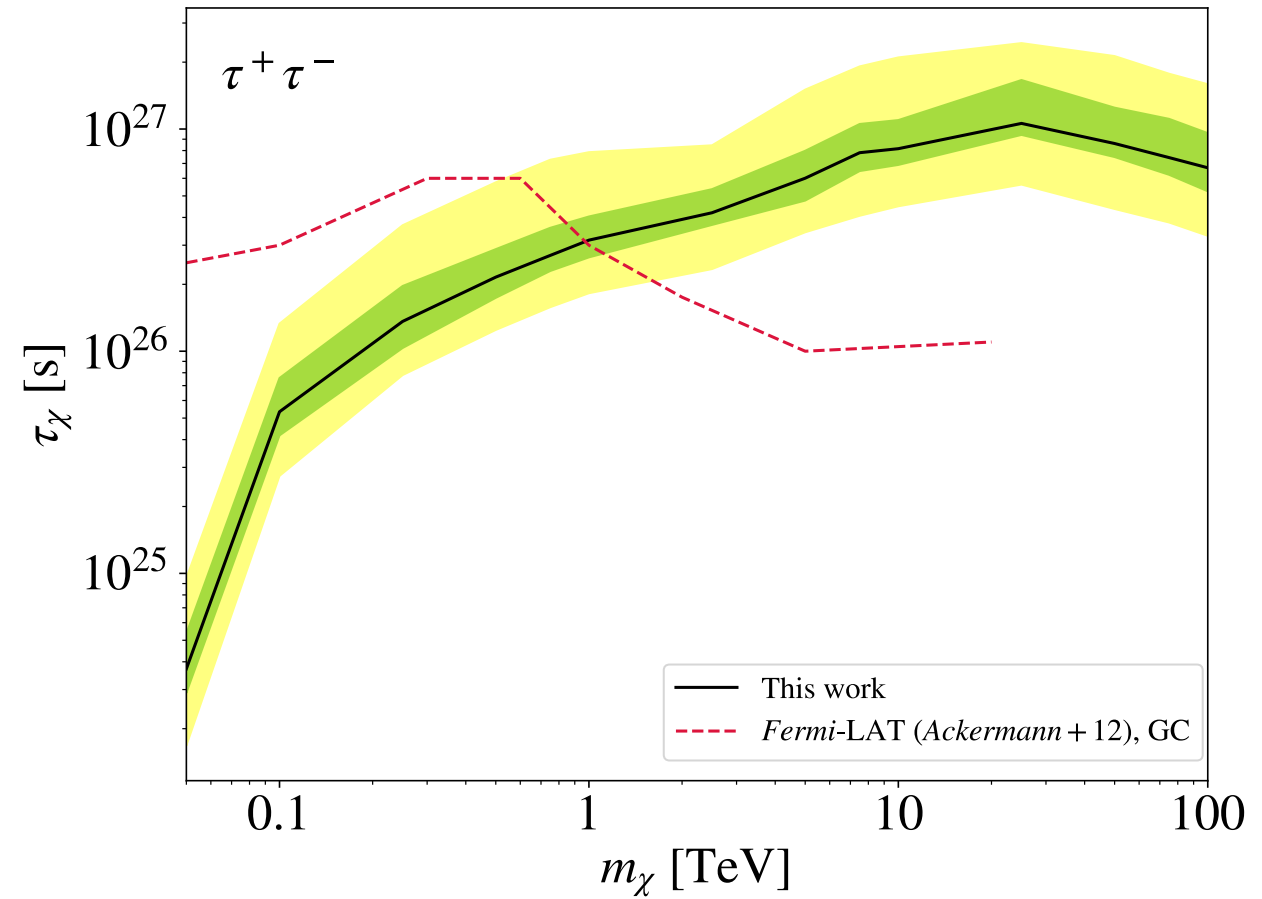
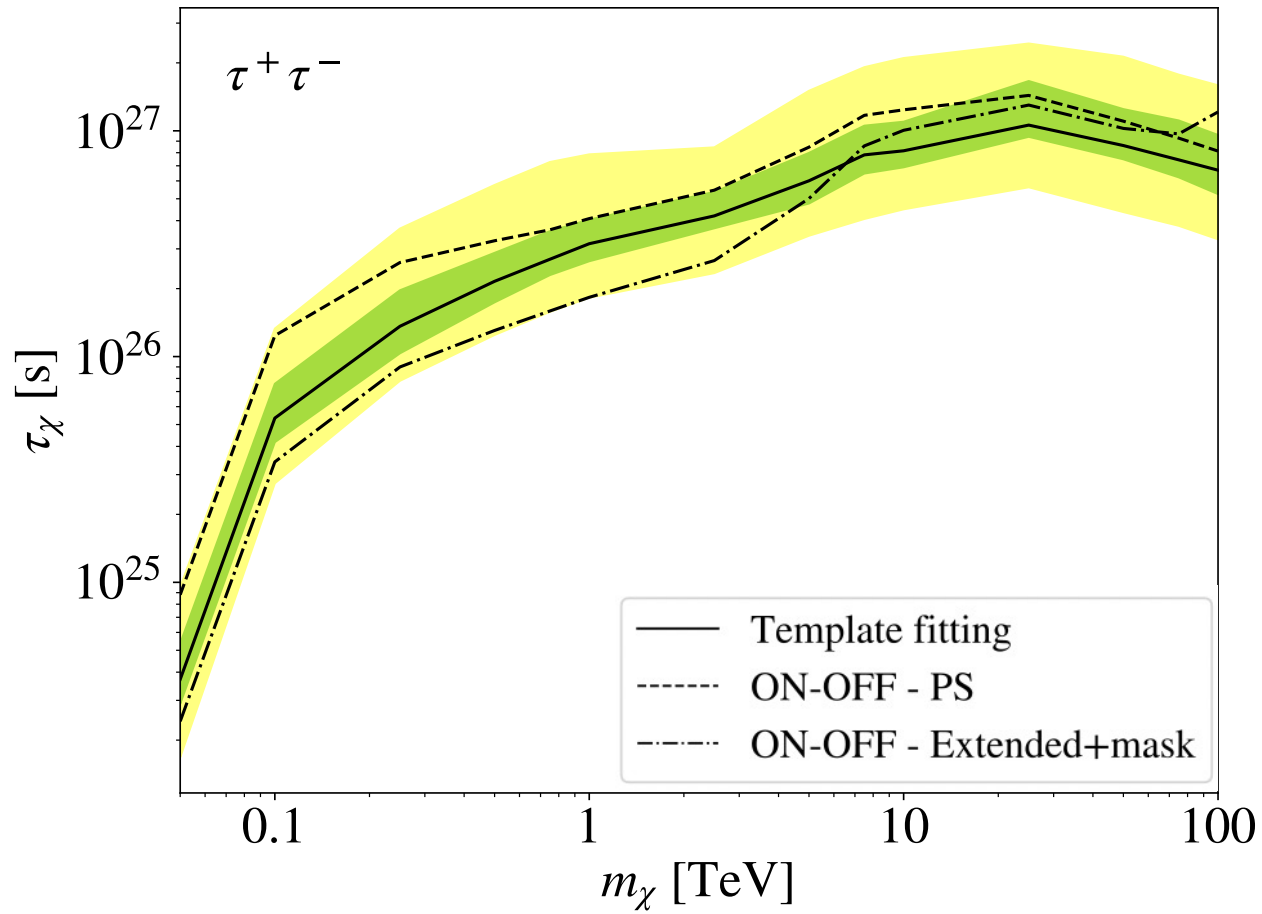
INSIGHT RESULTS: DM CONSTRAINTS

Decay



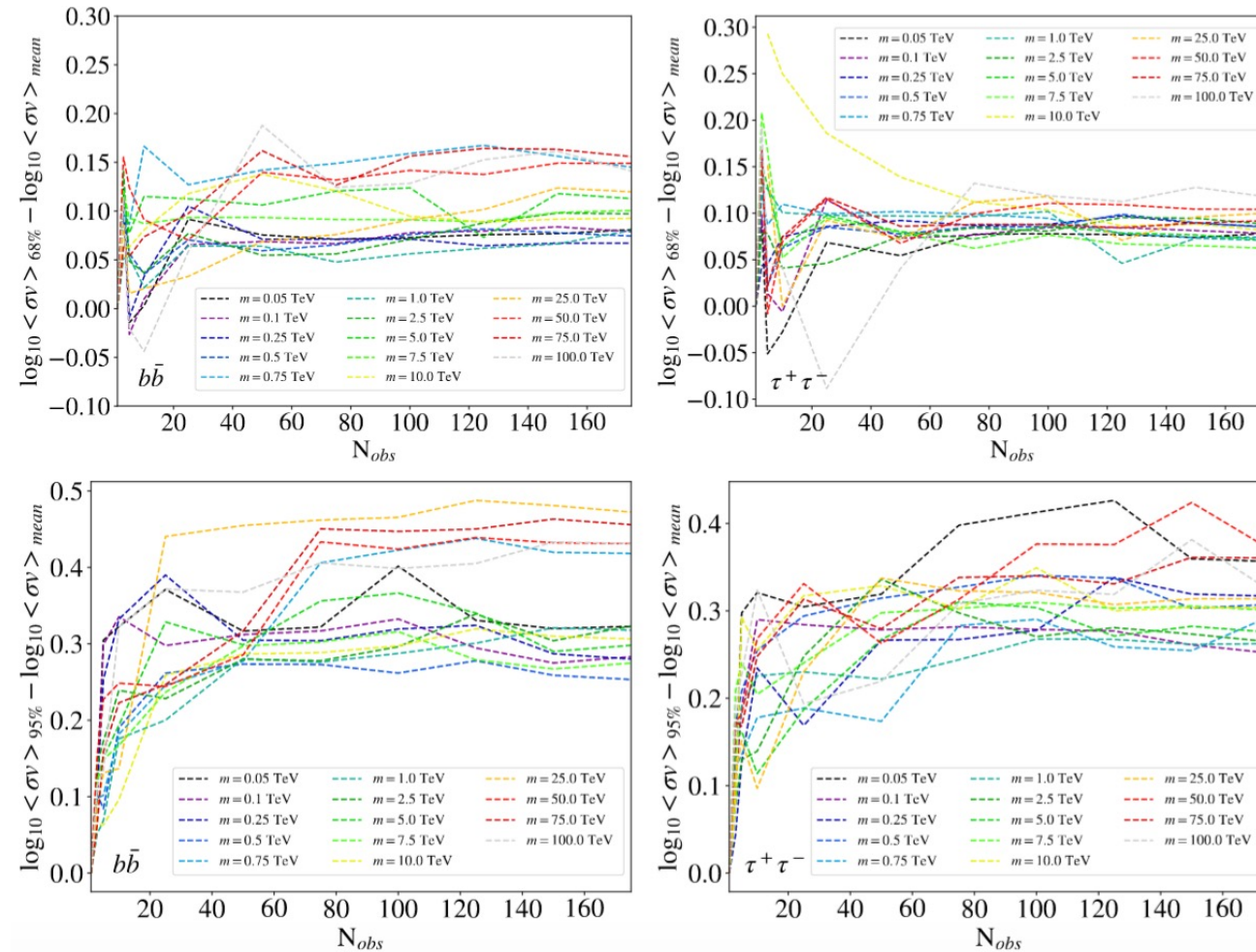
INSIGHT RESULTS: DM CONSTRAINTS

Decay



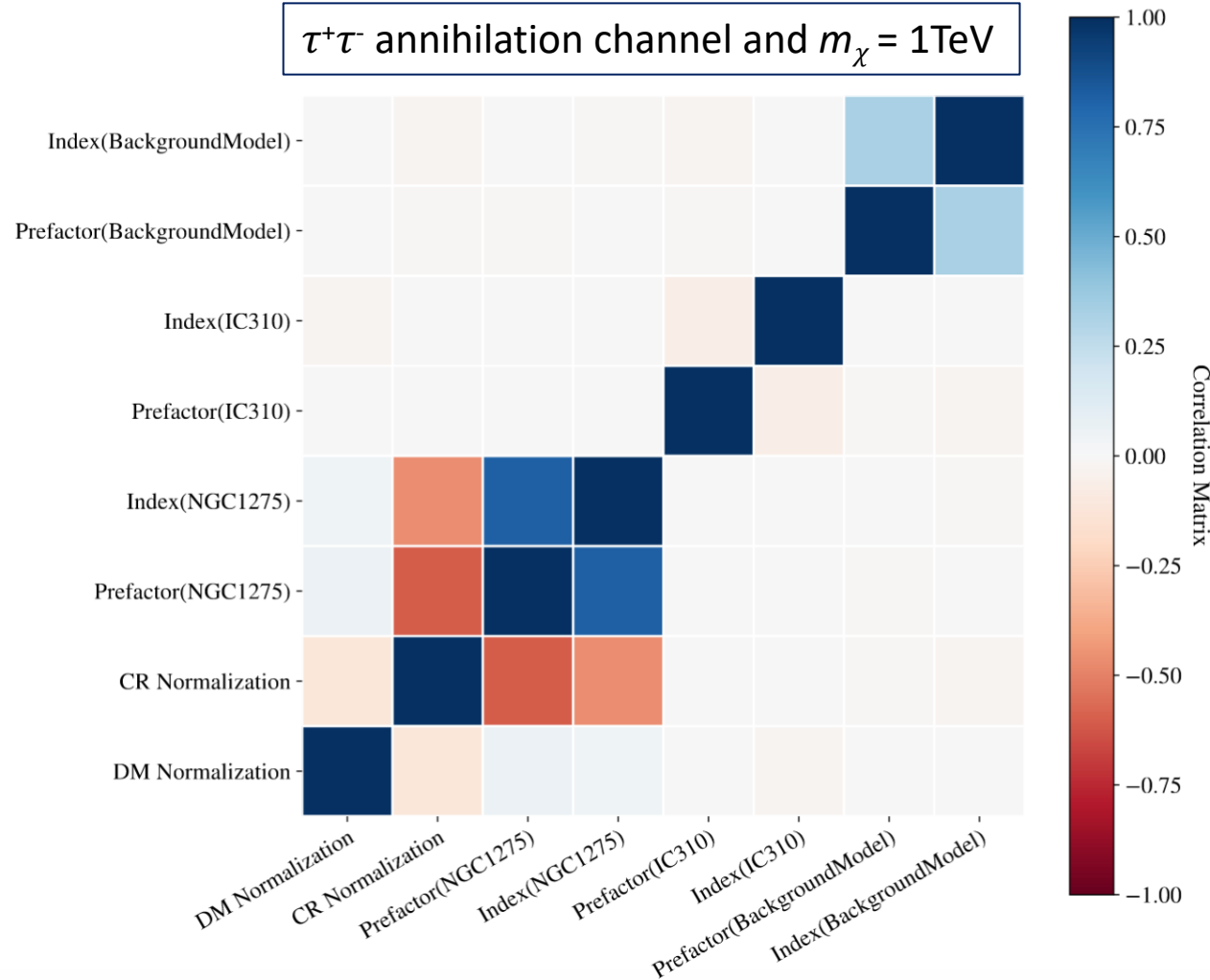
DM CONSTRAINTS: SCATTER BANDS

One-sided 1σ & 2σ scatter bands evolution with the number of realizations
(annihilation MED model, template fitting)



CTA ANALYSIS: INTERPLAY BETWEEN COMPONENTS

$\tau^+\tau^-$ annihilation channel and $m_\chi = 1\text{TeV}$



- Recovered mean values for CRs, NGC 1275, IC 310 and IRF-BKG within 1σ , independently of the channel or m_χ
- May be dependent on the considered DM scenario (annihilation/decay), channel or m_χ
- DM flux should not be neglected, as it seems to affect the correlations of CR normalization and NGC 1275

CTA ANALYSIS CONFIGURATION (II): ON-OFF ANALYSIS

- First analysis approach
 - Only includes γ -ray emission from DM and background from IRFs
 - Assumes the DM emission template
 - Circular mask of 0.1 deg in the centre
 - Historically used in Imaging Air Cherenkov Telescopes (IACTs) as MAGIC

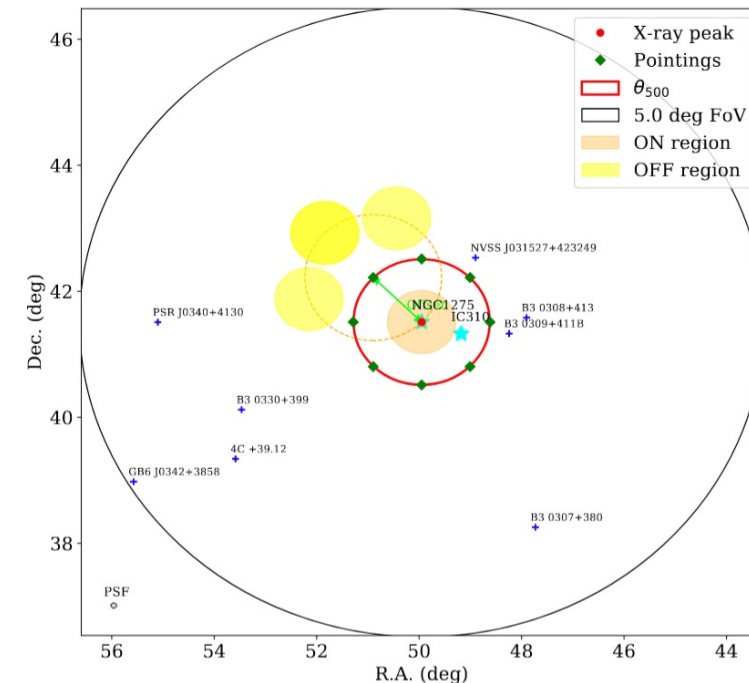
Lowest level of complexity,
more constraining results

Direct comparisons

- Different set-ups tested, best results for:

| | |
|-----------------------|------------------|
| Regions | 1 On/3 Off |
| Regions radius [deg] | 0.5 |
| Pointing (l, b) [deg] | (150.57, -13.26) |
| Offset [deg] | 1 |

| | |
|--------------------|----------------------|
| N_{obs} | 100 |
| T_{obs} [h] | 300 |
| IRFs | North_z20_50h, prod5 |
| Energy range [TeV] | 0.03 - 100 |

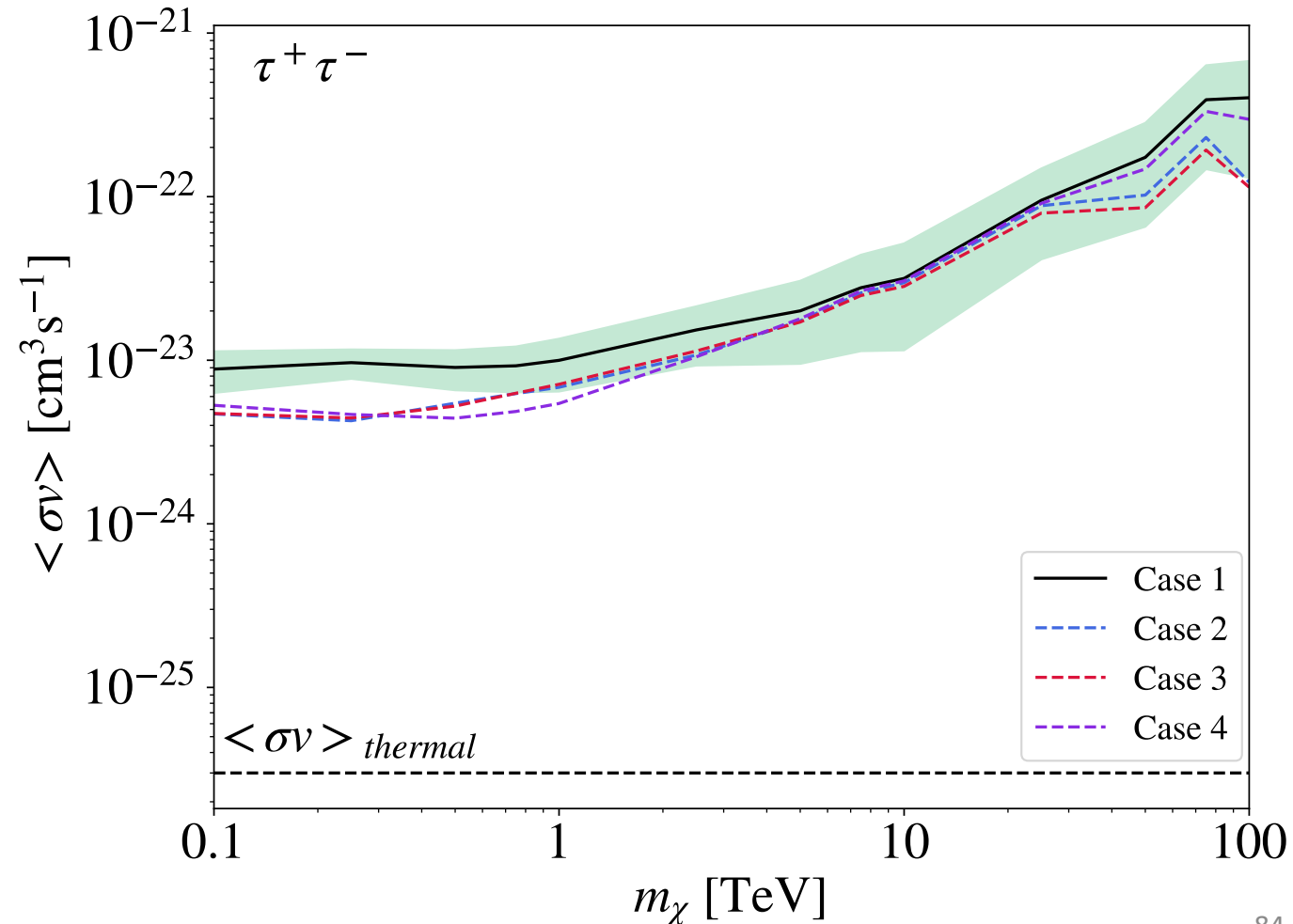


DM CONSTRAINTS: ON-OFF SET-UPS

Different configurations tested
with the ON-OFF set-up

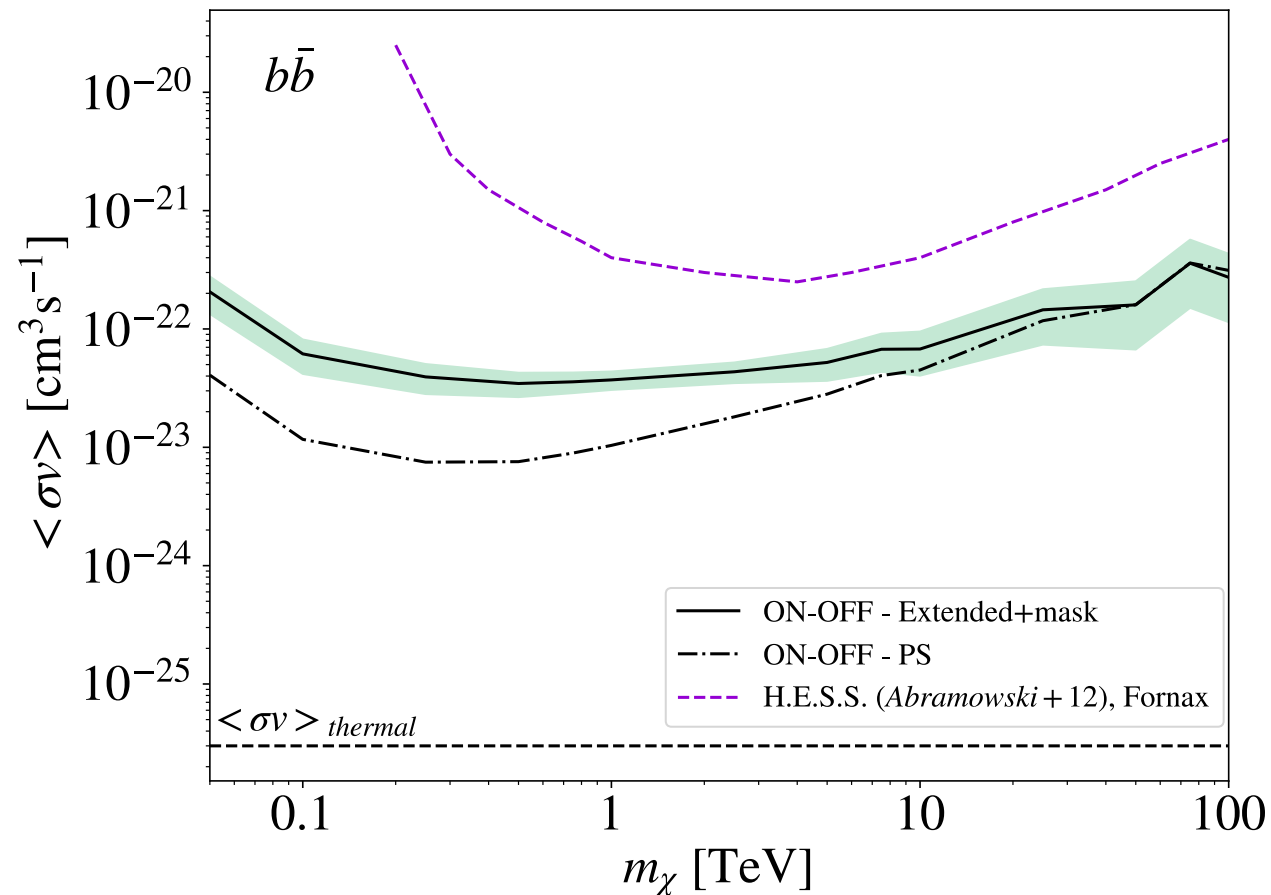
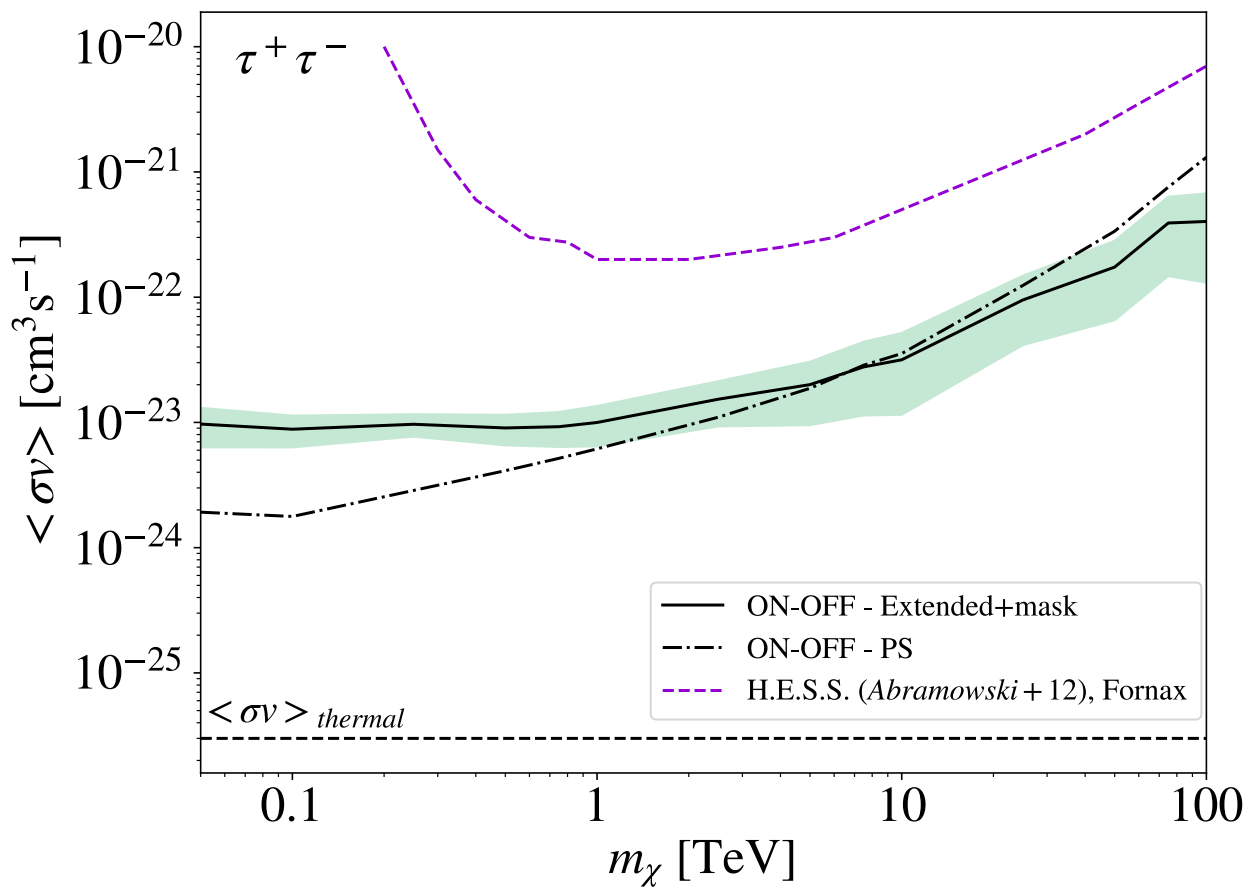
| Case | θ_{pointing} [deg] | θ_{ON} [deg] | N_{OFF} | κ |
|----------|----------------------------------|----------------------------|------------------|----------|
| 1 | 1 | 0.5 | 3 | 3 |
| 2 | 0 | 1 | 3 | 3 |
| 3 | 0.5 | 0.5 | 3 | 3 |
| 4 | 1 | 0.5 | 5 | 5 |

Limits for Perseus for MED annihilation model
(DM template + mask)



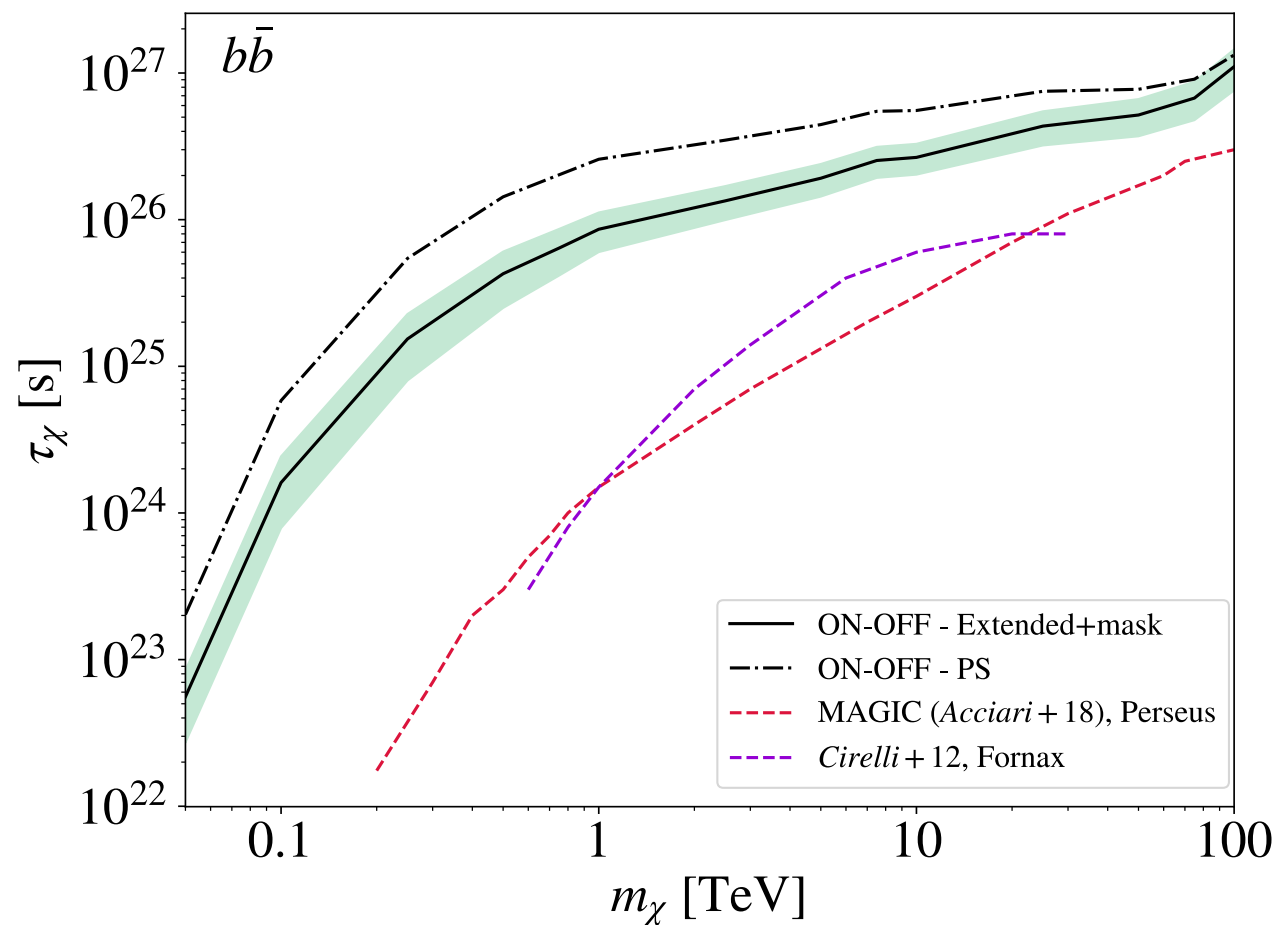
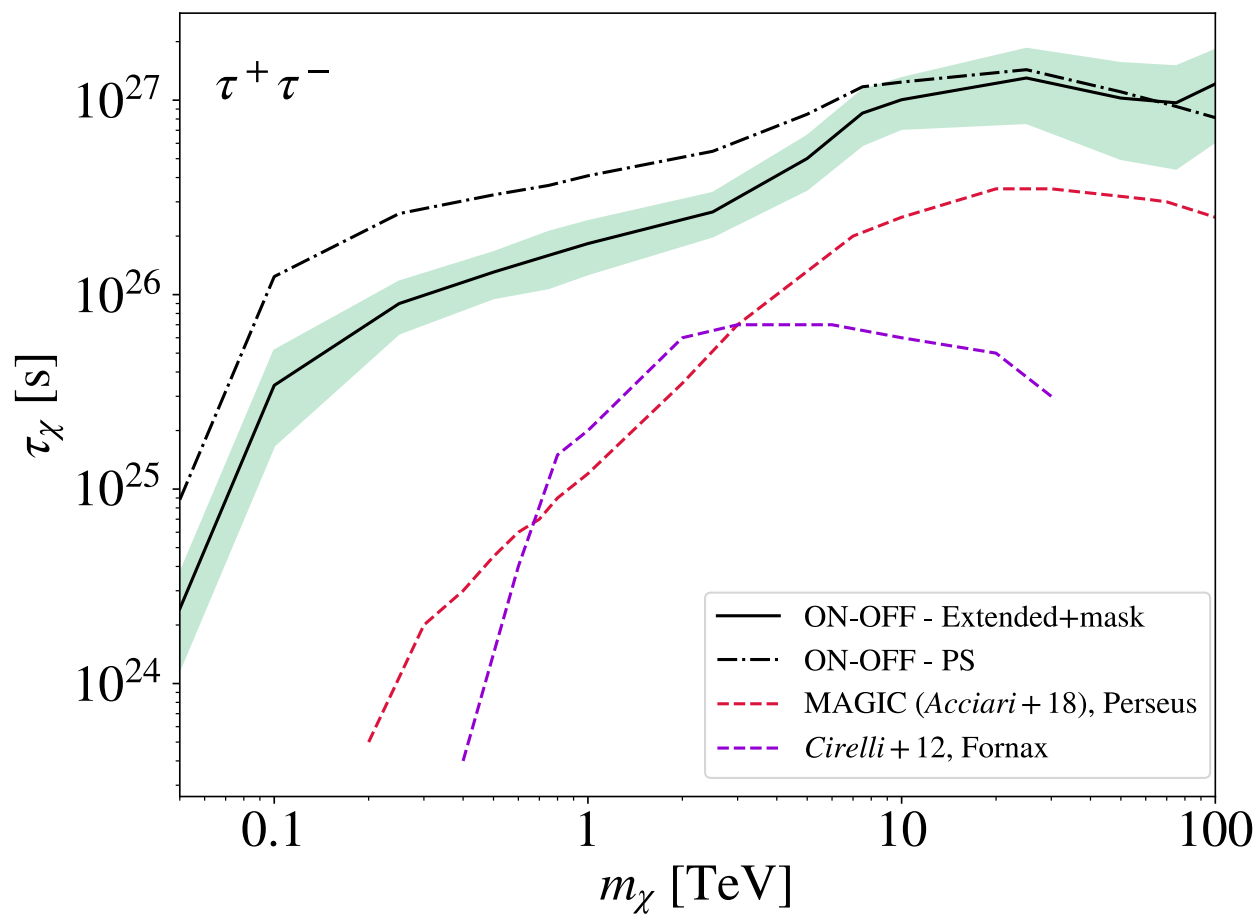
ON-OFF RESULTS: DM CONSTRAINTS

Annihilation (MED)



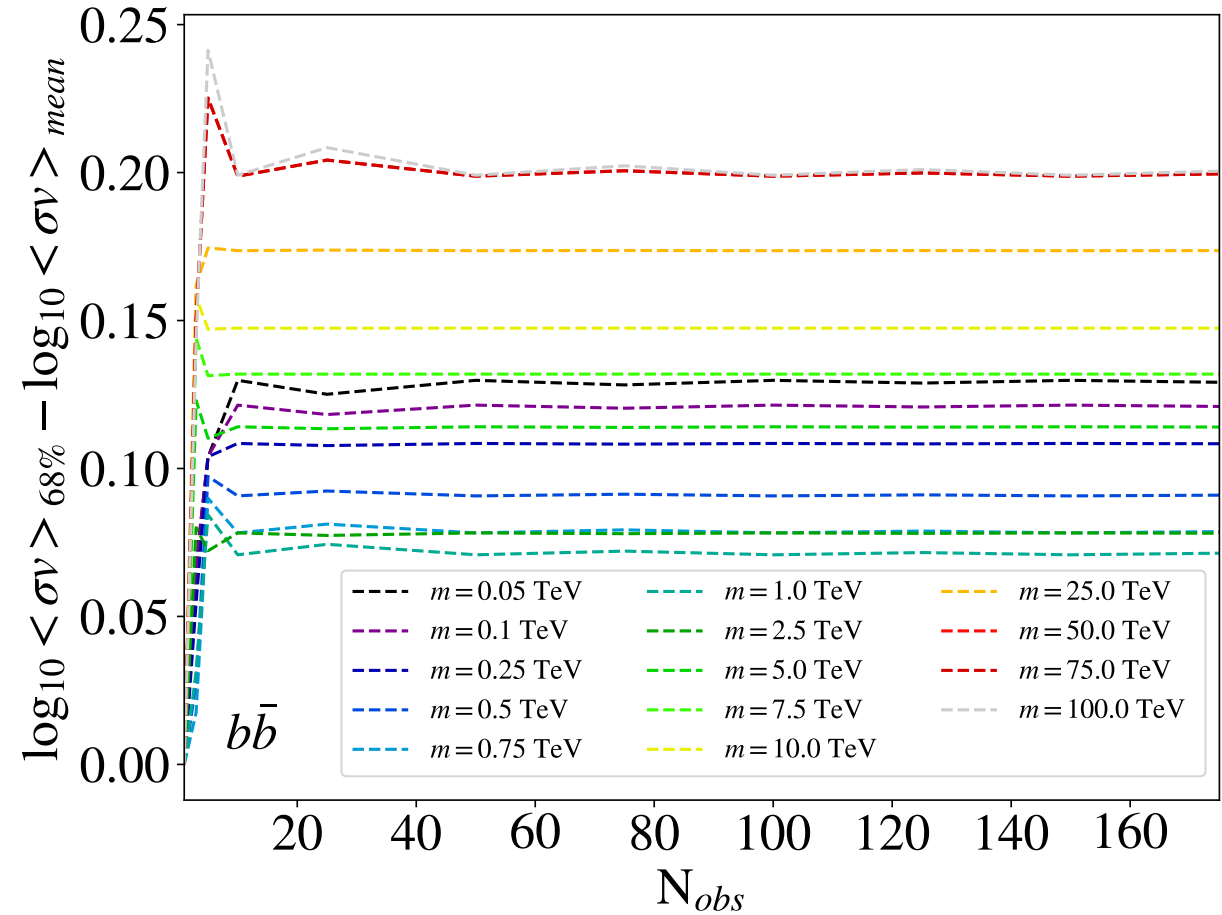
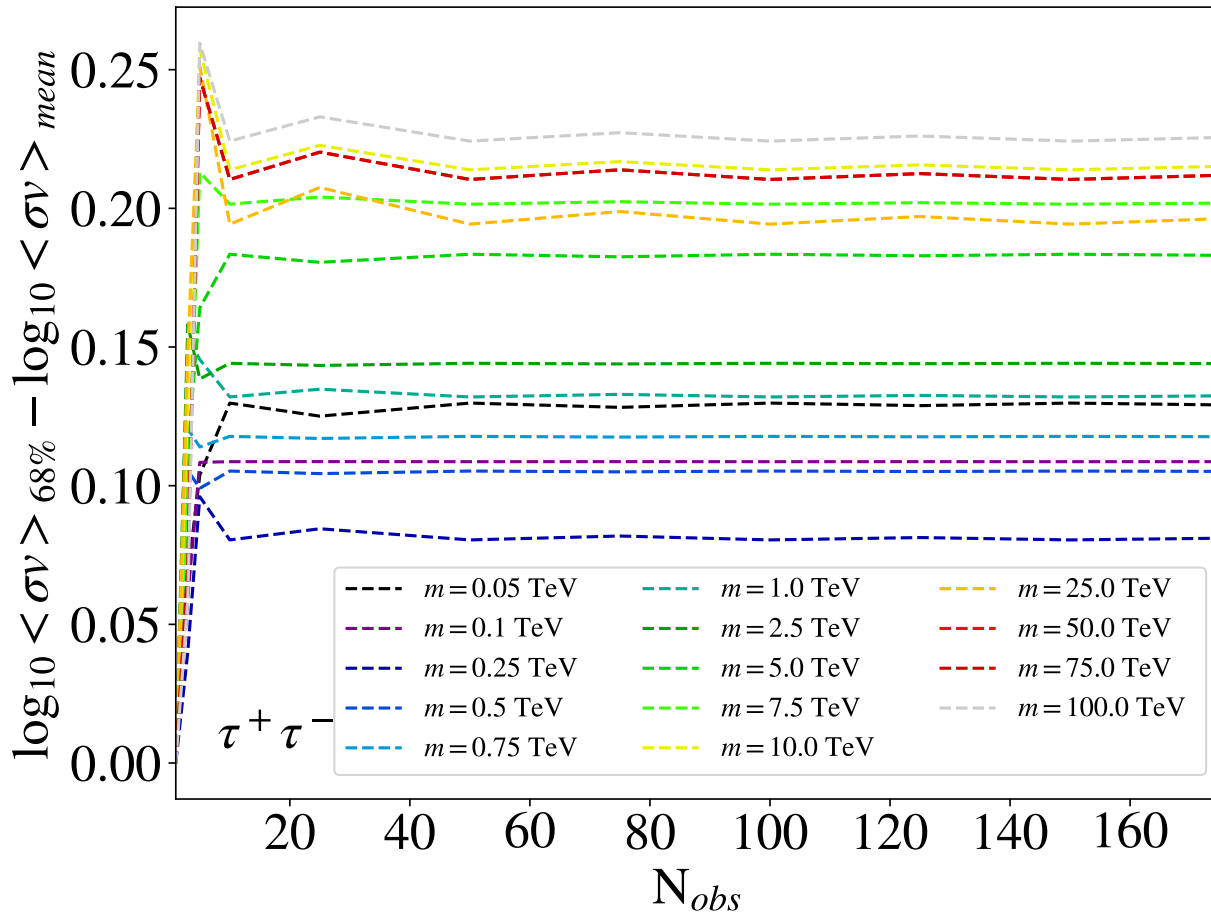
ON-OFF RESULTS: DM CONSTRAINTS

Decay

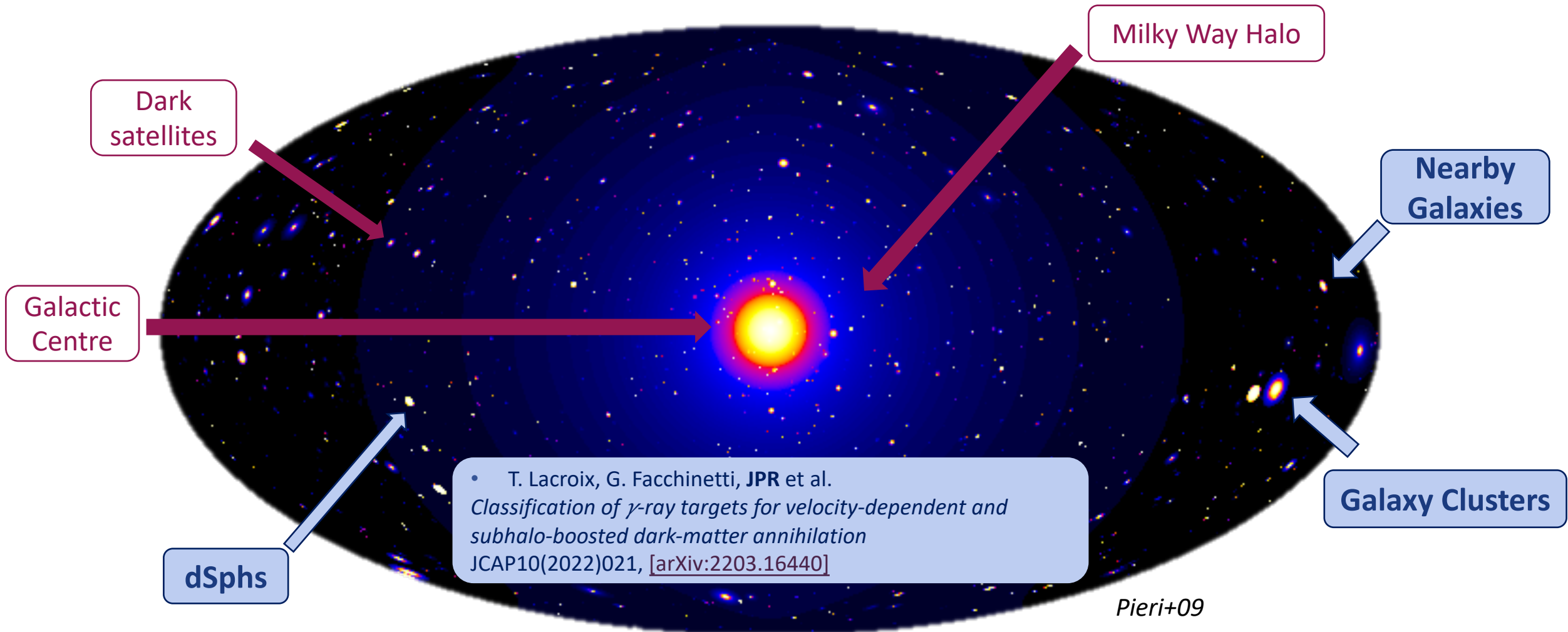


ON-OFF RESULTS : SCATTER BAND

One-sided 1σ band evolution with the number of realizations
(annihilation MED model, ON-OFF - Extended+mask)



γ -RAY DM SEARCHES IN DIFFERENT ASTROPHYSICAL OBJECTS



DIRRS AS TARGETS FOR γ -RAY DM SEARCHES

- Dwarf Irregular Galaxies (dIrrs)

- Rotationally supported objects

- High DM density ✓

DM density from their rotation curves (RCs)

- Located in our Local Volume:

$0.5 \text{ Mpc} < d_L < 10 \text{ Mpc}$

Closeby ✓

- Have masses between $10^8 - 10^{10} M_\odot$

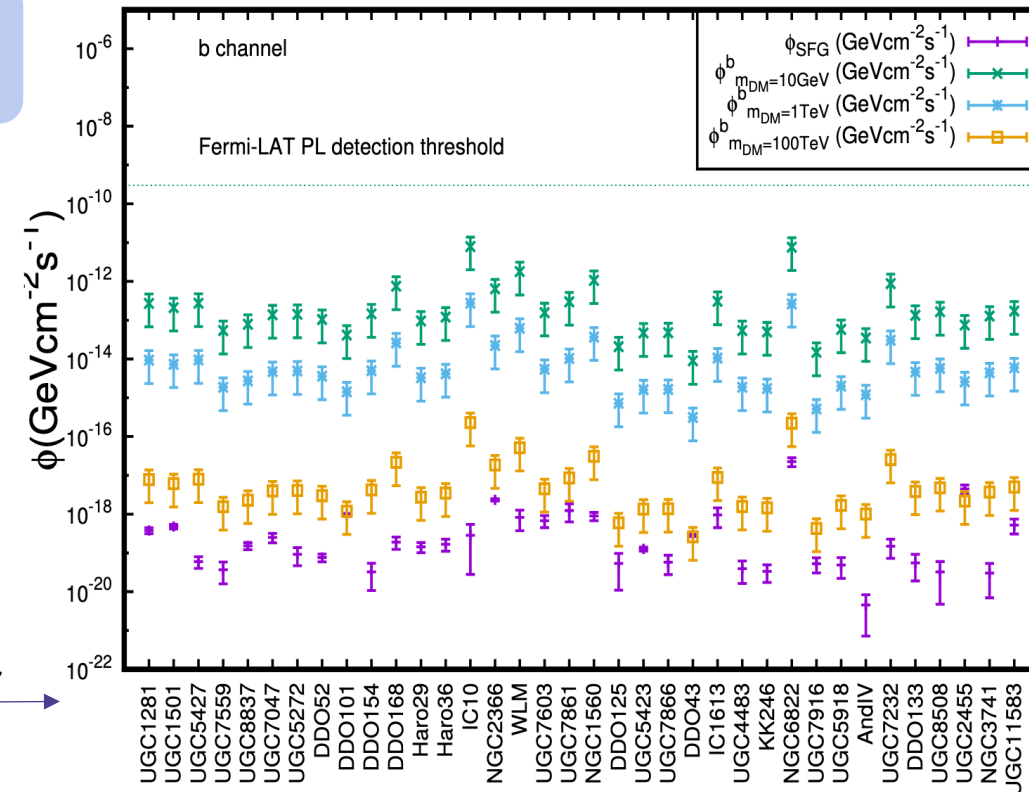
Massive objects

Population of substructures expected

- Star-forming galaxies

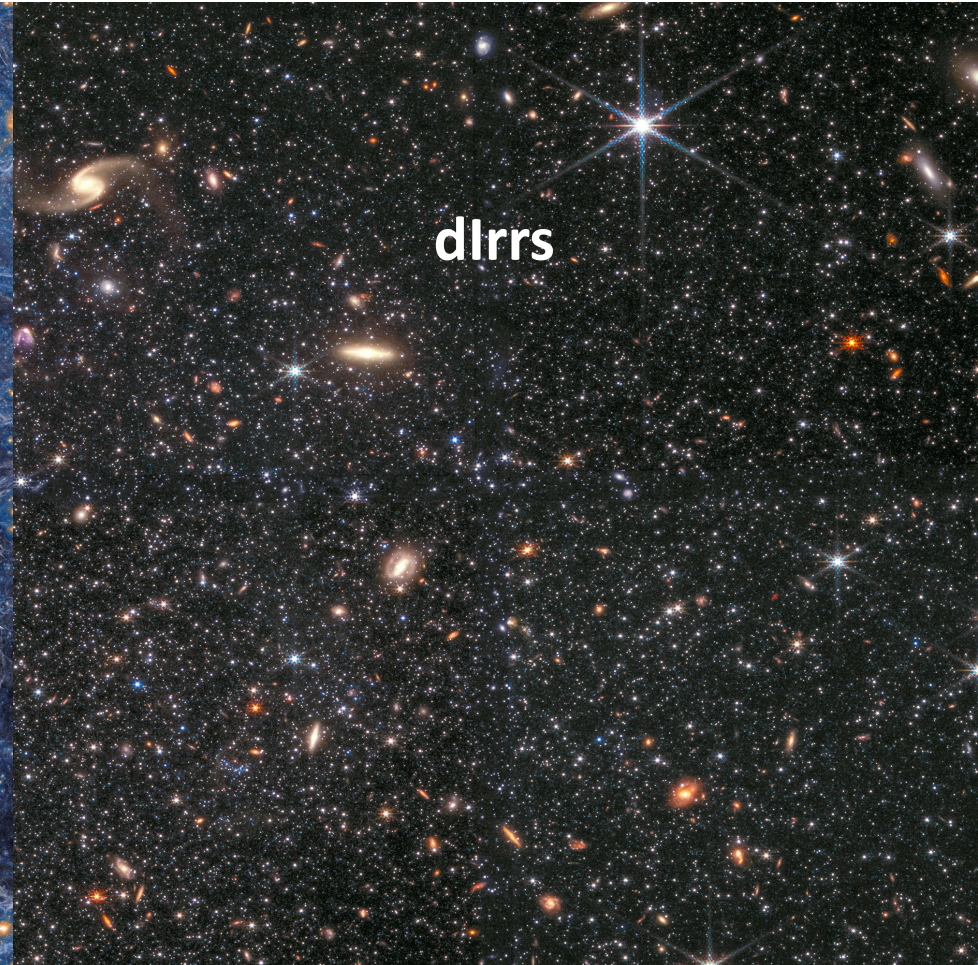
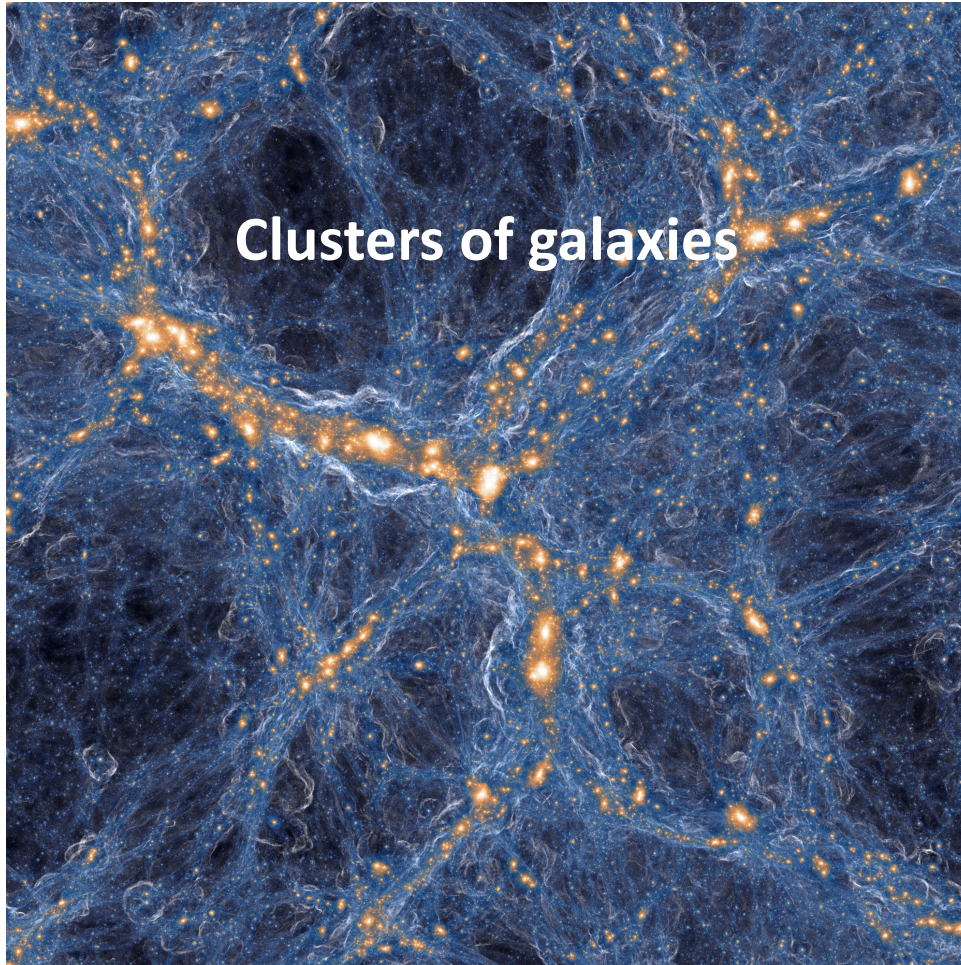
Negligible γ -ray background

Gammaldi+17



CAN WE CLASSIFY THE STUDIED TARGETS?

- Several astrophysical objects studied, with pros and cons



CAN WE CLASSIFY THE STUDIED TARGETS?

- Several astrophysical objects studied, with pros and cons

Clusters of galaxies

- Most massive - 10^{14} - $10^{15} M_{\odot}$
- Further - $z < 0.1$
- Higher substructure boost - $B \sim 9$
- Best targets for decay
- Astrophysical γ -ray emission
- Up to $\log_{10} J_{\text{MED}} \sim 18.40$

dIrrs

- Less massive - $10^8 - 10^{10} M_{\odot}$
- Closer - $d_L < 1$ Mpc
- Lower substructure boost - $B \sim 4$
- Not studied for decay
- Negligible astrophysical γ -ray emission
- Several at $\log_{10} J_{\text{MED}} \sim 18.50$



dSphs

- Classical
- Ultra-faint

CAN WE CLASSIFY THE STUDIED TARGETS?

- Build intra- and inter-family ranking of targets for γ -ray DM searches
- The absence of firm detection of vanilla-WIMP DM

Let us broaden the theoretical particle framework...

| | | | |
|--|--|--|---|
| Velocity dependence of $\langle\sigma v\rangle$ | Canonical s-wave partial wave may be naturally suppressed | Mediator is a scalar | \rightarrow p -wave dominates $\sigma v_{\text{rel}} \propto v_{\text{rel}}^2$ |
| Modification of the short-range $\langle\sigma v\rangle$ | Exchange of light mediator induces a long-range interaction between DM particles | Complex dark sectors | \rightarrow Sommerfeld enhancement |
| Contribution of DM subhalos | Dependent on host halo mass and their structural properties | Λ CDM structure formation paradigm | \rightarrow Boost computation for velocity-dependent annihilations |

CLASSIFY THE STUDIED TARGETS

- Build intra- and inter-family ranking of targets for γ -ray DM searches
- The absence of firm detection of vanilla-WIMP DM


Let us broaden the theoretical particle framework...

Jointly included and systematically studied for the three families of targets

| | | | |
|--|---|--|--|
| Velocity dependence of $\langle\sigma v\rangle$ | Suppressed | Mediator is a scalar | $\sigma v_{\text{rel}} \propto v_{\text{rel}}^2$ |
| Modification of the short-range $\langle\sigma v\rangle$ | range interaction between DM particles | Complex dark sectors | Sommerfeld enhancement |
| Contribution of DM subhalos | Dependent on host halo mass and their structural properties | Λ CDM structure formation paradigm | Boost computation for velocity-dependent annihilations |

Our work: provide DM models for dlrrs and clusters

DM MODELS FOR SELECTED DIRRS

- Use the DM models that just developed  V. Gammaldi, *JPR et al., Dark Matter search in dwarf irregular galaxies with the Fermi Large Area Telescope*, Phys. Rev. D 105, 083006, [[arXiv:2204.00267](https://arxiv.org/abs/2204.00267)]
- Select the most promising targets of the studied according to:
 - Highest J-factors
 - More available kinematic data
- Use core&cusplike profiles to account for model uncertainties:

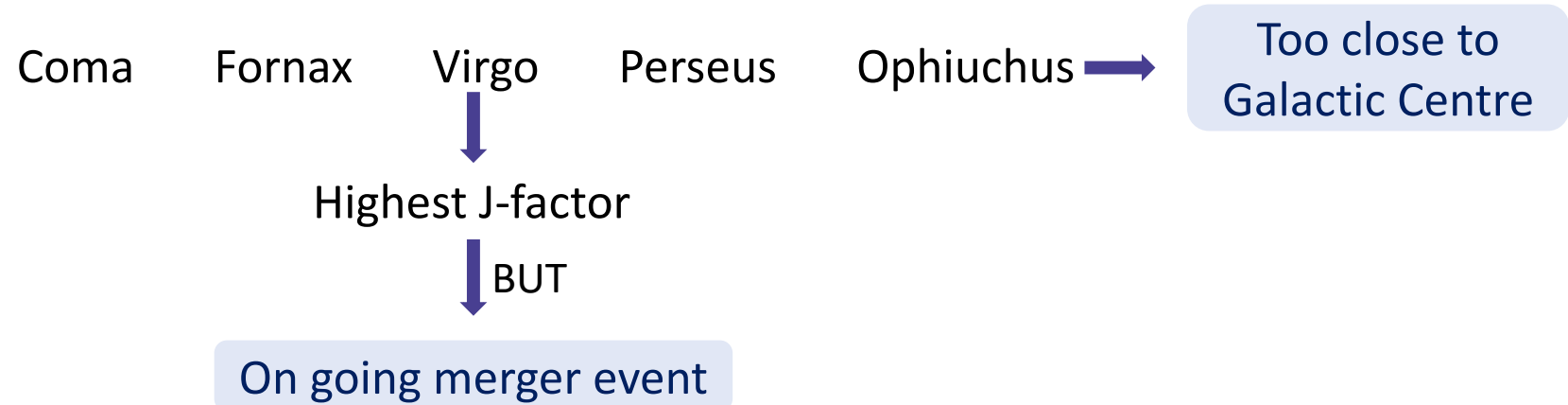
$$\rho_{\text{Bur}}(r) = \frac{\rho_c r_c^3}{(r + r_c)(r^2 + r_c^2)}$$

$$\rho_{\text{NFW}}(r) = \frac{\rho_0}{\left(\frac{r}{r_s}\right) \left(1 + \frac{r}{r_s}\right)^2}$$

| dIrr | (l, b) [deg] | D [kpc] | M_{200} [$10^{10} M_{\odot}$] | Profile | ρ [$10^7 M_{\odot} \text{ kpc}^{-3}$] | r [kpc] | R_{200} [kpc] |
|---------|-------------------|--------------|--------------------------------------|----------|---|--------------|--------------------|
| NGC6822 | (25.34, -18.40) | 480 | 3.16 | Burkert* | 3.16 | 3.3 | 62.9 |
| | | | | NFW | 0.79 | 5.9 | 62.6 |
| IC10 | (118.96, -3.33) | 790 | 3.98 | Burkert* | 15.85 | 2.0 | 71.3 |
| | | | | NFW | 0.63 | 6.8 | 70.3 |
| WLM | (75.87, -73.86) | 970 | 0.40 | Burkert* | 6.31 | 1.3 | 33.3 |
| | | | | NFW | 1.00 | 2.8 | 33.6 |

DM MODELS FOR SELECTED CLUSTERS

- Start from a smaller sample: *Sánchez-Conde+11*



DM MODELS FOR SELECTED CLUSTERS

- Start from a smaller sample: *Sánchez-Conde+11*



- Build NFW profiles from M_{200} : *Schellenberger&Reiprich17* *Reiprich&Böhringer02*

- Model uncertainties from:

M_{200} X-ray measurements

- $M_{200} < 5 \times 10^{14} h^{-1} M_{\odot} \rightarrow M_{\text{hydro}}/M_{SZ} = 0.86 \pm 0.01$
- $M_{200} > 5 \times 10^{14} h^{-1} M_{\odot} \rightarrow M_{\text{hydro}}/M_{SZ} = 1.46 \pm 0.08$

Underestimated 20%

(c-M) scatter

$\sigma_c = 0.14$ dex

Overestimated 50%

$$\left. \begin{aligned} & c_{200}(M_{200}^{(\max)}) \times 10^{+\sigma_c} \\ & c_{200}(M_{200}^{(\min)}) \times 10^{-\sigma_c} \end{aligned} \right\}$$

DM MODELS FOR SELECTED CLUSTERS

- Start from a smaller sample: *Sánchez-Conde+11*



- Build NFW profiles from M_{200} : *Schellenberger&Reiprich17* *Reiprich&Böhringer02*

| Cluster | (l, b) [deg] | D [Mpc] | Mass estimate | M_{200} [$10^{14} M_{\odot}$] | R_{200} [10^2 kpc] | ρ_0 [$10^6 M_{\odot} \text{kpc}^{-3}$] | r_s [10^2 kpc] |
|---------|-------------------|--------------|------------------|--------------------------------------|----------------------------|--|------------------------|
| Coma | (58.09, 87.96) | 102.18 | Hydrostatic | 13.16 | 23.19 | 2.29 | 3.38 |
| | | | Lower* | 8.77 | 20.26 | 5.37 | 5.58 |
| Fornax | (236.72, -53.64) | 20.35 | Hydrostatic* | 0.51 | 7.83 | 7.42 | 1.86 |
| | | | Upper | 0.61 | 8.32 | 3.20 | 1.05 |
| Perseus | (150.57, -13.26) | 80.69 | Hydrostatic | 7.71 | 19.41 | 2.35 | 2.80 |
| | | | Lower* | 5.14 | 16.96 | 5.57 | 4.59 |

BARYONIC CONTENT OF CLUSTERS

- From the X-rays surface brightness $S(r) = S_0 \left(1 + (r/r_c)^2\right)^{-3\beta+1/2}$ Beta-model

See Schellenberger&Reiprich 17

$$\rho_{\text{gas}}(r) = \rho_{\text{gas}}(0) \left(1 + \frac{r^2}{r_c^2}\right)^{-\frac{3}{2}\beta}$$

$$\rho_{\text{gas}}(0) = m_e n_e(0) + m_p n_p(0) + m_{\text{He}} n_{\text{He}}(0)$$

$$n_e(r) = n_e(0) \left(1 + \frac{r^2}{r_c^2}\right)^{-\frac{3}{2}\beta} + n_X(r) = \frac{\mu_Y}{\mu_X} n_Y(r)$$

Main responsible
of X-rays emission

Thermal electron density

From the beta-model

Thermal X density

Thermal ICM

Where μ are the
mean molecular
weights


$$\begin{cases} \mu_e &= \frac{1}{(1-\frac{1}{2}Y-\frac{1}{2}Z)} \approx 1.15 \\ \mu_p &= \frac{1}{1-Y-Z} \approx 1.35 \\ \mu_{\text{He}} &= \frac{4}{Y} \approx 14.6, \end{cases}$$

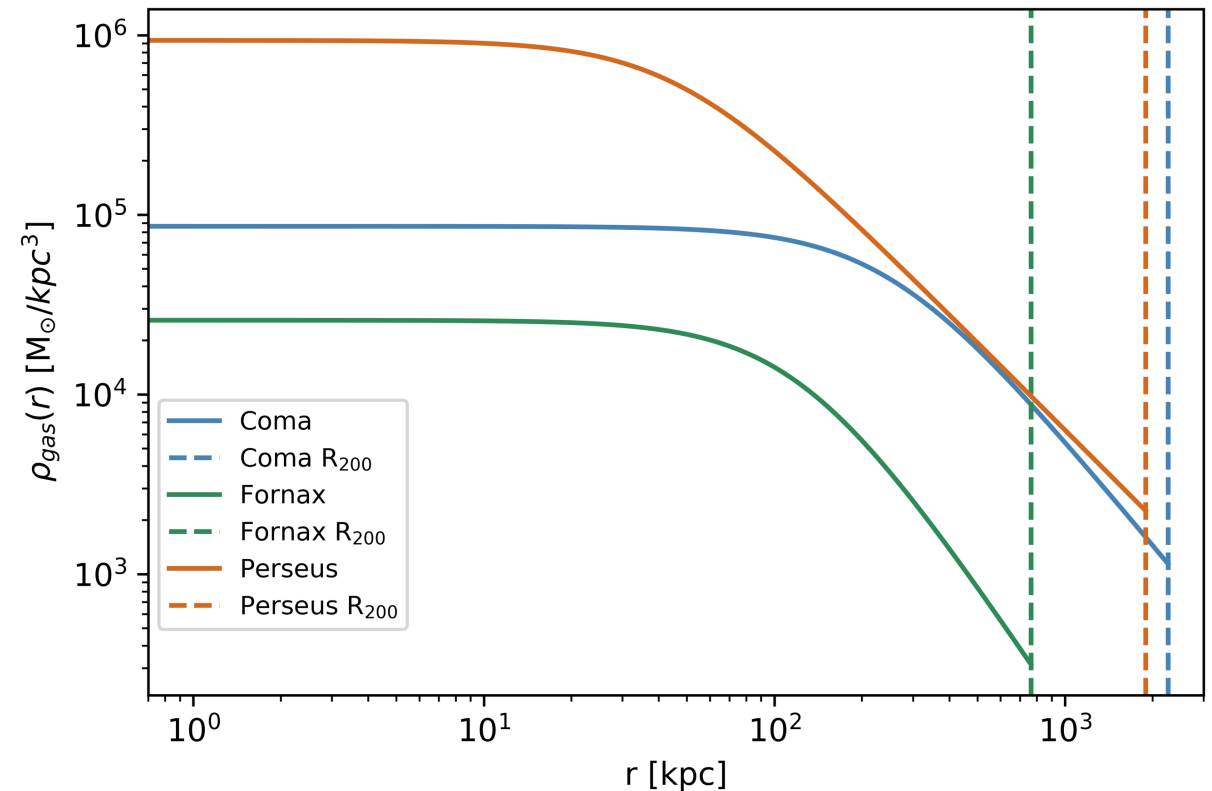
Adam+20

BARYONIC CONTENT OF CLUSTERS

- *Chen+09* performed a state-of-the-art X-ray analysis for nearby clusters and found the following parameters

| Name | β | r_c [kpc] | n_{center} [10^{-2}cm^{-3}] | $\rho_{gas}(0)$ [$M_{\odot}\text{kpc}^3$] |
|---------|---------|----------------|---|--|
| Perseus | 0.540 | 63 | 3.25 | 86402 |
| Fornax | 0.804 | 173 | 0.09 | 25921 |
| Coma | 0.654 | 343 | 0.30 | 936017 |

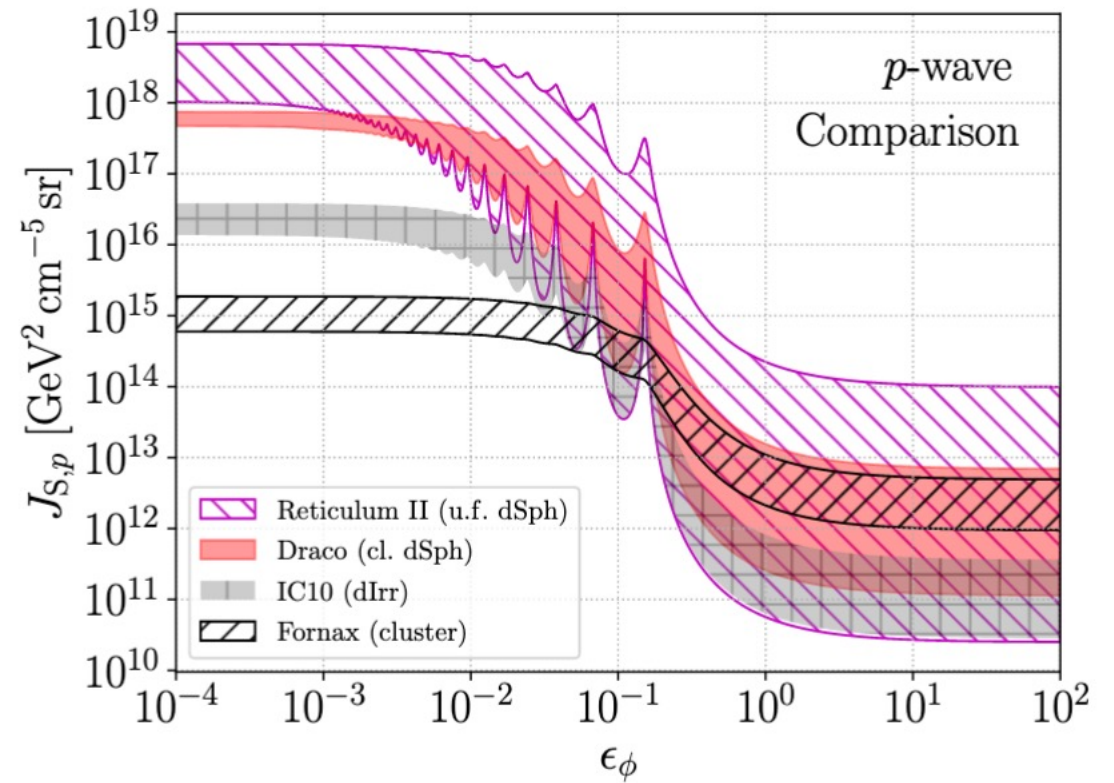
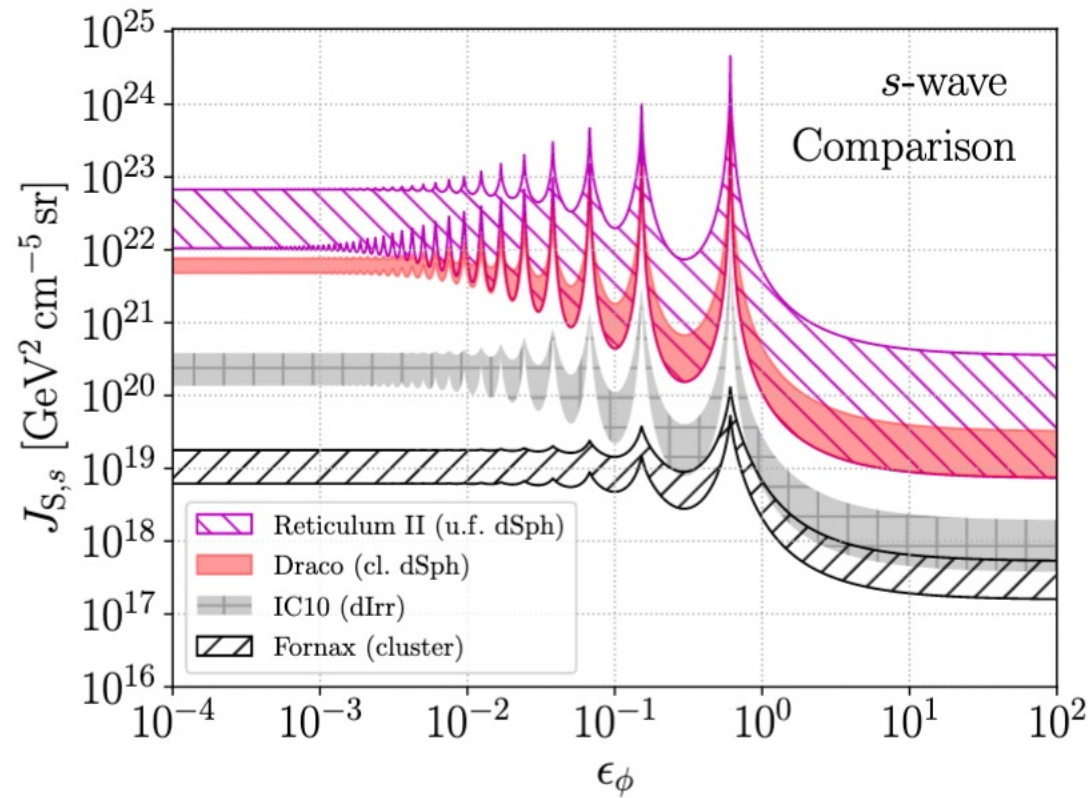

 MINOT software (*Adam+20*)



RESULTS ON CLASSIFICATION OF TARGETS

Main halos

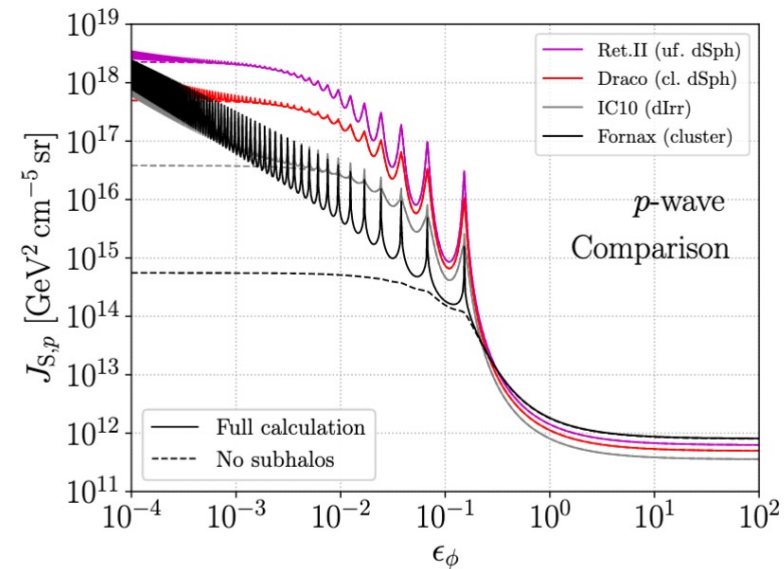
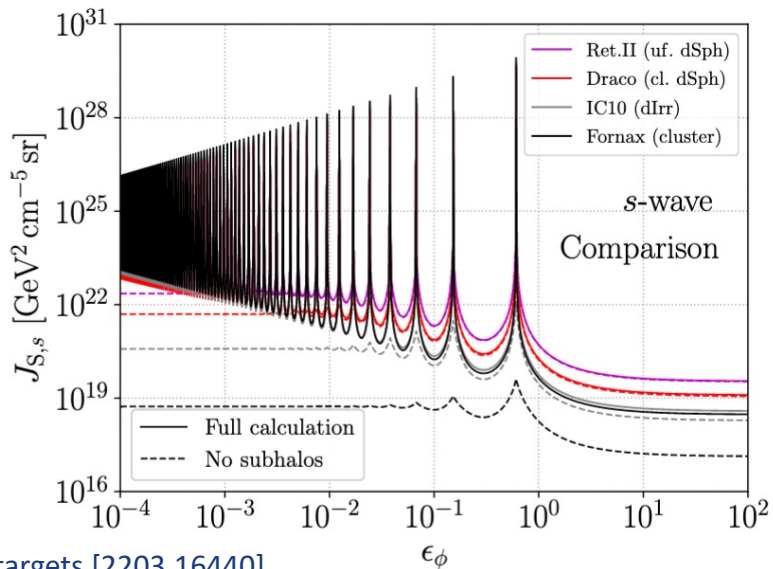
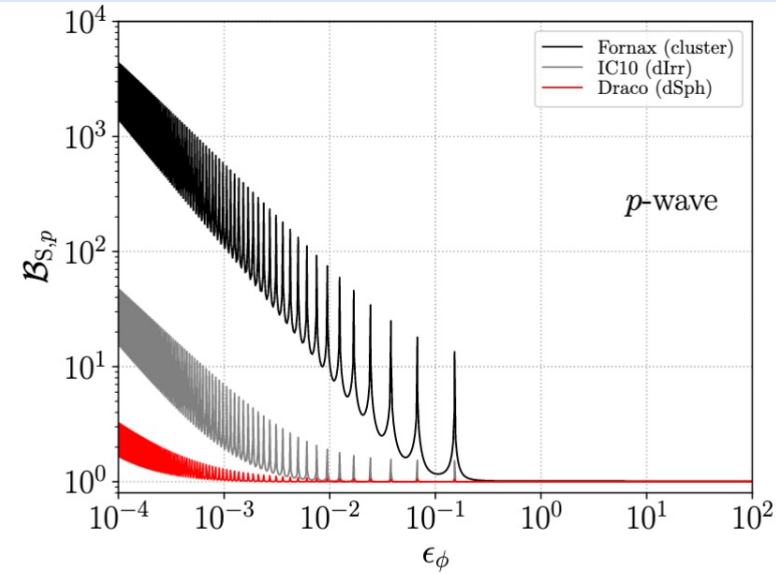
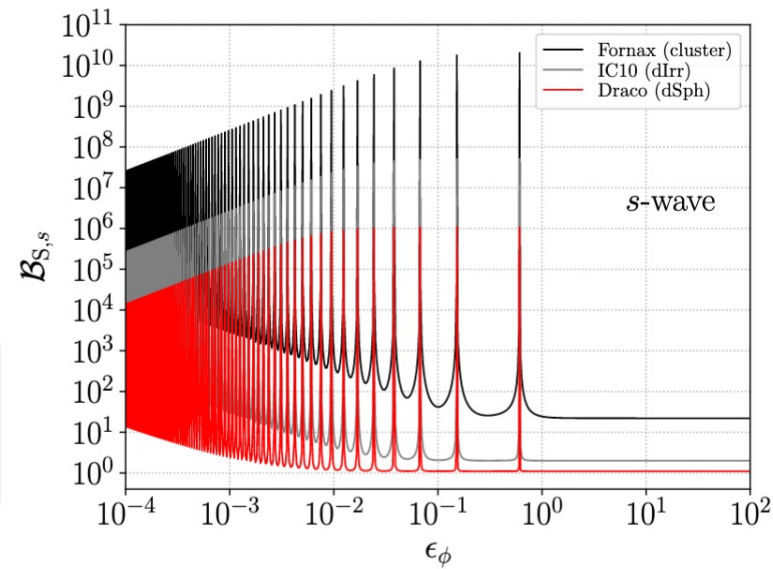
$$\epsilon_\phi \equiv \frac{m_\phi}{\alpha_D m_\chi}$$



RESULTS ON CLASSIFICATION OF TARGETS

Main halos
+
substructures

$$\mathcal{B}_S = \frac{J_{S,\text{tot}}}{J_{S,\text{host}}}$$



CLASSIFICATION OF TARGETS: SUMMARY

- Diversification of targets allows to distinguish and understand the impact of the systematics that each target suffers
- If DM detection is present in any of them, we should see it in others, as DM properties are universal
- After studying several targets, important to build intra- and inter-family ranking of targets under same theoretical framework
- These DM models take into account the specific uncertainties of each kind of object

CLASSIFICATION OF TARGETS: SUMMARY

- Diversification of targets allows to diversify systematic uncertainties that affect the results of the analysis
- Starting point to compute generalized J-factors, including p -wave annihilation, Sommerfeld enhancement and boost from subhalo population
- If DM annihilation is present in any of them, we should consider their specific properties are universal
- Ranking (where typically dSphs rank first) can be drastically modified: most striking case is s -wave on resonances and p -wave in the no-Sommerfeld enhancement regime, where galaxy clusters can outshine all others
- After spherically averaged DM density profiles are computed, we can perform intra- and inter-family ranking of targets in a theoretical framework
- These DM models take into account the specific uncertainties of each kind of object

CTAO DM SEARCHES

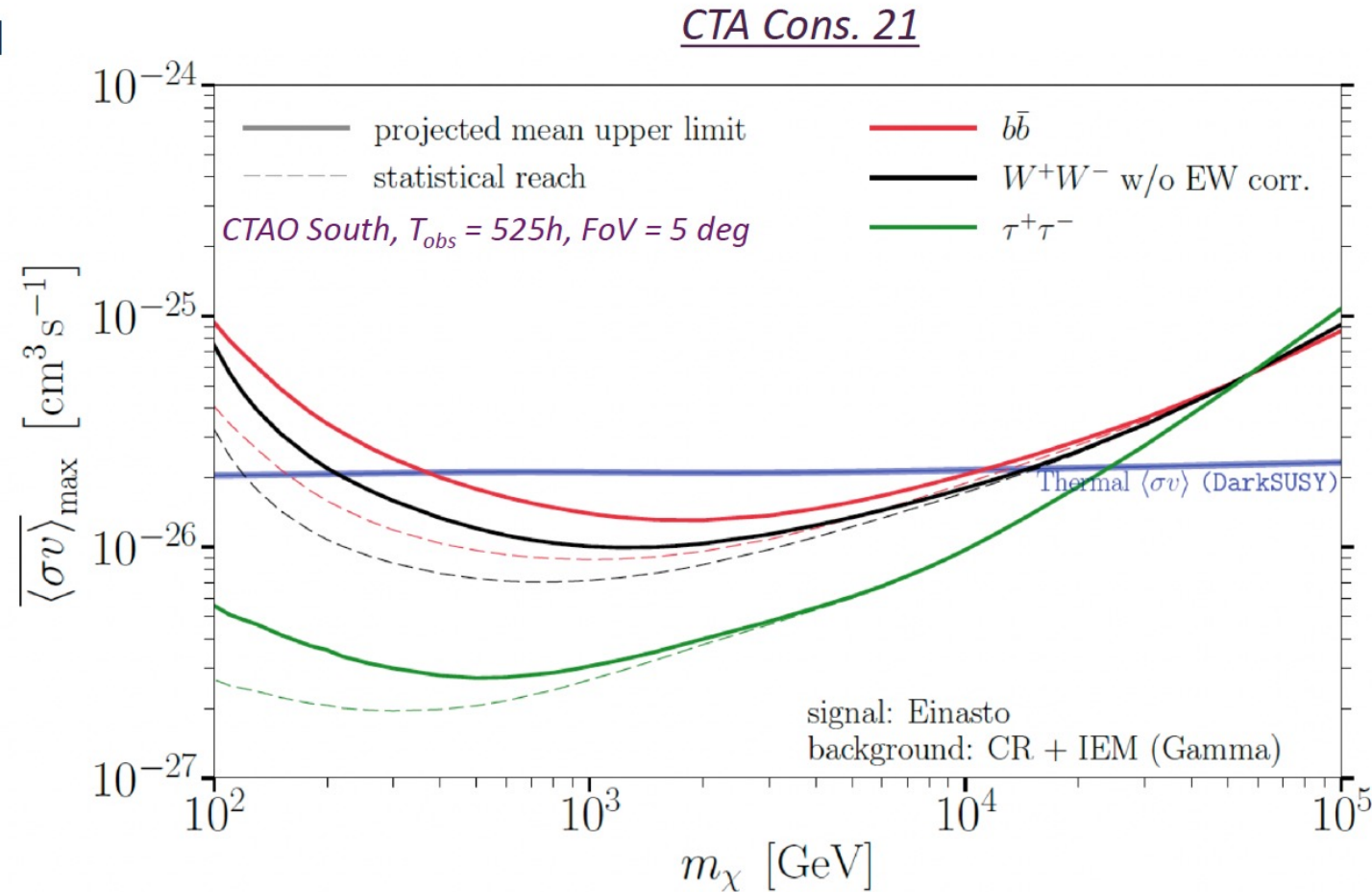
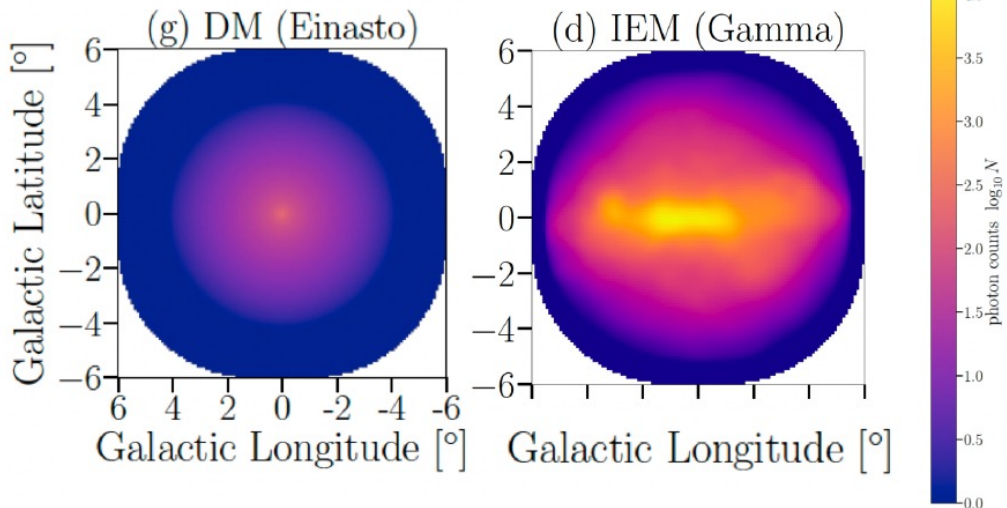
Properties of the Galactic Center

- Very close ($d_L = 8.5$ kpc), highly DM dominated object

$$\log_{10} J_{Ein} = 22.85$$

- Astrophysical γ -ray emission expected from:

- Point-like sources
- Inter-stellar emission (IEM)
- Fermi bubbles



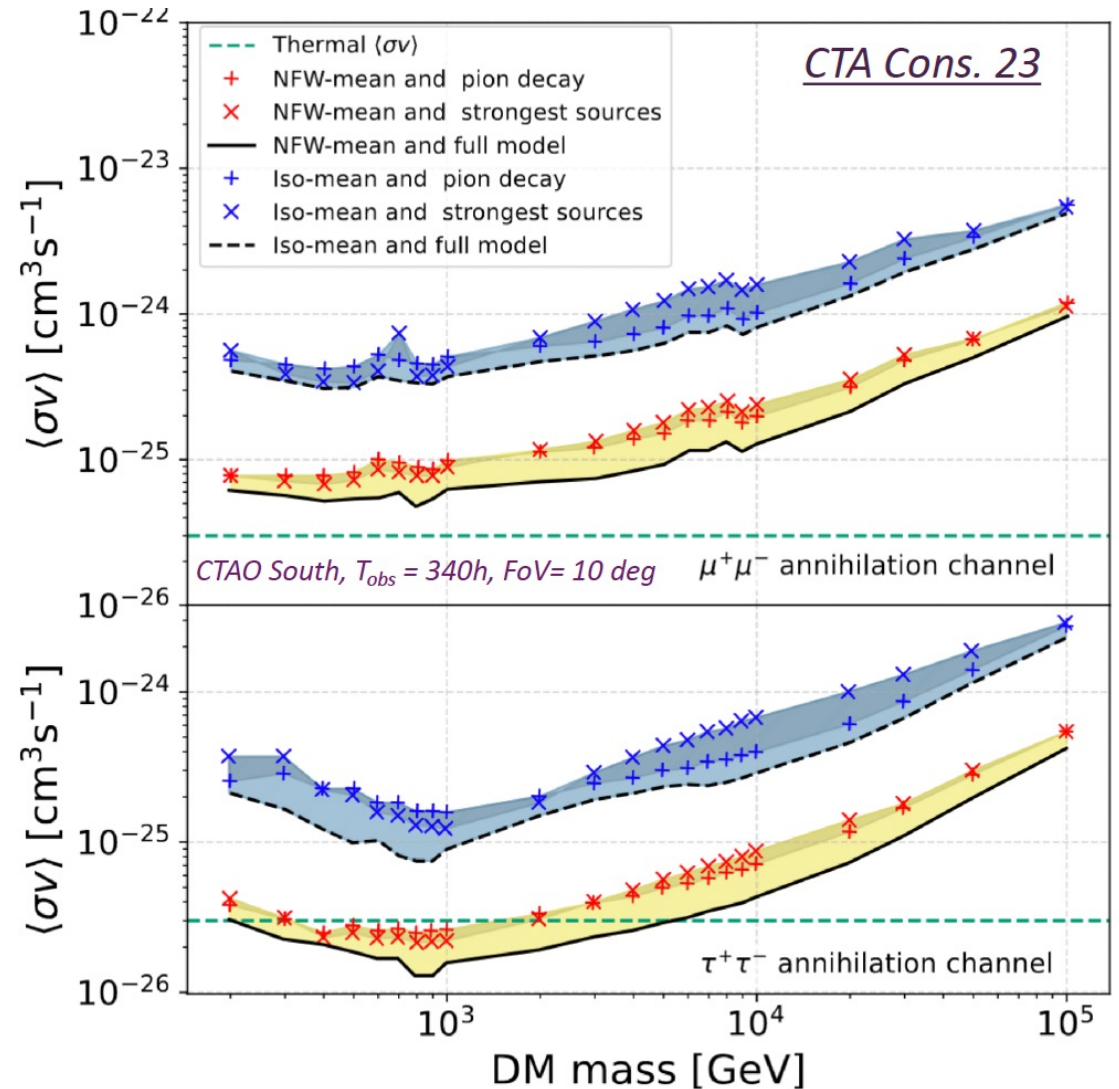
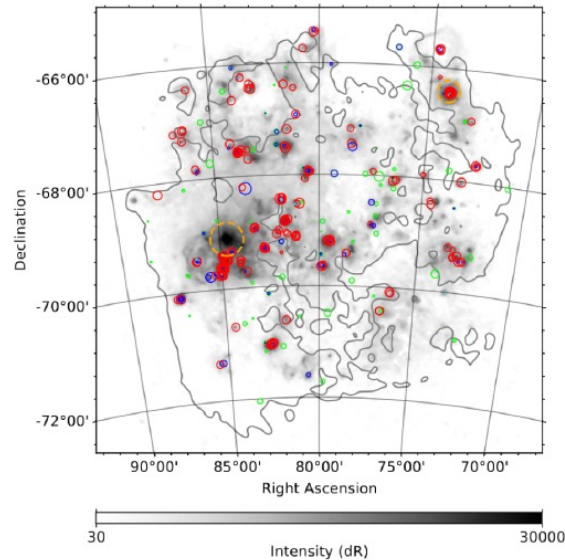
CTAO DM SEARCHES

Properties of the LMC

| | | | |
|-------|------------|---------------------------|---------------------------|
| d_L | 50.1 kpc | $M (\leq 10 \text{ deg})$ | $1.2 \times 10^8 M_\odot$ |
| l | 279.65 deg | b | -33.34 deg |

- MW satellite
- High star-forming region
- Astrophysical γ -ray emission expected from:
 - 4 known very high energy sources
 - SNRs, PWNs and pulsar halos
 - IEM

$$\log_{10} J_{\text{NFW-MEAN}} = 21.14$$



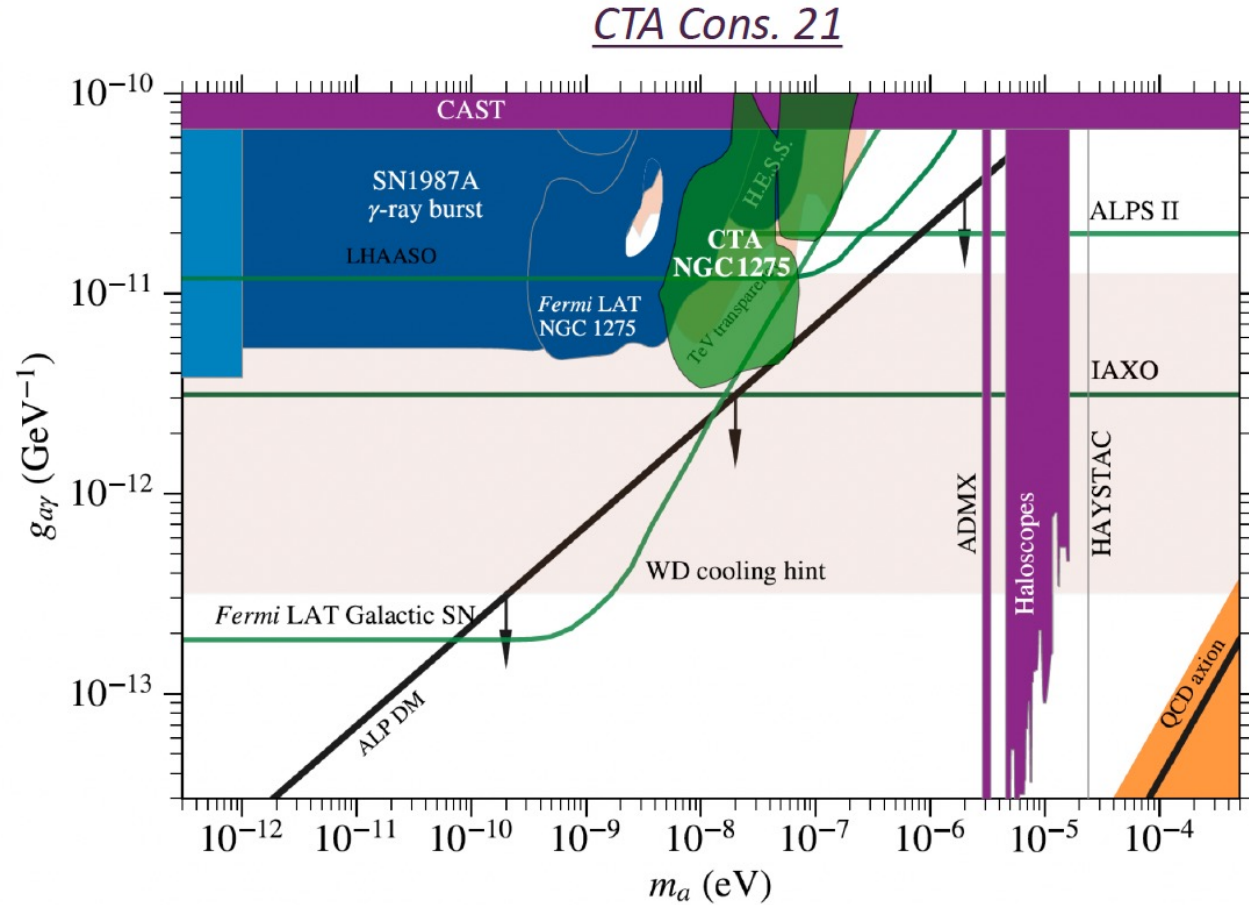
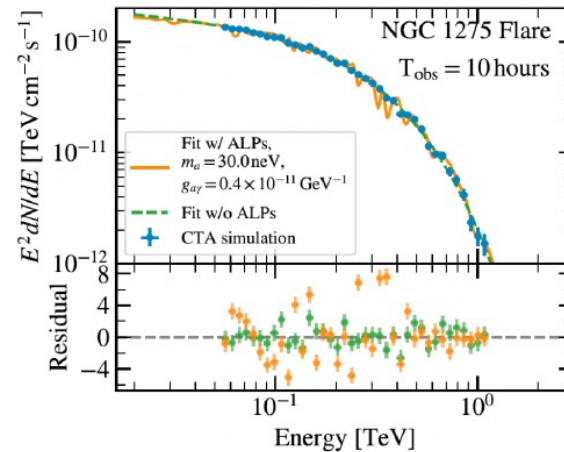
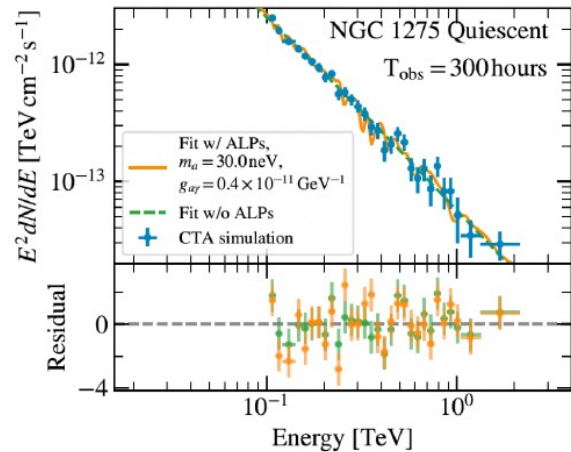
CTAO DM SEARCHES

- Target: NGC1275 – Brightest AGN of Perseus cluster

- At energies around:

$$E_{\text{crit}} \sim 2.5 \text{ GeV} \left(\frac{|m_a - \omega_{\text{pl}}|}{1 \text{ neV}} \right)^2 \left(\frac{B}{1 \mu\text{G}} \right)^{-1} \left(\frac{g_{a\gamma}}{10^{-11} \text{ GeV}^{-1}} \right)^{-1}$$

oscillatory patterns are expected in the AGN spectra



About SMASH program



SMASH

machine learning for science and humanities postdoctoral program

- SMASH is intersectoral, career-development training program for **postdoctoral researchers**, centered on developing cutting-edge machine learning applications for science and humanities, cofunded by **Marie Skłodowska Curie COFUND Action**.
- Duration: 2023 – 2028 - 3 calls for applicants will be launched in the period 2023 – 2028
- Coordinator: University of Nova Gorica, Dr. Gabrijela Zaharijas
- SMASH offers 2-year fellowships to 50 talented postdoc individuals to harness the potential of VEGA, one of Europe's newest petascale High-Performance Computers
- 5 host organisations in SLOVENIA: University of Nova Gorica, University of Ljubljana, Jožef Stefan Institute, Institute of Information Science and Slovenian Environment Agency
- 5 key research areas (and 17 sub-areas): <https://smash.ung.si/research-areas/>
- Website: <https://smash.ung.si/>

University of Ljubljana



REPUBLIC OF SLOVENIA
MINISTRY OF THE ENVIRONMENT,
CLIMATE AND ENERGY
SLOVENIAN ENVIRONMENT AGENCY



Co-funded by
The European Union



SMASH

machine learning for science and humanities postdoctoral program